Synthesis of Transition Metal Complexes Supported by Mixed Donor PSiP' Bis-Phosphino Silyl Pincer Ligands

by

Marshall R. Hoey

Submitted in partial fulfilment of the requirements
for the degree of Master of Science

at

Dalhousie University
Halifax, Nova Scotia
March 2016

Table of Contents

List of Tables

List of Figures

List of Schemes

Abstract

In an effort to explore new metal mediated reactivity and further the versatility of metal pincer chemistry, research in the Turculet group has targeted the synthesis of novel bis(phosphino)silyl PSiP pincer complexes. Given the profound influence that ligand design can have on the reactivity of the ensuing metal complexes, pincer ligands that feature a mixed neutral donor set have emerged as an intriguing ligand class that offers enhanced control over the steric and electronic features of a metal pincer complex. In this context the synthesis and reactivity of metal complexes supported by unsymmetrical PSiP' ligation was pursued.

In this work three novel PSiP' ligands were synthesized: (Cy-PSiP'-Ph)H, (Ph-PSiP*-^{i}Pr)H and (Cy-PSiP*-^{i}Pr)H. Group 10 complexes of the type (Cy-PSiP'-Ph)MX (M = Pt, Pd, Ni; X = Cl, Me, Ph) were prepared. The Pd and Ni chloride complexes were structurally characterized and found to exhibit approximate square planar coordination geometry in the solid state, with the silyl donor coordinated trans to the chloride ligand. The Me derivatives proved to be surprisingly unreactive with hydrosilanes, which is unlike the related Cy-PSiP analogues previously reported by the Turculet group. Amido complexes of the type (Cy-PSiP'-Ph)M(NHR) (M = Pt, Ni; R = H, Ph) and (Cy-PSiP'-Ph)Pd(NH_2) were also synthesized. While the latter complexes proved to be quite stable, related complexes of the type (Cy-PSiP'-Ph)Pd(NHR) (R = Ph, ^{t}Bu) underwent facile rearrangement processes involving Si-C (sp^2) bond cleavage in the ligand backbone. Such processes have previously been reported for related (Cy-PSiP)MX (M = Ni, Pd; X = alkyl, amido) species. Group 10 complexes supported by alternative PSiP' ligands including (Ph-PSiP*-^{i}Pr)PtCl and (Cy-PSiP*-^{i}Pr)MCl (M = Pt, Ni) were also synthesized. The complex (Cy-PSiP*-^{i}Pr)PdCl was structurally characterized and found to exist as a dimeric species in the solid state, with the $CH_2P^iPr_2$ ligand arms bridging between Pd centers. Solution NMR data suggests that in some cases, κ^3-coordination of Ph-PSiP*-^{i}Pr and Cy-PSiP*-^{i}Pr is achieved.

Finally preliminary studies revealed that Group 8 and 9 complexes supported by such PSiP' ligands are synthetically viable.

List of Abbreviations and Symbols Used

Anal. Calcd = Analysis Calculated
br = broad
cat. = catalyst
COE = cyclooctene
COD = 1,5-cyclooctadiene
[Cy-PSiP*-^{i}Pr]H =

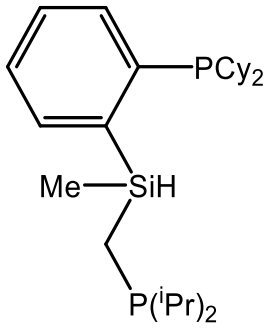

[Cy-PSiP'-Ph]H =

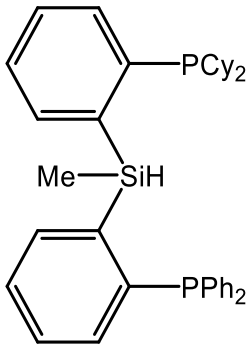

COSY = Homonuclear Shift *CO*rrelation Spectroscop*Y*
d = doublet
δ = chemical shift
DEPT = *D*istortionless *E*nhancement by *P*olarization *T*ransfer
η = indicator of hapticity in π-bonding ligands
E = main group element
equiv. = equivalents
EXSY = *EX*change Spectroscop*Y*
h = hour
HMBC = *H*eteronuclear *M*ultiple *B*ond *C*orrelation
HSQC = *H*eteronuclear *S*ingle *Q*uantum *C*orrelation
IR = infrared
$^{n}J_{XX'}$ = n bond coupling constant between atom X and atom X'
κ = indicator of hapticity in σ-bonding ligands
L = neutral two electron donor ligand
μ = descriptor for a bridging ligand
m = multiplet

M = generic transition metal or mol/L
min = minutes
NMR = *N*uclear *M*agnetic *R*esonance
ppm = parts per million
[Ph-PSiP*-^{i}Pr]H =

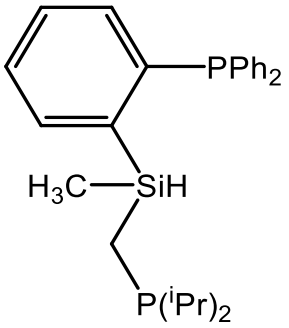

ORTEP = Oak Ridge Thermal Ellipsoid Plot
s = singlet
t = triplet
THF = tetrahydrofuran
X = anionic donor ligand

Acknowledgements

The completion of a thesis is not done on one's own and this one is no different. I would first like to thank my supervisor Dr. Laura Turculet for her help and support throughout this process, not only in the preparation of this document but also throughout the whole of my graduate studies. Her insights and guidance have been invaluable over the last two years. Working in her lab has allowed me to develop and grow more as a chemist than I thought possible.

I would also like to thank my supervisory committee, Drs. Mark Stradiotto and Alison Thompson for their support and guidance throughout my studies. I have to thank Dr. Mike Lumsden for his extensive help with running various NMR experiments for which I am extremely grateful. I am also thankful Mr. Xiao Feng for his help with mass spectrometry. I would also like to thank Drs. Robert Mcdonald and Mike Ferguson from the University of Alberta for X-ray crystallography experiments reported in this thesis. I would also like to thank the staff of the Department of Cshemistry at Dalhousie University for helping with various problems I have encountered.

A big thank you goes to the Turculet group members (past and present) for making working in the lab more enjoyable. I would also like to thank the Stradiotto group members for helpful discussion and allowing me to borrow seemingly anything from their lab.

Over the completion of my degree I have made several friends outside of the lab who have showed me the importance of a life outside of the lab. A special mention goes to my friend Laura Cole whose many discussions have helped me get through grad school and made it a more enjoyable experience.

Chapter 1: Introduction

1.1 Overview

Organometallic transition metal complexes play an important role in chemical synthesis, as demonstrated by the fact that the Nobel Prize in Chemistry was awarded in 2001, 2005 and 2010 for the development of transition metal catalyzed synthetic methods that have proven to be of broad scope and utility. Namely, the 2001 Nobel was awarded to Knowles, Noyori and Sharpless for their work in developing asymmetric catalysts,[1-3] the 2005 prize went to Grubbs, Schrock and Chauvin for the development of olefin metathesis,[4-6] and the 2010 award was made to Heck, Negishi and Suzuki for their seminal contributions in the field of Pd-catalyzed cross-coupling reactions.[6-8] The discovery of such useful catalysts is rooted in the development of new types of organometallic complexes and the fundamental study of their stoichiometric reactivity. In this regard, there is continued interest in the synthesis and study of transition metal complexes supported by novel ancillary ligands that can confer unique reactivity properties to the ensuing complexes.

In this context, the research described in this thesis details the synthesis and reactivity of platinum group metal complexes supported by novel bis(phosphino)silyl (PSiP) 'pincer'-type ancillary ligands. Specifically, the development of synthetic routes targeting "unsymmetrical" PSiP' pincer ligands and their corresponding metal complexes will be described. To help place this work in context, this chapter highlights prominent developments from the field of transition metal pincer chemistry, with specific emphasis

on reports involving related "unsymmetrical" pincer ligands as well as silyl pincer ligation.

1.2 Transition Metal Pincer Complexes

Pincer ligands are a diverse class of tridentate ancillary ligands that have been shown to support highly reactive transition metal centers.[9-11] Such ligands feature three donor groups that typically coordinate to the metal center in a *mer*-configuration (Figure 1-1). The three donors can be formally neutral (L) or anionic (X) and are connected by an organic backbone. Pincer ligands come in many variations, although the most ubiquitous are symmetric PCP ligands that feature a central anionic carbon donor group flanked by two neutral phosphine donors (Figure 1-1: A, B). Pincer ligands can also be "unsymmetrical" in nature, with numerous examples of mixed donor PCN and PNN metal complexes having been reported (Figure 1-1: D, E).[12-15] The modular design of pincer ligands provides numerous opportunities to tune the reactivity of their corresponding metal complexes by changing the nature of the donor groups and of the ligand backbone. As well, the tridentate nature of pincer ligands has been demonstrated to impart stability to their ensuing metal complexes (relative to analogous complexes supported by monodentate ligands) as a result of the chelate effect,[16-18] and this stability has led to unique reactivity, such as catalytic alkane dehydrogenation at elevated temperatures.[18]

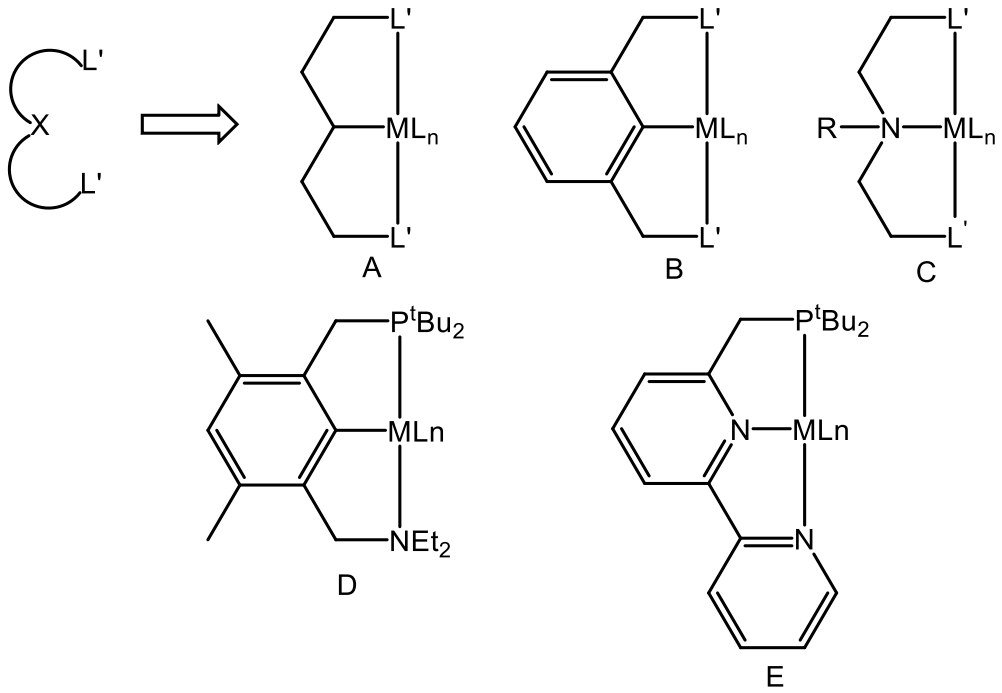

Figure 1-1. General form of pincer complexes and examples of LCL, LNL, PCN and PNN pincer coordination to a metal center.

The first report of pincer complexes in the literature was published by Shaw and coworkers in 1976,[19] although they were yet to be referred to as such until later reports of similar complexes. In this early work several different cyclometalated platinum group metal complexes were synthesized utilizing 2,6-bis[(di-t-butylphosphino)methyl]phenyl as the supporting tridentate ligand (Scheme 1-1). Since this first report by Shaw, pincer complexes have become quite prominent in the literature,[20-27] with numerous applications in catalysis, materials synthesis and stoichiometric bond activation.

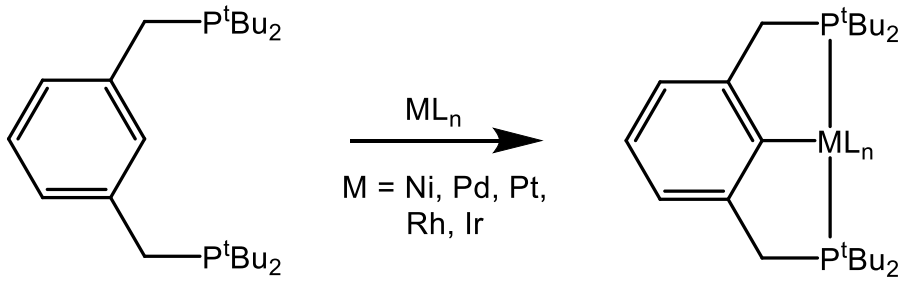

Scheme 1-1. Synthesis of platinum group metal pincer complexes by Shaw and co-workers using the 2,6-bis[(di-t-butylphosphino)methyl]phenyl ligand.

The nature of the L and X substituents can have profound effects (steric and electronic) on the resulting pincer metal complexes. While pincer complexes where L = PR_2, NR_2, SR, OR, SeR, AsR_3, CR_2, SiR_2 and GeR_2 have been reported,[112-115] the most common neutral donors employed are alkyl or aryl phosphino donors. Phosphino donors can provide control over sterics by varying the substituents on phosphorus, and also offer control over electron density at the metal by having more or less electron donating substituents on phosphorus. The backbone linkers can also provide control over the electronic properties of the complex, as aliphatic linkers can be more electron releasing than aromatic or benzylic linkers. The central anionic donor (X) also provides control over electronic features, most prominently via trans effects in square planar complexes. However, while numerous reports detailing the effects of changing L donors in pincer chemistry have appeared, relatively few examples of varied X donors have been reported, with X = C^- and N^- pincers dominating the literature.[18]

Further to the discussion of donor effects in pincer ligands, mixed donor pincers allow for even greater opportunities to tune the properties of the resulting complexes (electron donating properties, sterics and hemilability). The most common forms of mixed donor pincers are PCN and PNN species.[13,15,28] Changing one of the donors from a

phosphino to an amino derived donor can have profound effects on reactivity as amino donors are less electron donating as compared to phosphino groups. Furthermore, amino donors bind less tightly to electron rich late metal centers due to a hard/soft mismatch in donor/acceptor properties, and as a result there is also the possibility of N donors being hemilabile, thus allowing for coordinative unsaturation at the metal, which can facilitate substrate transformations that are not possible in otherwise saturated PCP and PNP complexes.[111]

1.3 Catalytic Applications of Pincer Complexes: Alkane Dehydrogenation

Although transition metal pincer complexes have found numerous applications in catalysis,[29] the utility of Ir pincer species in alkane dehydrogenation catalysis stands out as a rare example of catalytic alkane functionalization. The selective, transition metal catalyzed functionalization of unactivated alkanes is often regarded as one of the greatest challenges in synthetic chemistry.[30,31] This can be a useful method for the conversion of alkanes directly to alkenes, alcohols, amines and other valuable products that could have large implications in the production of fuels, fine chemicals and pharmaceuticals. A key step in such alkane functionalization chemistry involves C-H bond activation (or cleavage) at a reactive metal center.[30,32] One of the particular challenges in discovering metal species able to undergo this type of chemistry is that the active-site needed for C-H bond activation is often inhibited by coordination of reagents needed for the functionalization step, by the oxidized product itself, or by other species generated in the course of the reaction.[33] The previously mentioned reasons are why the number of

catalytic C-H bond functionalization reactions is quite small, even though numerous examples of stoichiometric C-H bond cleavage are now known.[32]

Transition metal catalyzed alkane dehydrogenation in the presence of a sacrificial hydrogen acceptor was long sought as a viable C-H bond functionalization reaction (Scheme 1-2). One of the primary challenges associated with this reaction is that heating to relatively high temperatures is required for the release of the product alkene from intermediate complexes. Under such conditions, many of the organometallic complexes that had been investigated as catalysts for this reaction undergo decomposition. For example, Crabtree and coworkers showed that $[IrH_2(Me_2CO)_2(P(p\text{-}FC_6H_4)_3)_2][SbF_6]]$ can dehydrogenate alkanes at 85 ºC in the presence of the hydrogen acceptor *tert*-butylethylene (TBE), but heating to 135 ºC was required for the efficient release of alkene.[34] The system failed to catalytically turn over because the catalyst decomposed above 130 ºC. In this context, the enhanced thermal stability of Ir pincer complexes proved highly advantageous in the development of viable alkane dehydrogenation catalysts. The modular nature of pincer ligation allowed for tuning of such catalysts to optimize their performance.

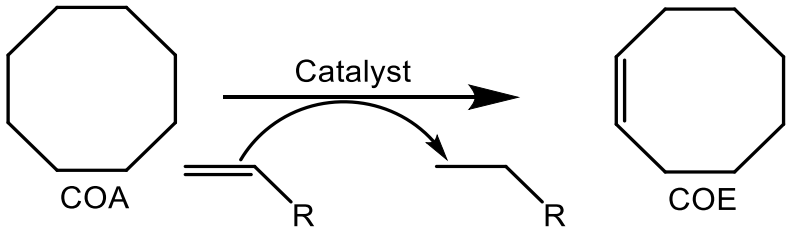

Scheme 1-2. Transition metal catalyzed alkane dehydrogenation of cyclooctane in presence of a sacrificial hydrogen acceptor.

1.3.1 Alkane Dehydrogenation Catalyzed by (PCP)Ir Complexes

The first example of pincer-ligated Ir complexes employed in the catalytic dehydrogenation of alkanes was reported by Jensen, Kaska and co-workers in 1996,[27] who prepared (^{t}Bu-PCP)IrH$_2$ and tested it for activity in the transfer dehydrogenation of cyclooctane (COA) in the presence of TBE (Scheme 1-3).

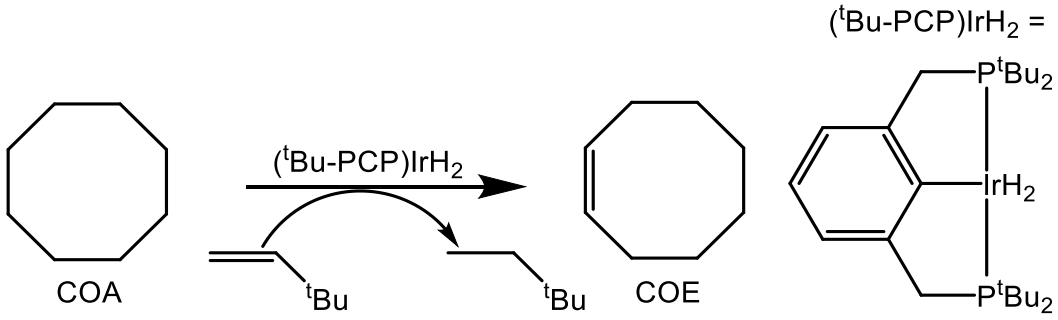

Scheme 1-3. Catalytic dehydrogenation of COA by (^{t}Bu-PCP)IrH$_2$ with TBE as the sacrificial hydrogen acceptor.

The Ir pincer complex showed high activity towards COA/TBE transfer dehydrogenation giving 82 turnovers/h at a temperature of 150 °C. This same complex also showed high thermal stability with no observable decomposition over one week at 200 °C. In similar work by Kaska and Jensen the same Ir complex was shown to also efficiently dehydrogenate other cycloalkanes such as cyclohexane, methylcyclohexane and decalin, in some cases yielding aromatic products.[35] The high thermal stability of (^{t}Bu-PCP)IrH$_2$ also allowed for the first demonstration of efficient acceptorless dehydrogenation of cyclodecane under reflux conditions with 360 turnovers observed after 24 h (Scheme 1-4).[36] Utilizing the less sterically crowded isopropyl phosphino analogue (^{i}Pr-PCP)IrH$_4$ under similar conditions resulted in close to 1000 turnovers in the dehydrogenation of cyclodecane (Scheme 1-4) and the first reported example of acceptorless dehydrogenation of an acyclic alkane (n-undecane).[37]

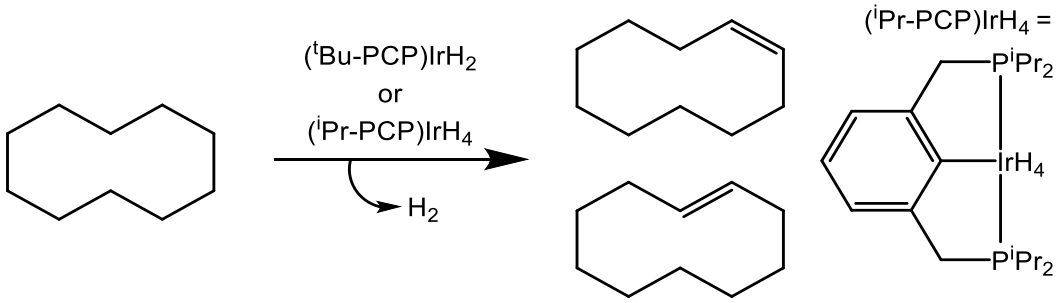

Scheme 1-4. Acceptorless dehydrogenation of cyclodecane by (^{t}Bu-PCP)IrH$_2$ and (^{i}Pr-PCP)IrH$_4$.

Mechanistic studies on both the transfer hydrogenation and acceptorless dehydrogenation processes were performed, and the proposed mechanistic pathway is shown in Scheme 1-5.[38] Key to both processes is the generation of a low coordinate (PCP)Ir^{I} species that is formally a 14-electron complex. This highly reactive intermediate mediates the C-H bond activation step necessary for catalytic turnover to occur.

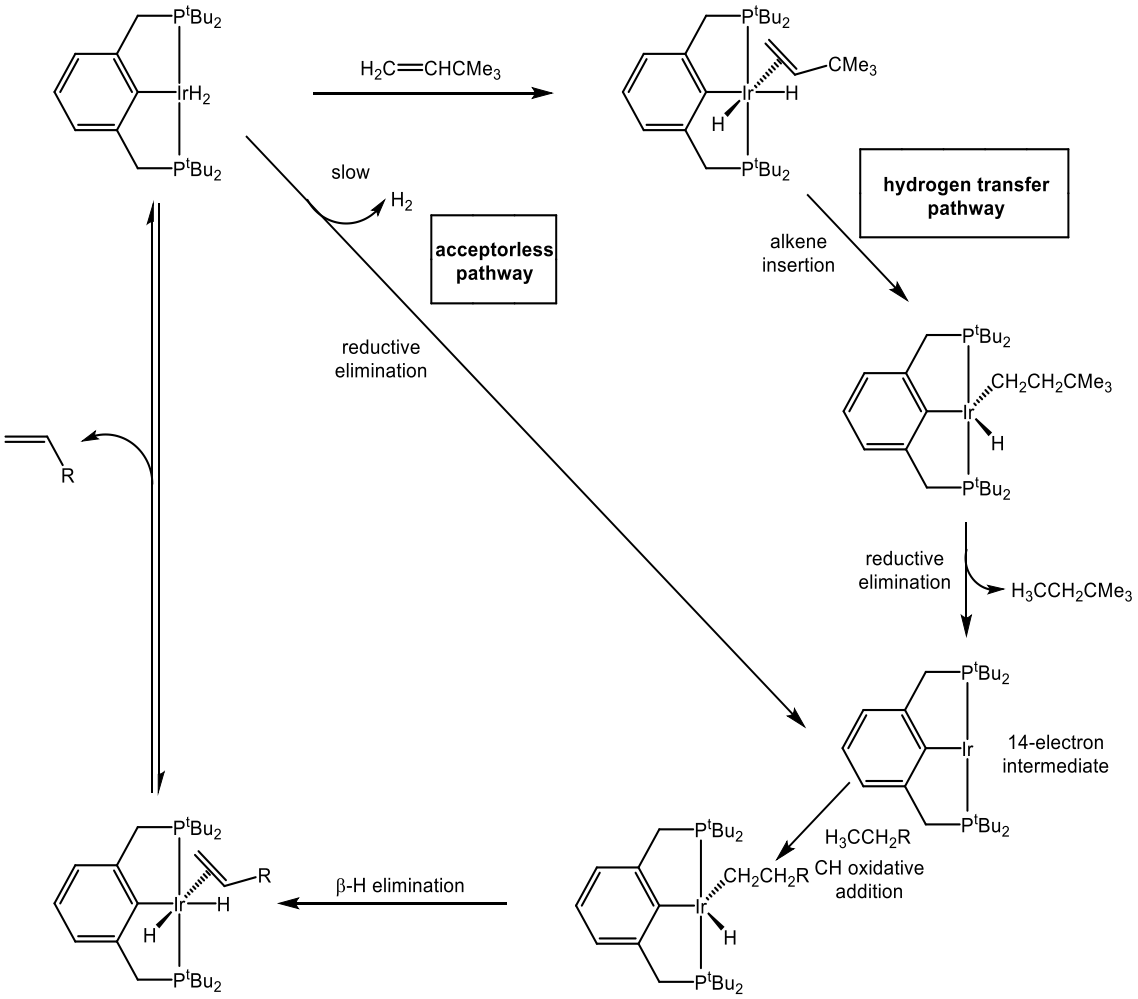

Scheme 1-5. Proposed catalytic cycle for transfer dehydrogenation and acceptorless dehydrogenation of alkanes catalyzed by)PCP)Ir pincer complexes.

1.3.2 Bis(phosphinite) Ir Pincer Complexes for Catalytic Alkane Dehydrogenation

After the initial reports of (PCP)Ir complexes being able to catalyze the dehydrogenation of alkanes it was of interest to modify the ligands further in hopes of increasing the reactivity of these catalysts. Perhaps the most notable modifications of the PCP ligand is seen in the bis(phosphinite) Ir pincer complexes (R-POCOP)Ir (R-POCOP = κ^3-2,6-$C_6H_3(OPR_2)_2$) which were prepared independently by the Brookhart (R = ^{t}Bu)[39]

and Jensen (R = ^{i}Pr)[40] groups (Scheme 1-6). Both of these newly prepared catalyst species exhibited greater activity in the transfer dehydrogenation of COA (Scheme 1-6) than the (^{t}Bu-PCP)Ir complex previously reported.[27] In particular (^{t}Bu-POCOP)Ir showed activity an order of magnitude higher than that of (^{t}Bu-PCP)Ir.[18]

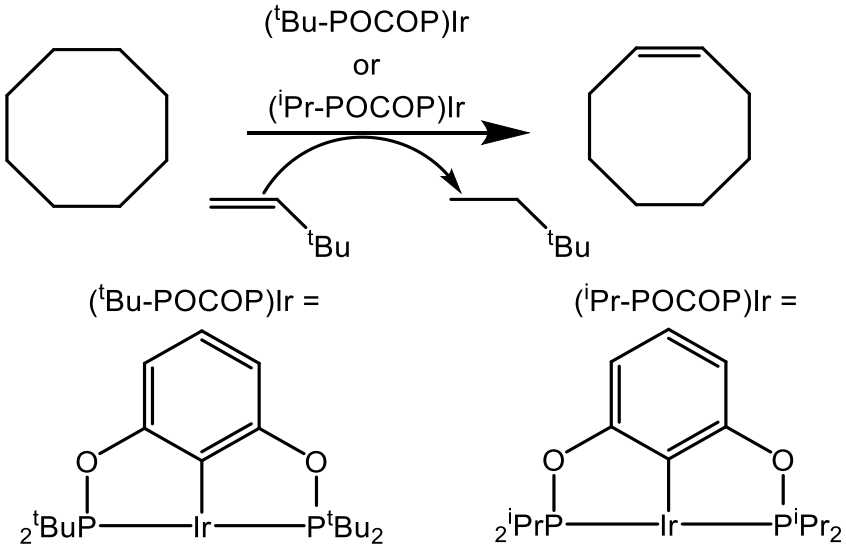

Scheme 1-6. Transfer dehydrogenation of COA catalyzed by bisphosphinite Ir pincer complexes.

In terms of the mechanism of dehydrogenation (,^{t}Bu-POCOP)Ir follows a similar pathway to that of (^{t}Bu-PCP)Ir (Scheme 1-5). The greater catalytic activity exhibited by the former complex has been attributed primarily to steric differences between these two pincer species, with the (bis-phosphinite) Ir pincer complex being much less sterically hindered than the analogous (PCP)Ir complex. Recently performed DFT calculations as well as X-ray crystallographic data appear to confirm this hypothesis (Figure 1-2).[18] Surprisingly, the electronic differences between these two catalysts appear to be fairly subtle.[18] While the electronegative oxygen atoms in the bis(phosphinite) pincer might be considered electron-withdrawing, DFT calculations showed that the oxygen atoms donate

substantial π-electron density to the aryl ring of the ^{t}Bu-POCOP ligand. This results in the Ir center of (^{t}Bu-POCOP)Ir being slightly more electron rich than that in (^{t}Bu-PCP)Ir.[42] However, due to the subtle nature of this effect, steric factors are overall considered to play a more defining role in the reactivity differences between POCOP and PCP ligated Ir.

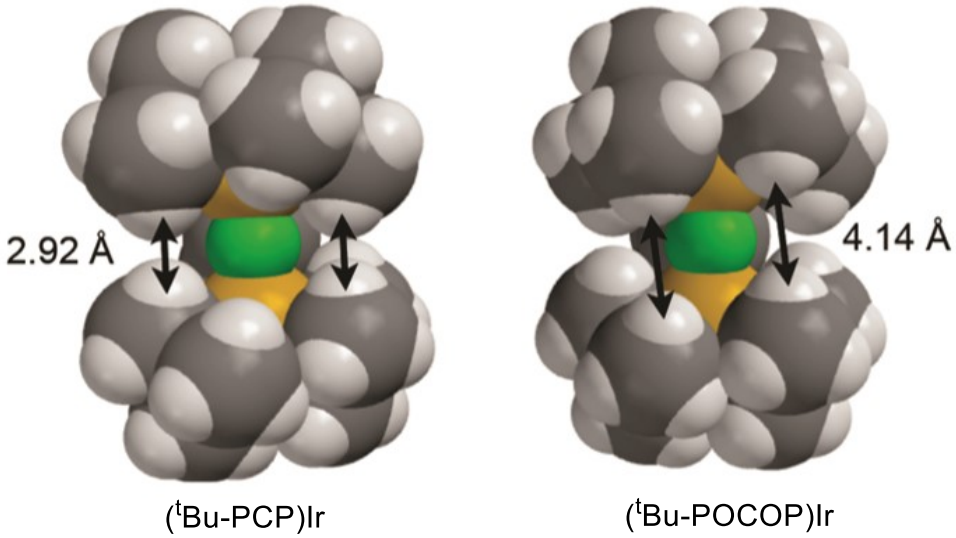

Figure 1-2. DFT calculated structures showing steric hindrance differences between (^{t}Bu-PCP)Ir and (^{t}Bu-POCPO)Ir.[18]

1.3.3 Alkane Metathesis

Alkane metathesis is a remarkably challenging reaction that has substantial applications in fuel and chemical production. Although no homogeneous catalysts have been developed that can perform this challenging transformation in a direct fashion, one can envision combining catalytic alkane dehydrogenation with olefin metathesis to achieve catalytic alkane metathesis (Scheme 1-7).[43]

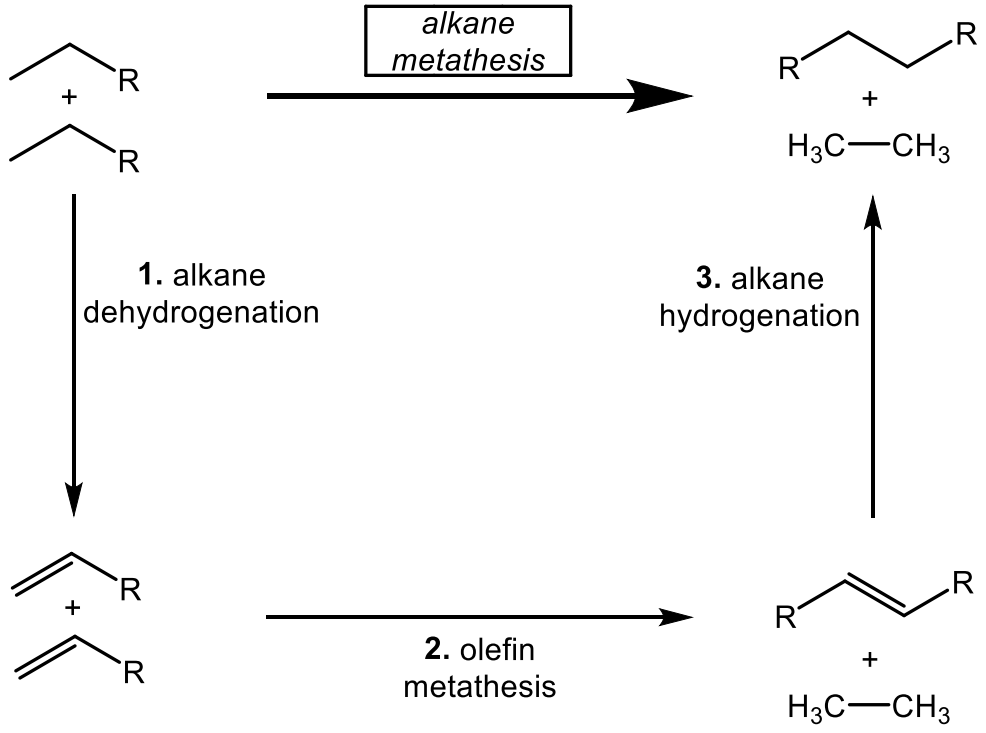

Scheme 1-7. Combination of alkane dehydrogenation with olefin metathesis to achieve alkane metathesis.

This approach represents a highly promising application of alkane dehydrogenation catalysis. In collaboration, Goldman, Brookhart and co-workers initially attempted this reaction by combining the transfer dehydrogenation catalyst (^{t}Bu-PCP)IrH_2 (Scheme 1-3) and two equiv. of the sacrificial acceptor TBE with the Grubbs olefin metathesis catalyst $(Cy_3P)_2Cl_2Ru$=CHPh (Figure 1-3, A).[43,44] However, this system did not yield any observable alkane metathesis and instead led to the formation of a catalytically inactive species. In subsequent studies the dehydrogenation catalyst precursors (^{t}Bu-PCP)IrH_2 and (^{t}Bu-IrPOCOP)IrH_2 were used in tandem with the Schrock olefin metathesis catalyst Mo-F12 (Figure 1-3, B).[39,41,45] Both Ir complexes performed with high efficiency, with overall product (C_2 – C_{15} alkanes) concentrations of 2.05 M (for (^{t}Bu-POCOP)Ir) and 1.25 M (for (^{t}Bu-PCP)Ir) obtained from 7.6 M n-hexane using

10 mM Ir catalyst and 16 mM metathesis catalyst after 1 day at 125°C. Studies revealed that turnover numbers for alkane metathesis are limited by the decomposition of the olefin metathesis catalyst under the high temperatures required for the alkane dehydrogenation chemistry. Thus, addition of further amounts of Mo-F12 to the metathesis reaction samples reinitiated catalytic activity.[46] In an effort to access more robust olefin metathesis catalysts, it was found that W-based catalysts outperformed the Mo-analogues in the tandem-catalyzed metathesis of n-octane. The most effective olefin metathesis catalyst discovered in the course of these studies was W(NAr)-($CHCMe_2Ph$)($OSiPh_3$)$_2$ (W-Si2) (Figure 1-3, C),[45] which afforded 3.0 M product. In conjunction with these studies, efforts to develop selective alkane dehydrogenation pincer-based catalysts that are more active at lower temperatures also play an important role in the further exploitation of catalytic alkane metathesis.

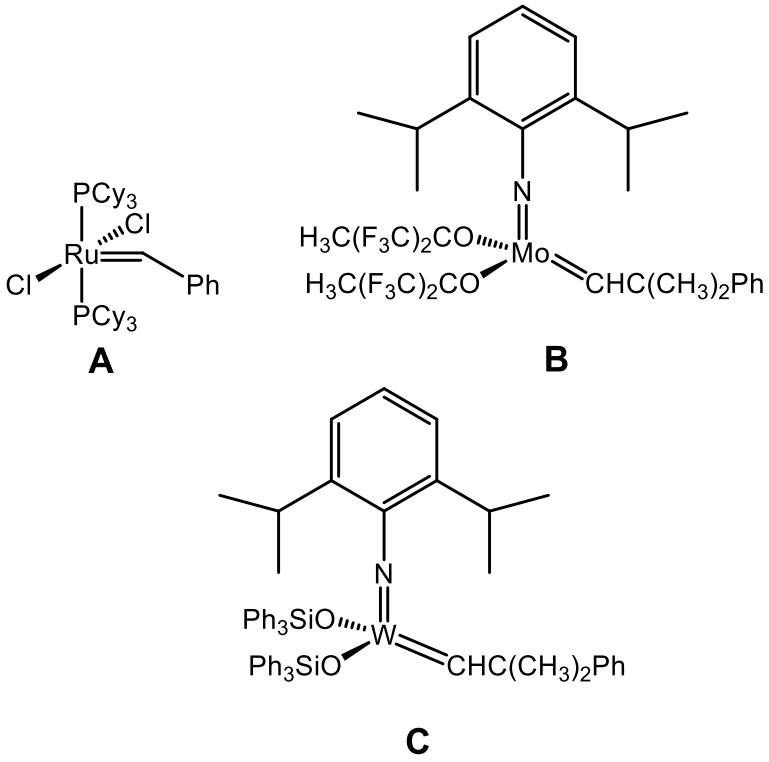

Figure 1-3. Olefin metathesis catalysts used in alkane metathesis.

1.4 Catalytic Applications of Mixed Donor Pincer Complexes

Tridentate pincer ligation featuring a mixed set of neutral donors (LXL') has garnered increased interest in recent years. The incorporation of two different L-type donors into the pincer architecture provides an additional means by which one can fine-tune the steric and electronic features of the ensuing metal complexes. Some of the more prominent examples of novel reactivity involving such complexes have come from the Milstein group, who have developed a series of PNN-ligated Ru species that have found widespread applications in catalysis (Figure 1-4).[28] As opposed to the more traditional bis(phosphino) PCP- or PNP-ligated pincer complexes, mixed donor species of this type feature a mismatch between the relatively soft, electron-rich metal center and the hard amine donor, leading to relatively poor coordination of the amino donor to the metal center. As such, the neutral N-donor could act as a hemilabile donor that undergoes reversible coordination and dissociation from the metal center, resulting in the transient formation of coordinatively unsaturated complexes. Such coordinatively unsaturated complexes are typically very reactive and are often invoked as intermediates in catalysis.

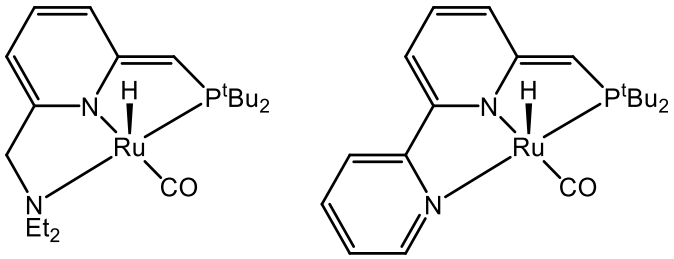

Figure 1-4. Series of (PNN)Ru complexes synthesized by Milstein and co-workers.

A key design feature of Milstein's PNN pincers is a central pyridine donor. Treatment of such PNN-ligated Ru species with a strong base leads to dearomatization of the pyridine ring, transforming the central nitrogen to an anionic donor (Scheme 1-8, A).[47] This dearomatized complex can effectivey function as a hydrogen shuttle, as it can be rearomatized upon reaction with H_2 (Scheme 1-8, B).[47] The resulting (PNN)Ru dihydride complex can, in turn, reductively eliminate H_2 at room temperature followed by a hydride transfer from the benzylic ligand backbone to reform the dearomatized species.

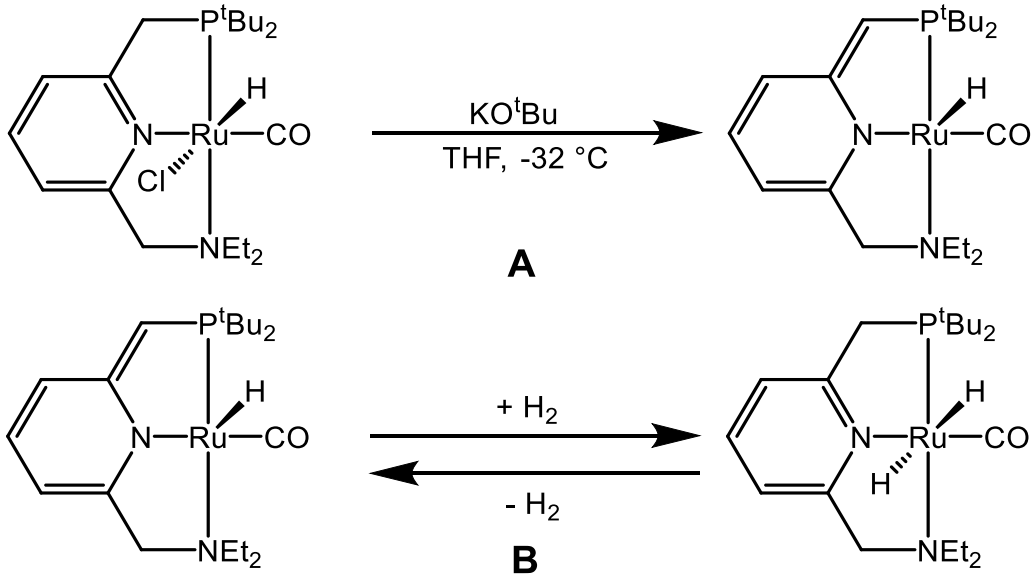

Scheme 1-8. Dearomatization of a PNN pincer complex with a strong base (**A**). Reversilbe dearomatizaton and rearomatization of PNN pincer complexes (**B**).

Such (PNN)Ru pincer complexes are capable of carrying out a wide variety of catalytic reactions involving hydrogenation/dehydrogenation steps,[28,47] including the hydrogenation of organic carbonates, carbamates and formates,[48] the transformation of alcohols to carboxylic acid salts and H_2 using water as the oxygen atom source,[49] the direct hydrogenation of amides to alcohols and amines under mild conditions,[50] the efficient hydrogenation of biomass-derived cyclic diesters to 1,2-diols,[51] catalytic

hydrogenation of urea derivatives to amines and methanol,[52] catalytic coupling of nitriles with amines to selectively form imines under mild hydrogen pressure,[53] and the direct synthesis of pyrroles by dehydrogenative coupling of β-aminoalcohols with secondary alcohols.[54] The mixed P,N donor set has proven key to achieving efficient catalysis in these systems. For the purpose of this document I will highlight two such processes: the dehydrogenative coupling of alcohols and amines and the hydrogenation of organic carbonates, carbamate and formates.

1.4.1 Dehydrogenative Coupling of Alcohols and Amines

Amides, imines and amines are all important fundamental building blocks for the chemical industry. The conventional synthesis of these compounds utilizes reagents such as carboxylic acids and derivatives thereof, as well as promoters or coupling reagents leading to the production of high amounts of waste.[55,56] With this in mind Milstein and coworkers have developed catalytic processes for the synthesis of these products directly from alcohols and amines with the H_2 or H_2O being the only reaction byproducts and utilizing no toxic reagents.

The reaction of primary alcohols with amines was undertaken with the possibility of three different reaction outcomes (Scheme 1-9). Dehydrogenation of a primary alcohol to form an aldehyde was envisioned as the first step, following which reaction of the aldehyde with an amine could form an intermediate hemiaminal that could undergo spontaneous elimination of water to form an imine that could then undergo hydrogenation with the liberated H_2 to yield a secondary amine. Alternatively, dehydrogenation of the hemiaminal could lead to the formation of an amide. Lastly, the aldehyde could react

with a second equivalent of alcohol to produce a hemiacetal that could be dehydrogenated to produce an ester.

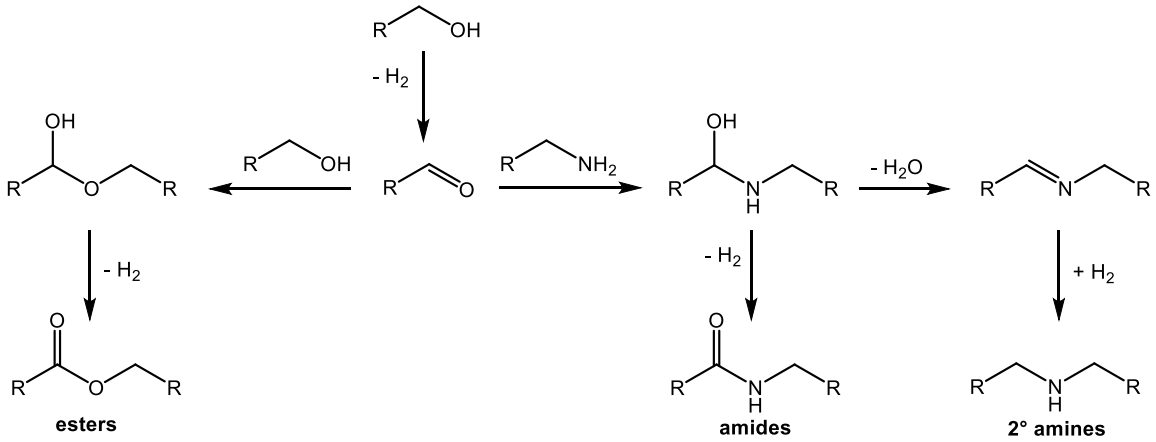

Scheme 1-9. Possible pathways for the reaction of primary alcohols and amines.

Milstein and co-workers initially targeted the synthesis of amides using a dearomatized (PNN)Ru catalyst (Scheme 1-10).[50] Amide yields ranging from 58-99 % were obtained from a variety of primary amines and primary alcohols utilizing 0.1 mol % catalyst under reflux conditions. Sterically hindered substrates resulted in lower yields of amides. Also, in the case of less nucleophilic amines such as aniline, ester formation becomes competitive. Lastly, the reactivity is restricted to primary amines, with no reactivity observed for secondary amines such as dibenzyl amine.

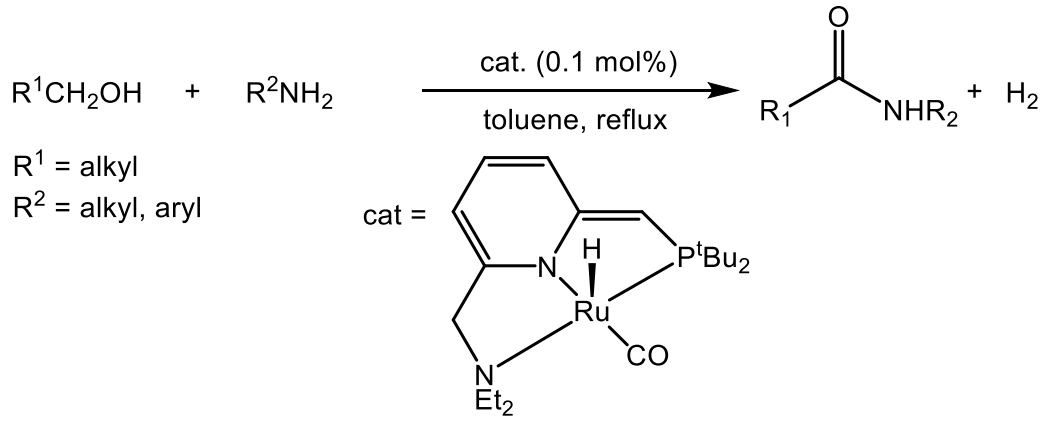

Scheme 1-10. Dehydrogenative coupling of alcohols and amines to form amindes.

The proposed catalytic cycle for this amidation reaction is shown in Scheme 1-11, and features dissociation of the amine ligand arm as a key step. Initial dissociation of the amine ligand arm from complex A results in the formation of a coordinatively unsaturated Ru species that can coordinate the alcohol substrate and undergo subsequent rearomatization to form the hydrido alkoxy complex B. β-hydride elimination from B leads to formation of an intermediate aldehyde and the trans-dihydride complex D which reductively eliminates H_2 to regenerate the dearomatized complex A. In the presence of amines the aldehyde reacts to form a hemiaminal that is subsequently dehydrogenated by complex A to form the desired amide product.

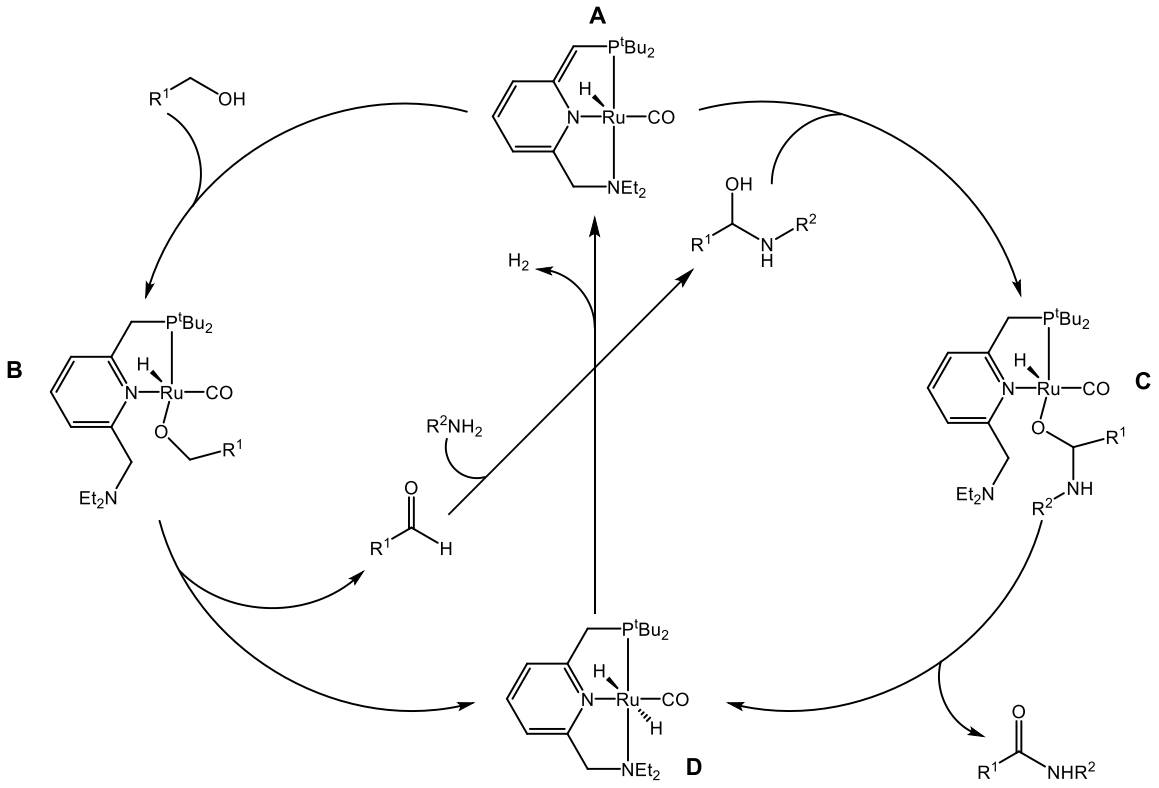

Scheme 1-11. Catalytic cycle for dehydrogenative coupling of alcohols and amines to form amides.

The use of related (PNP)Ru catalysts under these conditions does not result in amide formation. Rather, imines result via dehydration of the hemiaminal intermediate.[59] This difference in reactivity is striking and highlights the powerful impact of ligand design on the reactivity of pincer metal complexes. The difference has been attributed to the ability of the Ru complex to coordinate the intermediate aldehyde.[59] In the case of PNN species, due to the presence of the hemilabile amine arm, the aldehyde remains coordinated to the metal center and undergoes nucleophilic attack by the primary amine to form a quaternary ammonium intermediate (Scheme 1-12). Intramolecular proton transfer to the dearomatized phosphine arm follows, and β-hydride elimination generates the amide product. In the case of the PNP complex the attack of the aldehyde by the

amine takes place after the aldehyde is released into solution to generate a free hemiaminal intermediate that then eliminates water and forms an imine.[59]

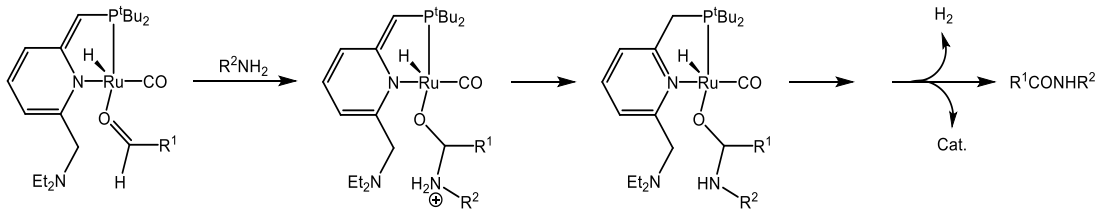

Scheme 1-12. Formation of amides with the use of a PNN Ru catalyst.

The coupling of primary alcohols and amines has recently been applied to the synthesis of peptides and pyrazines from β-amino alcohols, both of which are important molecules in chemistry and biology.[60] Use of a (PNN)Ru catalyst led to the dehydrogenative coupling of β-amino alcohols to form cyclic dipeptides (Scheme 1-13, A). Yields ranging from 64 - 99% were obtained using a 1 mol % catalyst loading in refluxing 1,4-dioxane (19 h). In the case of the less bulky substrate (*S*)-(+)-2-amino-1-propanol (R = Me in Scheme 1-13), a 72% yield of poly(alanine) was obtained. This reactivity is remarkable as, in contrast to traditional peptide synthesis, only H_2 is formed as a reaction byproduct. Interestingly, when a related (PNP)Ru catalyst was utilized under similar conditions, the resulting products were pyrazine derivaties (Scheme 1-13, B), which are proposed to form via a 1,4-dihydropyrazine intermediate.

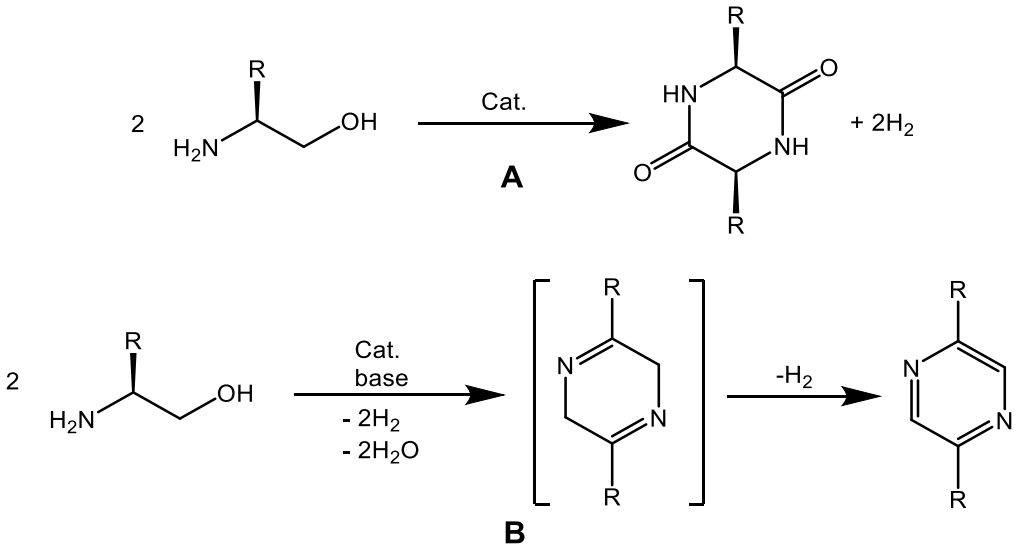

Scheme 1-13. Formation of cyclic peptides through dehydrogenative coupling of β-amino alcohols with the use of a PNN catalyst (**A**). Formation of pyrazines through the dehydrogenative coupling of β-amino alcohols using a PNP catalyst (**B**).

This coupling methodology has also been applied to the synthesis of polyamides from the reaction of diols and diamines. Milstein's (PNN)Ru catalyst was used to couple diols and diamines of various chain length and functionality (aliphatic, aromatic, linear and cyclic spacers were used; Scheme 1-14). In most cases >99% conversion and good (65-95%) yields were obtained at a 1 mol % catalyst loading after 48 h at 120°C. The resulting polyamides featured average molecular weights of ~ 10 – 30 kDa.[61]

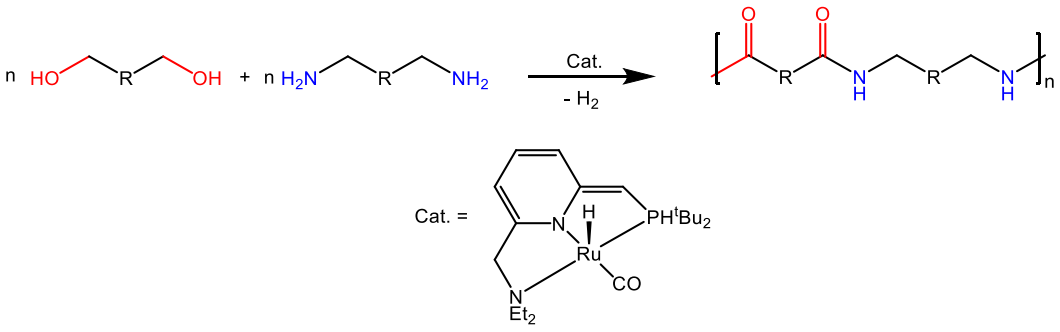

Scheme 1-14. Synthesis of polyamides through PNN catalyzed reaction of diols and diamines.

1.4.2 Hydrogenation of Organic Carbonates, Carbamate and Formates

Given the causative role of rising atmospheric CO_2 levels on global warming, there is significant interest in the development of efficient methodologies for the reduction of CO_2 to methanol, which can in turn be utilized as a chemical feedstock or as a fuel. The synthesis of methanol by the reaction of atmospheric CO_2 with hydrogen has in fact been referred to as the most economic way to mitigate the greenhouse effect (the "methanol economy").[63,64] Although a practical direct catalytic process of this type has yet to be developed, the hydrogenation of dimethyl carbonate, methyl formate or organo-carbamates to afford methanol represents an indirect hydrogenation of CO_2 to methanol, as all three species are readily obtained from CO_2 (Scheme 1-15).[65-67] As such, there is significant interest in developing mild, efficient catalytic protocols for the hydrogenation of such compounds to form methanol.

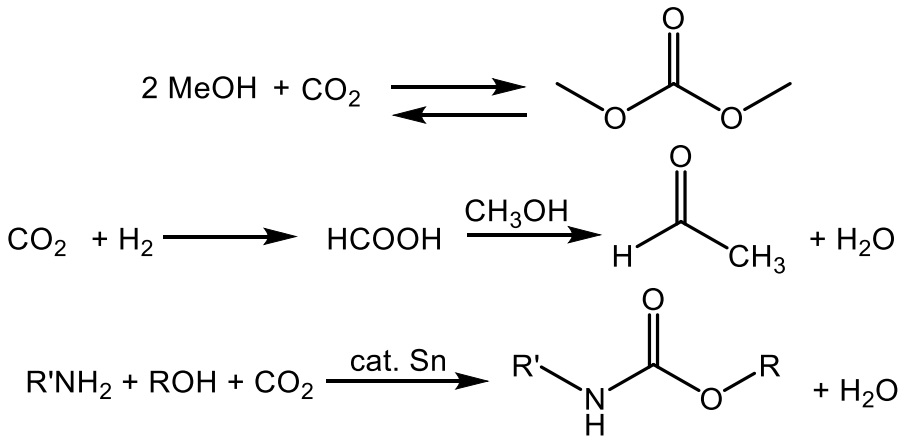

Scheme 1-15. Synthesis of dimethyl carbonate, methyl formate and organo-carbamates from CO_2.

In this regard, Milstein and co-workers reported that dearomatized (PNN)Ru(H)(CO) species (**A** and **B** as shown in Figure 1-4) are effective catalysts for the hydrogenation of organic carbonates and formates under mild, neutral conditions to afford alcohols, and for the hydrogenation of organic carbamates to form the corresponding alcohol and amine.[18] These represent the first such examples of catalytic hydrogenation involving organic carbonates and carbamates and the first example of homogeneuously catalyzed hydrogenation of alkyl formates. The reactions presented are selective, have reasonably high turnover numbers and can be carried out under neat conditions (i.e. without added solvent), thus generating no waste.

Both (PNN)Ru complexes **A** and **B** (Figure 1-4) were used for the hydrogenation of dimethyl carbonate to form methanol, with 0.1 mol% **B** affording >99% conversion and >99% yield of methanol after 8 h at 100 °C under solvent-free conditions and at relatively low pressure (10 atm H_2; TON >990; 89% conversion observed after 2 h). Turnover numbers as high as 4,400 were obtained at higher H_2 pressures (50 atm; after 14 h at 110 °C in THF). Complex **B** also catalyzed the hydrogenation of other organic carbonates to the corresponding alcohols. Diethyl carbonate was selectively hydrogenated to ethanol (91%) and methanol (89%) (8 h, 100 °C, 10 atm, solvent-free) with almost complete conversion (93%) and a good TON (910 based on ethanol).

Complex **B** (0.01 mol%) also catalyzed the hydrogenation of methyl carbamates to methanol and the corresponding amine, with methyl *N*-benzylcarbamate selectively affording methanol and benzylamine in quantitative yields (10 atm H_2, 110 °C in THF, 48 h). Remarkably, benzyl carbamates were also selectively hydrogenated under similar conditions, to yield methanol, the corresponding amines and benzyl alcohol, without

cleavage of the benzyl–O bond (Scheme 1-16, A). This is in contrast to the hydrogenolysis of benzyl carbamates using Pd/C catalyst, which leads to formation of the deprotected amine and free CO_2 (Scheme 1-16, B).

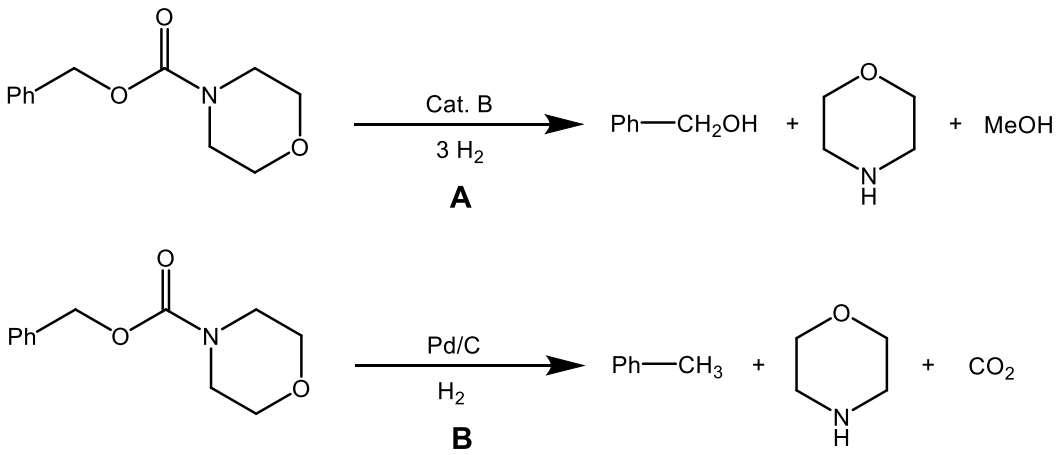

Scheme 1-16. Hydrogenation of benzyl carbamates with (**B**) and without (**A**) cleavage of the benzyl-O bond.

The hydrogenation of methyl formate is also efficiently catalyzed by complex **B** under solvent-free conditions, as in the case of dimethyl carbonate. Quantitative conversion of methyl formate selectively to methanol was achieved at a catalyst loading of 0.1 mol% upon heating at 80 °C for 8 h under H_2 (10 atm). The hydrogenation of other formate esters, such as ethyl and n-butyl formate, also proceeded efficiently under similar conditions to afford methanol and the corresponding alcohol (e.g. ethanol or n-butanol) in good yields.

Possible mechanisms for the hydrogenation of dimethyl carbonate (Scheme 1-17, **A**) and methyl formate (Scheme 1-17, **B**) were proposed on the basis of stoichiometric reactivity studies. Both proposed cycles operate in a similar manner and generate many of the same intermediates. In both cycles, dihydrogen addition to the dearomatized

(PNN)Ru(H)CO catalyst (***i***) results in aromatization to form the coordinatively saturated dihydride complex ***ii***. Subsequent hydride transfer to the carbonyl group of the carbonate (for cycle **A**) or formate ligand (for cycle **B**), leads to the formation of intermediate ***iii*** or ***v***, respectively. This process may involve direct hydride attack on the carbonyl or, alternatively, dissociation of the amino ligand arm to provide a site for coordination of either carbonate or formate to the Ru center. Deprotonation of the benzylic ligand arm by an adjacent methoxy group can result in liberation of methanol and the formation of either the formate adduct ***iv*** (for cycle **A**) or the formaldehyde adduct ***vi*** (for cycle **B**), respectively. Addition of another equivalent of H_2 (which may also involve amine arm decomplexation), followed by hydride transfer to either methyl formate (for cycle **A**) or formaldehyde (for cycle **B**), can generate either ***v*** or ***vii***, respectively. Deprotonation of the benzylic arm by a methoxy group generates a second equivalent of methanol and in the case of cycle **B**, regenerates catalyst ***i***. In the case of cycle **A** the formaldehyde intermediate ***vi*** is formed, which undergoes hydrogenation to the methoxy complex ***vii***. Methanol liberation from ***vii*** regenerates catalyst ***i***.

These results represent an unprecedented indirect approach to the difficult problem of CO_2 reduction to methanol. The reactions described are atom-economical and efficient. As the proposed mechanisms show, the pincer ligand design is key to this novel reactivity, and the mixed donor set may play an important role in providing access to available coordination sites.[48]

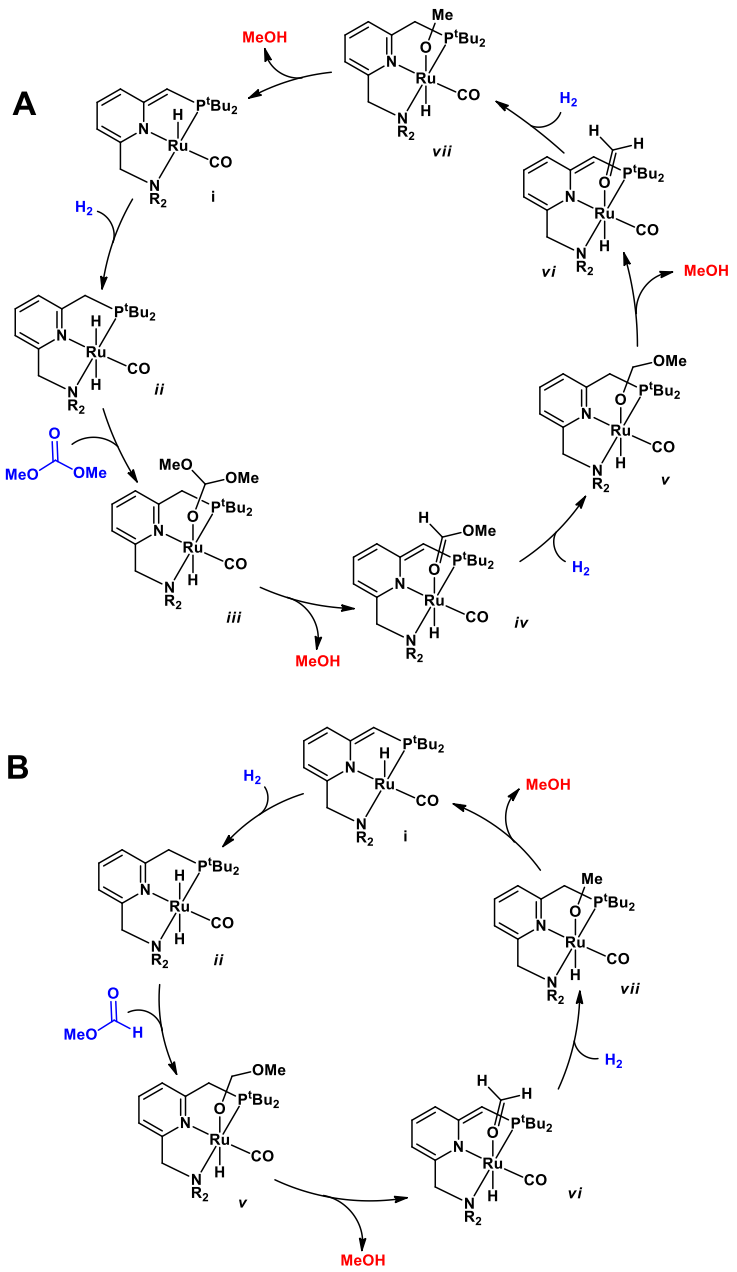

Scheme 1-17. Proposed mechanisms for the (PNN)Ru-catalyzed hydrogenation of dimethyl carbonate (**A**) and methyl formate (**B**).

1.5 Silyl Pincer Ligation

Although pincer ligands are highly modular and offer numerous opportunities to tune and specifically tailor both steric and electronic features, variability of the central anionic donor (X) in the pincer architecture has been vastly underexplored. The study of

pincer complexes that feature other types of central donor groups is an emerging area, with examples of pincer ligation featuring X = Si,[68] Ge,[69,70] Sn,[69,70] P, [71-80] and B [81-87] having been reported in recent years. Of these alternative pincer designs, silyl-based PSiP ligands are the most established and well-studied, and the Turculet group has been at the forefront of this research area.[10,11,88,89] In comparing PSiP pincer ligation with the closely related PCP derivatives highlighted in previous sections of this document, the increased electron-donating character of Si relative to C can lead to a more electron-rich late metal center, which in turn is more likely to undergo challenging oxidative addition reactions. In addition, the stronger trans-labilizing ability of Si can better promote coordinative unsaturation at the metal center, which is a characteristic of highly reactive metal complexes.[90] Such features can lead to significant structural and reactivity differences between PCP- and PSiP-supported complexes.

Literature precedent for the synthesis of silyl PSiP ligands was established by Stobart and co-workers in the 1980s, who prepared a series of platinum group metal complexes supported by bi-,[24] tri-,[25] and tetradentate[26] (phosphino)silyl ligands ligands featuring aliphatic and benzylic backbones (Figure 1-5). These early studies primarily addressed the fundamental coordination chemistry of such phosphino silyl ligands. Tilley and co-workers subsequently reported the synthesis of NSiN pincer complexes based on a bis(8-quinolyl)silyl framework (Figure 1-6).[91-93]

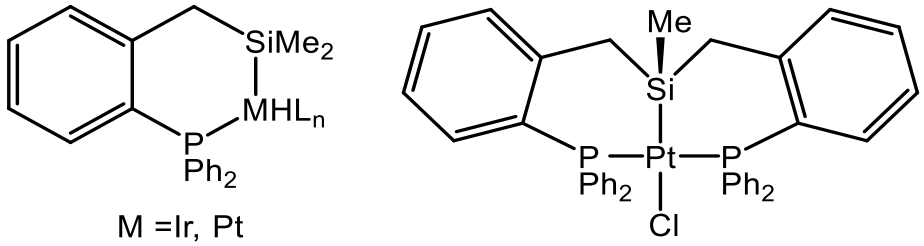

Figure 1-5. Bi-, tri-(phosphino) silyl ligands developed by Stobart and co-workers.

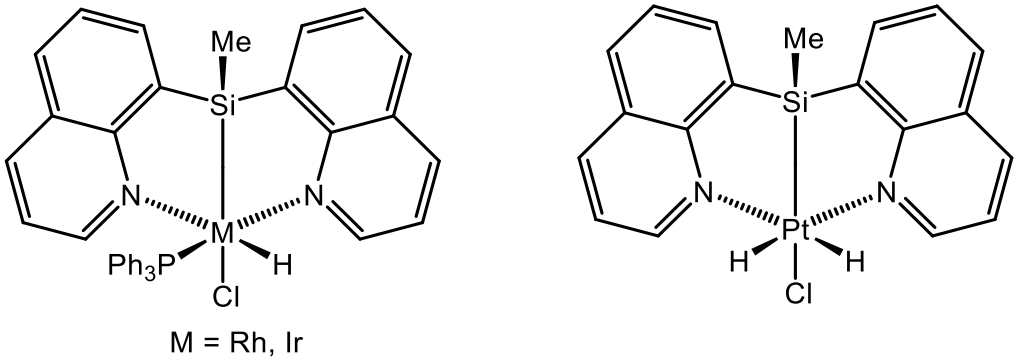

Figure 1-6. NSiN pincer complexes based on a bis(8-quinolyl)silyl framework.

More recently, the Turculet group has developed robust PSiP derivatives featuring a phenylene backbone (Figure 1-7) that have been shown to support very unusual and reactive late metal complexes. Examples of these complexes include formally 14-electron Ru complexes,[89] Ir complexes that undergo oxidative addition of ammonia,[10] Ni and Pd complexes that undergo unprecedented reversible sp^2-sp^3 and sp^3-sp^3 C-Si bond cleavage,[88] and unusual η^2-SiH Pt complexes that catalyze the reduction of CO_2.[11] The *ortho*-phenylene backbone of these ligands is rigid and contains no β-hydrogens, thereby eliminating the possibility of complexes undergoing decomposition by β-hydride elimination involving the ligand backbone. These ligands are highly modular as the substituents on the phosphine donors can easily be altered to achieve the desired steric and electronic effects in the resulting metal complexes. This modular design has been

extended to encompass the synthesis of mixed donor PSiN pincer ligands and their corresponding complexes.[111]

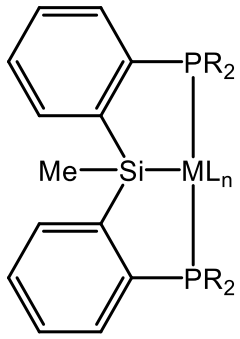

M = Ru, Rh, Ir, Pt, Pd, Ni
R = Cy, Ph, ^{i}Pr

Figure 1-7. PSiP pincer complexes featuring a phenylene backbone.

1.5.1 Unusual Trigonal Pyramidal (PSiP)Ru^{II} Complexes

Although coordinatively and electronically unsaturated late metal complexes that feature less than 16 valence electrons are invoked as key intermediates in a majority of metal-catalyzed processes, isolated species of this type are rare, especially in the absence of stabilizing features such as agostic interactions.[16,94,95] As such, there is significant interest in the synthesis of electron deficient, low-coordinate metal complexes in order to enable the study of their structure and reactivity properties. In the case of Ru^{II}, the vast majority of isolated complexes are either five- or six-coordinate species that feature 16- or 18-electron configurations, respectively.[91.94,95] By comparison, four-coordinate, formally 14-electron Ru^{II} complexes are exceedingly rare.[89]

Previously reported strategies for the synthesis of 14-electron Ru^{II} species included the incorporation of stabilizing agostic interactions between the metal center and

the ancillary ligands (Figure 1-8, **A** and **B**).[96-99] Alternatively, Caulton and co-workers demonstrated that the unusual square planar, 14-electron Ru^{II} complex $(({}^tBu_2PCH_2SiMe_2)_2N)RuCl$ (Figure 1-8, **C**) is stabilized by adopting a triplet spin state that prevents the formation of agostic interactions with the metal center.[100] Subsequently, Schneider and co-workers reported the synthesis of the closely related square planar complex $(({}^tBu_2PCH_2CH_2)_2N)RuCl$ (Figure 1-8, **D**) that adopts a singlet ground state as a result of increased π-donation from the chelating dialkyl amido ligand, relative to the disilyl amido ligand featured in Caulton's complex.[101] In contrast to these *cis*-divacant octahedral and square planar species, Turculet and co-workers reported the synthesis and structural characterization (X-ray) of unusual, diamagnetic, trigonal pyramidal Ru^{II} complexes of the type (Cy-PSiP)RuX (Scheme 1-18, Cy-PSiP = $[\kappa^3$-(2-$Cy_2PC_6H_4)_2SiMe]^-$, X = amido or alkoxo) that do not require agostic stabilization.[89] Rather, DFT analysis indicates that such (PSiP)RuX species are stabilized by the strongly donating central silyl donor of the PSiP ligand.

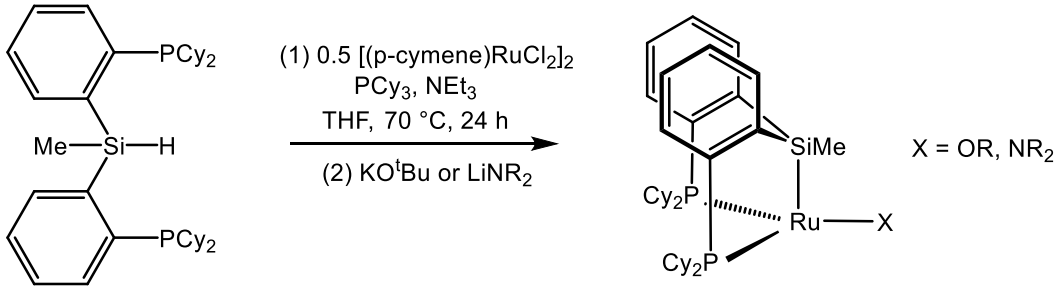

Scheme 1-18. Synthesis of (Cy-PSiP)RuX.

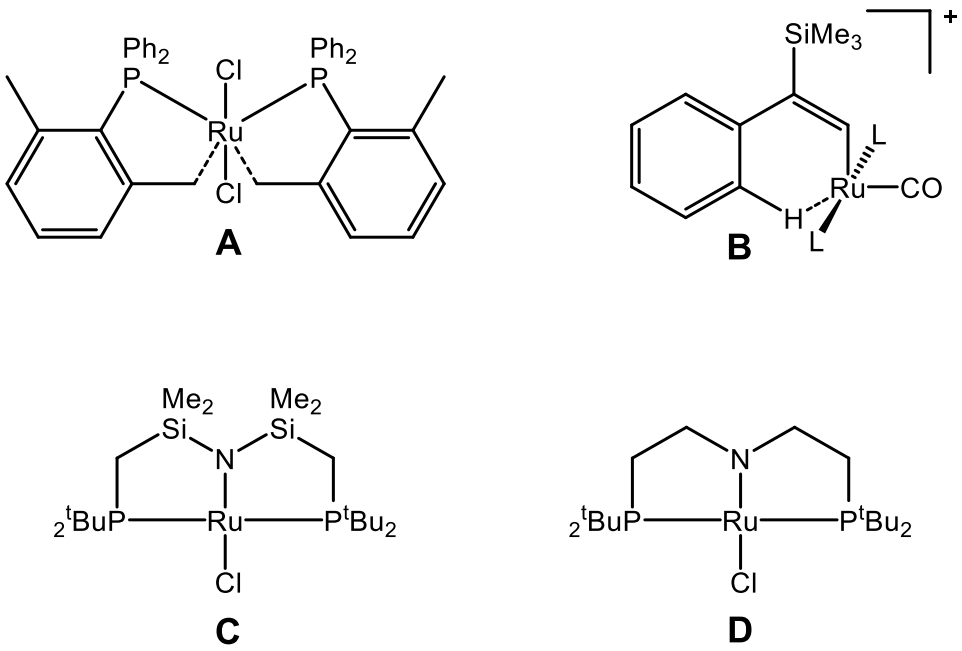

Figure 1-8. Examples of 14-electron Ru complexes.

DFT studies of complexes of the type (PSiP)RuX confirmed the slightly distorted trigonal pyramidal geometry that was observed crystallographically, where the alternative *mer*-κ^3-pincer–Ru^{II} coordination mode is significantly (on the order of 30 kcal mol^{-1}) higher in energy. The triplet spin state, which also favours a *fac*-κ^3-(PSiP)Ru^{II} ligation, was calculated to be higher in energy by more than 24 kcal mol^{-1}. Examination of the HOMO and LUMO for such complexes reveals that these are not particularly well suited to accommodate an agostic interaction at the vacant axial coordination site. Analogues of (PSiP)RuX that have the central silyl donor replaced by either C(sp^3)–Me, phosphido or amido donor groups were also studied computationally, and these studies revealed the following order of descending donating ability (based on NBO charge distribution): PSiP > PPP > PCP > PNP. The strength of C–H agostic interactions in such (PXP)Ru (X = Si; P, C(sp^3)–Me, or N) complexes directly correlates with the degree of electron deficiency

at Ru and hence increases in the following order X = Si < P < C(sp^3)–Me < N. The nature of the central donor group also profoundly influences the gap in stability between *fac*-κ^3- and *mer*-κ^3-(PXP)Ru^{II} forms, as well as the size of the gap between the singlet and triplet spin states, thereby reinforcing the pivotal role of a strongly donating silyl donor for the stabilization of such diamagnetic trigonal pyramidal complexes.

Although four-coordinate (PSiP)RuX (X = amido, alkoxo) species are stabilized by the strongly donating silyl group, they are nonetheless reactive and were shown to undergo multiple E-H (E = main group element) bond activation steps upon treatment with $H_3B{\cdot}NH_3$ to quantitatively form the bis(σ-B-H) complex (PSiP)RuH(η^2:η^2-H_2BNH_2), a rare example of a bis(σ-B-H) aminoborane complex (Scheme 1-19).[89] The mechanism of this reaction was studied computationally and was determined to proceed in a stepwise fashion via intramolecular deprotonation of ammonia and subsequent borane B–H bond oxidative addition. These studies confirm that such four-coordinate, formally 14-electron (R-PSiP)RuX complexes are capable of promoting multiple bond activation steps in a manner that may be synthetically useful in the transformation of main group substrates.

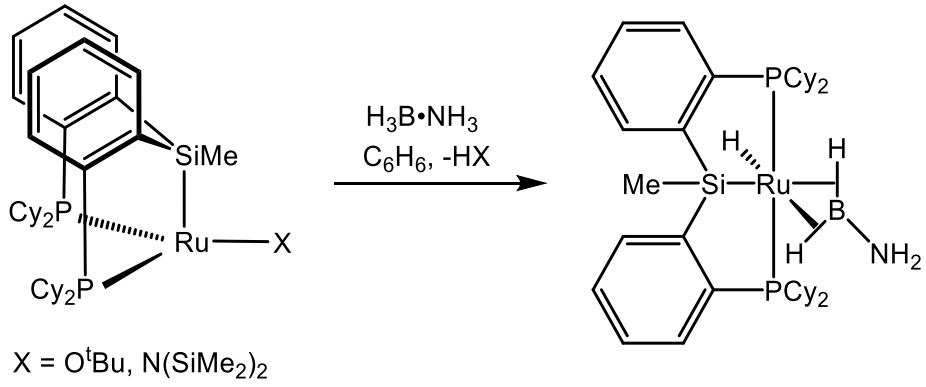

Scheme 1-29. Synthesis of (PSiP)RuH(η^2:η^2-H_2BNH_2).

1.5.2 N-H Bond Oxidative Addition by (PSiP)Ir^{I} Species

Although significant interest exists in developing new atom-efficient catalytic amination reactions that utilize ammonia as a substrate, well-documented examples of N-H bond oxidative addition to a metal center are exceedingly rare.[102-105] Having shown that complexes of the type (Cy-PSiP)Ir(H)Cl are precursors to highly reactive (Cy-PSiP)Ir^{I} species that can undergo arene C-H bond cleavage reactions,[106] research in the Turculet group shifted to the study of N-H bond cleavage involving such unsaturated Ir^{I} intermediates, with the goal of observing N-H bond oxidative addition of simple amines, anilines and ammonia. Prior to this work, only one example of an isolable, monomeric late metal $L_nM(H)(NH_2)$ species obtained from N-H bond oxidative addition of ammonia had been reported by Zhao, Goldman, and Hartwig, who used a (PCP)Ir pincer complex to achieve ammonia activation.[104]

Complexes of the type (Cy-PSiP)Ir(H)(NHR) (R = aryl, H) were prepared by the direct reaction of (Cy-PSiP)Ir(H)Cl with the appropriate LiNHR reagent. Such amido species proved readily isolable and did not undergo N-H reductive elimination upon heating or upon reaction with PMe_3. In contrast, related (PCP)Ir(H)(NHR) complexes undergo facile N-H reductive elimination, which can at times preclude their isolation.[103] X-ray crystallographic analysis of (Cy-PSiP)Ir(H)[NH(2,6-$Me_2C_6H_3$)] revealed distorted square-based pyramidal geometry at the metal center, with Si occupying the apical coordination site. This structure differs from that of the related complex [C_6H_3-2,6-($CH_2P^tBu_2$)$_2$]Ir(H)(NHPh), which features square pyramidal coordination geometry with the hydride occupying the apical position and, thus, oriented *cis* to the anilide ligand. This structural difference is likely a result of the strong *trans*-directing ability of the silyl

donor. Having determined that (Cy-PSiP)Ir(H)(NHR) (R = aryl, H) complexes are isolable species, N-H bond activation studies showed that treatment of (Cy-PSiP)Ir[I] (generated *in situ* in cyclohexane solution from (Cy-PSiP)Ir(H)Cl and $LiCH_2CMe_3$) with the corresponding H_2NR reagent led to the synthesis of (Cy-PSiP)Ir(H)(NHR) species via an N-H bond oxidative addition route (Scheme 1-20). This reactivity represents a rare example of N-H bond oxidative addition of ammonia, and provides some insight into the possible development of new atom-economical chemical transformations that incorporate N-H bond oxidative addition steps.

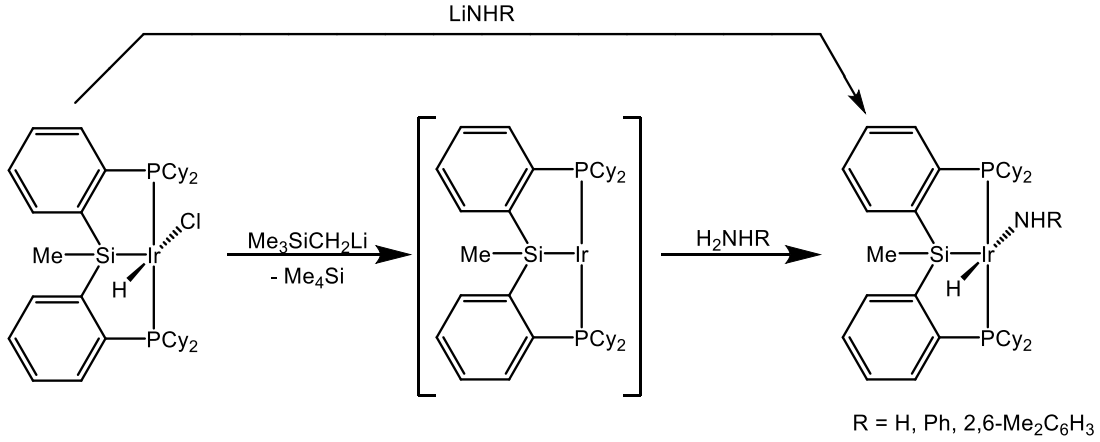

Scheme 1-20. Synthesis of (Cy-PSiP)Ir(H)(NHR) species via N-H bond oxidative addition.

1.5.3 Si-C Bond Cleavage Involving (PSiP)Ni and (PSiP)Pd Species

Although Si-C(sp^2) bond activation is well-documented,[95] examples of unstrained Si-C(sp^3) bond cleavage are extremely rare,[88] as Si-C bonds are quite strong (Si-C bond dissociation energy for $H_3Si\text{-}CH_3$ = 89.6 kcal mol^{-1} and C-C bond dissociation energy for $H_3C\text{-}CH_3$ = 90.1 kcal mol^{-1}).[107,108] In the pursuit of new (Cy-PSiP)M(alkyl) (M = Ni, Pd) complexes, Turculet and coworkers discovered an unusual ligand rearrangement that

involves remarkably facile Si-C(sp^3) and Si-C(sp^2) bond-cleavage processes.[88] Notably, for (Cy-PSiP)Ni species, these Si-C bond-activation processes are reversible on the NMR timescale.

The alkylation of (Cy-PSiP)PdCl (Scheme 1-21, **A**) with MeLi led to the formation of the corresponding Pd-Me complex (Scheme 1-21, **B**), which can be isolated in good yield. Howver, over time the Pd-Me complex was observed to undergo a rearrangement involving net transfer of the Pd-*Me* group to Si and cleavage of a Si-C(sp^2) bond in the pincer ligand backbone to yield a four-membered Pd-C-C-P metallacycle (Scheme 1-21, **C**). A possible mechanism for this rearrangement could involve the intermediacy of a bis-phosphine Pd^0 species (not directly observed and likely stabilized by solvent coordination or an agostic interaction), that undergoes Si-C(sp^2) oxidative addition (Scheme 1-21, **D**).

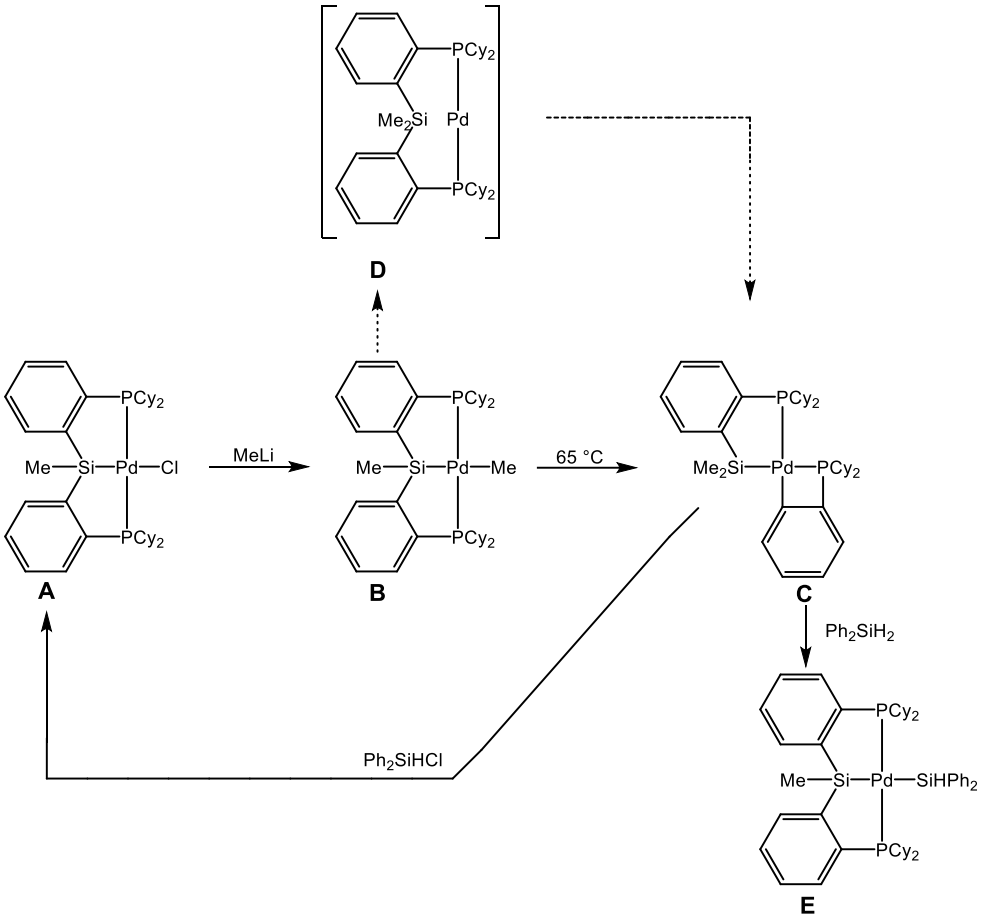

Scheme 1-21. Cleavage of a Si-C(sp^2) bond to form a four-membered metallacycle.

Remarkably, the Si-C(sp^2) bond cleavage process is reversible, as indicated by the reaction of the rearranged complex with either Ph_2SiH_2 or Ph_2SiHCl, which reformed the Cy-PSiP ligand and afforded the terminal Pd silyl and chloride complexes, respectively (Scheme 1-21). These reactions require cleavage of a Si-C(sp^3) linkage within the rearranged species in order to reform the Cy-PSiP framework. It is plausible that Si-C(sp^2) reductive elimination in the rearranged complex regenerates the bis-phosphine Pd^0 species, which undergoes subsequent Si-C(sp^3) bond cleavage to reform (Cy-PSiP)PdMe. The terminal Pd-Me species can then react with added silanes to ultimately provide the observed Pd silyl and chloride products.

Attempts to access (Cy-PSiP)NiMe led to the generation of an equilibrium mixture comprised of the terminal Ni-Me complex and the complex resulting from Si-C(sp^2) bond cleavage in the ligand backbone (Scheme 1-22), which were observed in a ca. 1:2 ratio.[88] Notably, ^{31}P-^{31}P EXSY NMR spectra of the product mixture revealed chemical exchange between the magnetically non-equivalent phosphorus environments in the rearranged species (in keeping with reversible Si-C(sp^2) bond cleavage), as well as cross-peaks indicative of exchange involving (Cy-PSiP)NiMe and the rearranged complex (in keeping with reversible Si-C(sp^3) bond cleavage). Under similar conditions, no chemical exchange involving the analogous Pd species was observed. The interconversion of the Ni-Me complex and its isomer was further confirmed by ^{1}H-^{1}H EXSY NMR experiments, which revealed chemical exchange between the Si*Me* and Ni*Me* environments in the two compounds. Thus, remarkably, in the case of Ni these Si-C bond activation processes are reversible on the NMR timescale in solution.

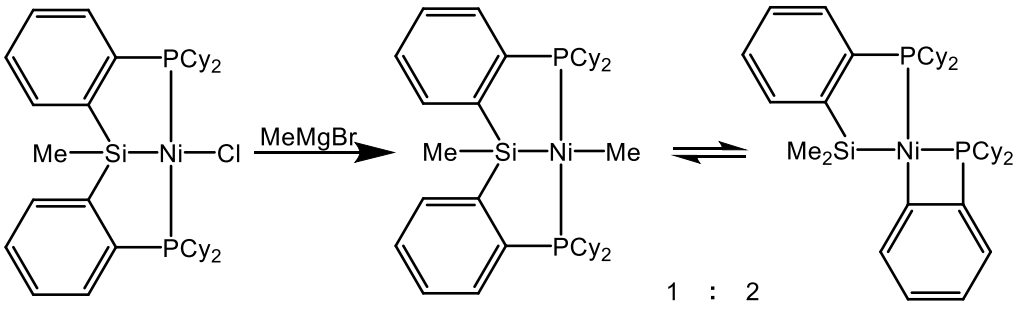

Scheme 1-22. Equilibrium mixture of (Cy-PSiP)NiMe and the complex resulting from Si-C(sp^2) cleavage.

1.5.4 Reduction of CO_2 with Tertiary Silanes Catalyzed by (PSiP)Pt Species

As described previously (*vide supra*), CO_2 is a significant contributor to global warming, and thus the current high level of CO_2 in the atmosphere is of great concern.[66] In this regard, there is significant interest in the development of efficient methodologies for the conversion of CO_2 into a hydrocarbon fuel, with the ultimate goal of achieving a carbon-neutral catalytic process.[66] As such, the pursuit of homogeneous catalysts for the conversion of CO_2 to methanol and/or methane is an area of growing interest.[65,66]

In an effort to address the issue of catalytic reduction of CO_2, Turculet and co-workers demonstrated that Pt and Pd complexes of the type [Cy-P*Si*(μ-H)P]*M* (**A**, Scheme 1-23; M = Pd, Pt) that feature a η^2-SiH coordination involving the tethered silicon fragment are effective precatalysts for the conversion of CO_2 to methane with a tertiary silane as the reductant.[11] At the time of publication, only two transition metal catalysts for the reduction of CO_2 to methane using hydrosilanes had been reported,[109,110] and no examples of formatoborate metal complexes had been described in the literature. The reduction involves the formation of zwitterionic Pd and Pt hydride complexes of the type (Cy-PSiP)*M*(μ-H)*B*(C_6F_5)$_3$ (**B**, Scheme 1-23) upon the reaction of [Cy-P*Si*(μ-H)P]*M* with the strong Lewis acid B(C_6F_5)$_3$. Such zwitterionic species are proposed to be the catalytically active species in the reduction of CO_2 to the bis(silyl)acetal $CH_2(OSiR_3)_2$, which occurs via the formation of formatoborate intermediates (**C**, Scheme 1-23). The bis(silyl)acetal is subsequently reduced down to methane and the corresponding bis (silyl)ether by B(C_6F_5)$_3$ mediated hydrosilylation.[11,109,110] Support for this proposal is

drawn from the observation that upon replacement of $B(C_6F_5)_3$ with the less Lewis acidic borane BPh_3 only the formation of the bis(silyl)acteal $CH_2(OSiR_3)_2$ was observed.

Using (Cy-PSiP)*Pt*(μ-H)*B*$(C_6F_5)_3$ (0.065 mol % relative to silane) as the catalyst with 1 atm of CO_2 and Me_2PhSiH (fluorobenzene solvent, 65 °C) afforded 1063 turnovers after 4 h, while (Cy-PSiP)*Pd*(μ-H)*B*$(C_6F_5)_3$ at the same loading resulted in 469 turnovers with heating at 85 °C. The bulkier silane Et_3SiH led to significantly decreased activity (22 turnovers with 0.065 mol % Pt catalyst, 1 atm CO_2, 65 °C, 4 h). Control experiments carried out in the absence of CO_2 confirmed that the observed silyl ether formation cannot be attributed to side reactions involving adventitious water or O_2.

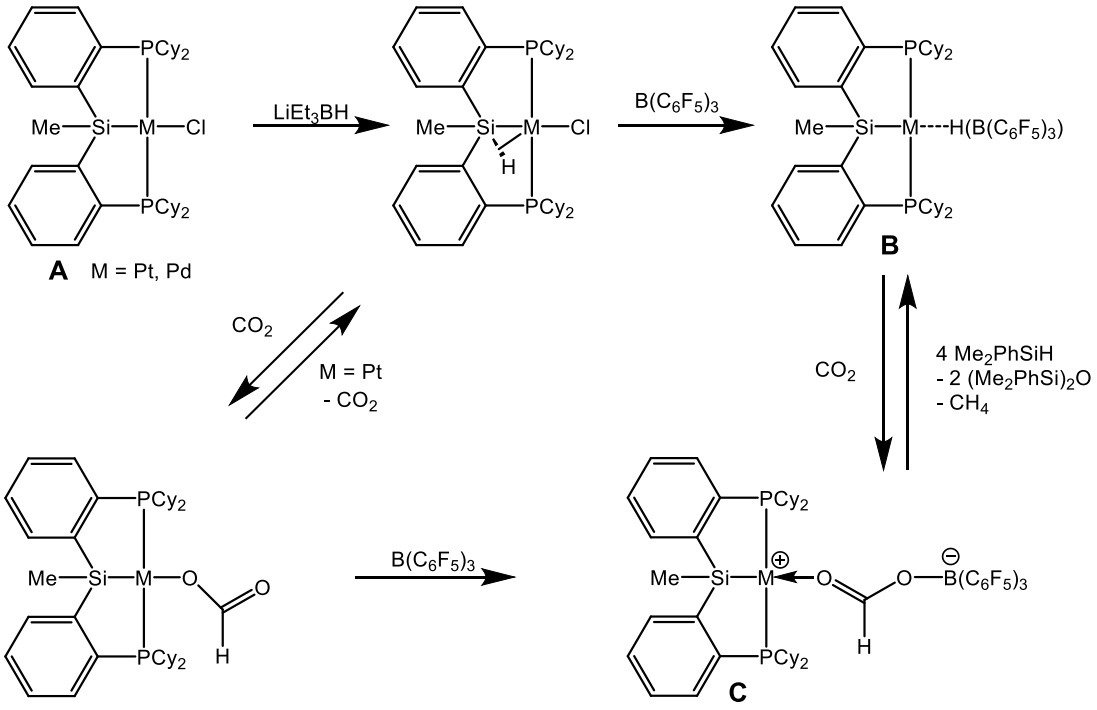

Scheme 1-23. Reduction of CO_2 with tertiary silanes catalyzed by a (CyPSiP)Pt species.

1.5.5 Synthesis of Platinum Group Metal PSiN Complexes

As highlighted above (*vide supra*), transition metal complexes featuring mixed donor pincer ligation have demonstrated the ability to perform a number of remarkable

catalytic reactions. Having observed a variety of new and interesting reactivity with PSiP-ligated transition metal complexes, the Turculet group sought to develop potentially hemilabile PSiN mixed donor species, with the goal of accessing increasingly reactive metal complexes.[111,112] At the outset, it was considered that the reversible coordination of the amine pincer arm may render PSiN-ligated complexes more responsive to the changing electronic and coordinative requirements at a metal center that arise during substrate transformations, thereby providing access to new and/or enhanced reactivity.

Tertiary (phosphinoamino)silanes that could function as pro-ligands for the synthesis of (phosphinoamino)silyl pincer complexes were accessed in a stepwise fashion by preparing the phosphino and amino ligand arms separately (Scheme 1-24).[111,112] Following Si-H oxidative addition and deprotonation, square planar complexes of the type (κ^3-^{t}Bu-PSiN-Me)MX (M = Pt, X = Cl; M = Pd, X = Br; ^{t}Bu-PSiN-Me = (2-^{t}Bu$_2$PC$_6$H$_4$)(2-Me$_2$NC$_6$H$_4$)SiMe$^-$) were readily isolated. Such complexes engaged in dynamic processes in solution involving decomplexation of the amine arm and inversion and rotation at N, which rendered the N*Me* groups equivalent at elevated temperatures. The amino PSiN ligand arm could also be displaced from the metal coordination sphere in these square planar comlexes, as well as the five-coordinate Rh complex (^{t}Bu-PSiN-Me)Rh(H)Cl, by the introduction of a more strongly coordinating donor ligand such as PMe$_3$. In the case of (κ^2-^{t}Bu-*PSi*N-Me)Pd(Br)(PMe$_3$), treatment with BPh$_3$ as a PMe$_3$ scavenger led to the quantitative regeneration of (κ^3-^{t}Bu-PSiN-Me)PdBr, which further highlights the hemilabile character of PSiN ligation.

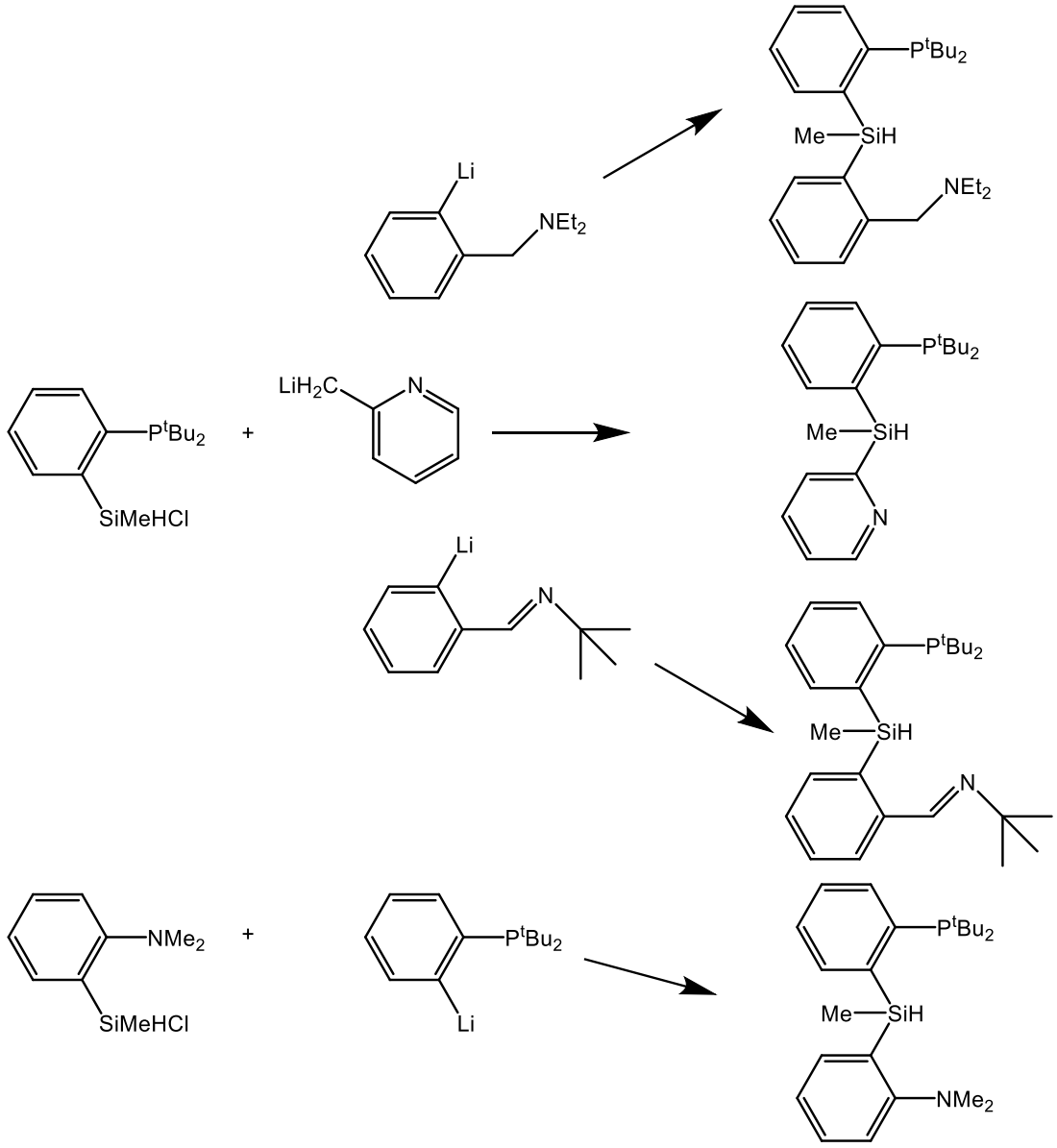

Scheme 1-24. Synthesis of mixed donor PSiN ligands.

Although square planar Group 10 halide species and five-coordinate complexes of the type (κ^3-PSiN)M(H)Cl proved isolable in many cases, typically such late metal complexes proved to be largely unstable both in solution and in the solid state and attempts to further pursue the chemistry of such complexes were limited by their reactive nature.[113] It can be concluded that the relatively poor ligating ability of the amino donor

arm in PSiN ligands resulted in a high degree of instability in the ensuing metal complexes relative to the related PSiP variants.

1.5.6 New Directions in Silyl Pincer Design: Towards Mixed Donor PSiP' Complexes

The goal of the research presented in this thesis is to extend the methodology developed for the preparation of mixed donor silyl pincer species to the synthesis of "unsymmetrical" PSiP' variants that feature two different phosphino donor arms (Figure 1-9). Having observed that mixed donor PSiN ligation led to relatively unstable transition metal complexes that often resisted isolation attempts, it is anticipated that replacing the amino donor with a phosphino group would lead to relatively more stable complexes. The "unsymmetrical" nature of PSiP' ligation would provide an added level of tunability to the pincer framework, such that the steric and electronic features of the ensuing complexes could be adjusted to access increasingly reactive species. The synthesis of such PSiP' ligands as well as their coordination chemistry with platinum group metals is described herein.

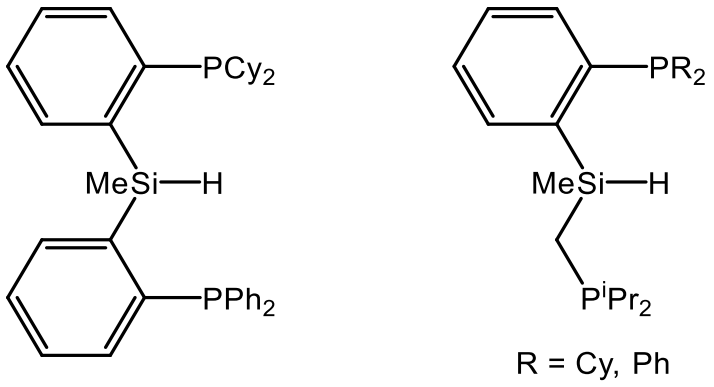

Figure 1-9. Unsymmetrical PSiP' ligands.

Chapter 2: Group 10 Metal Complexes Supported by Mixed Donor PSiP' Silyl Pincer Ligation

2.1 Introduction

Previous work in the Turculet group has focused on the chemistry of late transition metal complexes supported by PSiP silyl pincer ligands of the type [(2-$R_2PC_6H_4)_2SiMe]^-$ (R = aryl, alkyl). As highlighted in Chapter 1 of this document, such complexes have proven adept at a number of challenging stoichiometric and catalytic reactions, including N-H bond oxidative addition in amines,[11] Si-C(sp^3) bond cleavage,[88] and reduction of CO_2 to methane.[11] In an effort to better control this reactivity and potentially access increasingly reactive silyl pincer complexes for applications in bond activation and catalysis, mixed donor silyl pincer ligation is targeted in this work. Although numerous breakthroughs have been made in the area of mixed donor PCN and PNN pincers (see Chapter 1),[16] previous attempts in the Turculet group to develop PSiN pincer species resulted in metal complexes that were relatively unstable and difficult to isolate.[111,140] In light of these developments, the work detailed in this thesis targeted the synthesis of bis(phosphino) PSiP' mixed donor pincer species that feature two different types of phosphino donors. Such "unsymmetrical" silyl pincer ligands offer an added degree of tunability to the pincer framework, yet are anticipated to lead to more readily isolable metal complexes relative to the PSiN analogues.

Related examples of "unsymmetrical" PNP' pincer ligation were initially reported by Liang and co-workers, who prepared Ni and Al complexes supported by such ligands (Scheme 2-1, **A**).[116,117] Interestingly, the reactivity of the unsymmetrically substituted nickel hydride complex (Ph-PNP'-^{i}Pr)NiH (Ph-PNP'-^{i}Pr = (*o*-$Ph_2PC_6H_4$)(*o*-

$^{i}Pr_2PC_6H_4)N^-$) with respect to olefin insertion is inferior to that of the symmetrically substituted analogue (Ph-PNP)NiH (Ph-PNP = (o-$Ph_2PC_6H_4)_2N^-$) but superior to that of (^{i}Pr-PNP)NiH,[116] which highlights the level of control over reactivity that is afforded by such relatively minor changes in the donor properties of the pincer ligand. Subsequently, Goldberg, Kemp and co-workers reported on the coordination chemistry of related PNP' ligands with Group 10 metals.[118] As well, Ozerov and co-workers evaluated the electronic properties of a series of analogous PNP' pincer ligands and their Ni, Pd, Pt, and Rh complexes.[119] Group 10 (PNP')MCl (M = Ni, Pd, Pt) complexes were evaluated on the basis of redox potentials and (PNP')Rh(CO) complexes were evaluated based on their corresponding ν(CO) values. Ultimately the authors concluded that the judicious choice of the donor atoms and the nature of their substituents as well as modifications to the diarylamido ligand backbone allows for some control of the degree to which the redox activity of the ligand and the electronic effect of the ligand on a metal center are influenced. Finally, Morris and co-workers have recently reported on the synthesis of Fe complexes of unsymmetrical PNP' pincer ligands and their high activity and selectivity in catalytic asymmetric hydrogenation of ketones and imines (Scheme 2-1, **B**).[120]

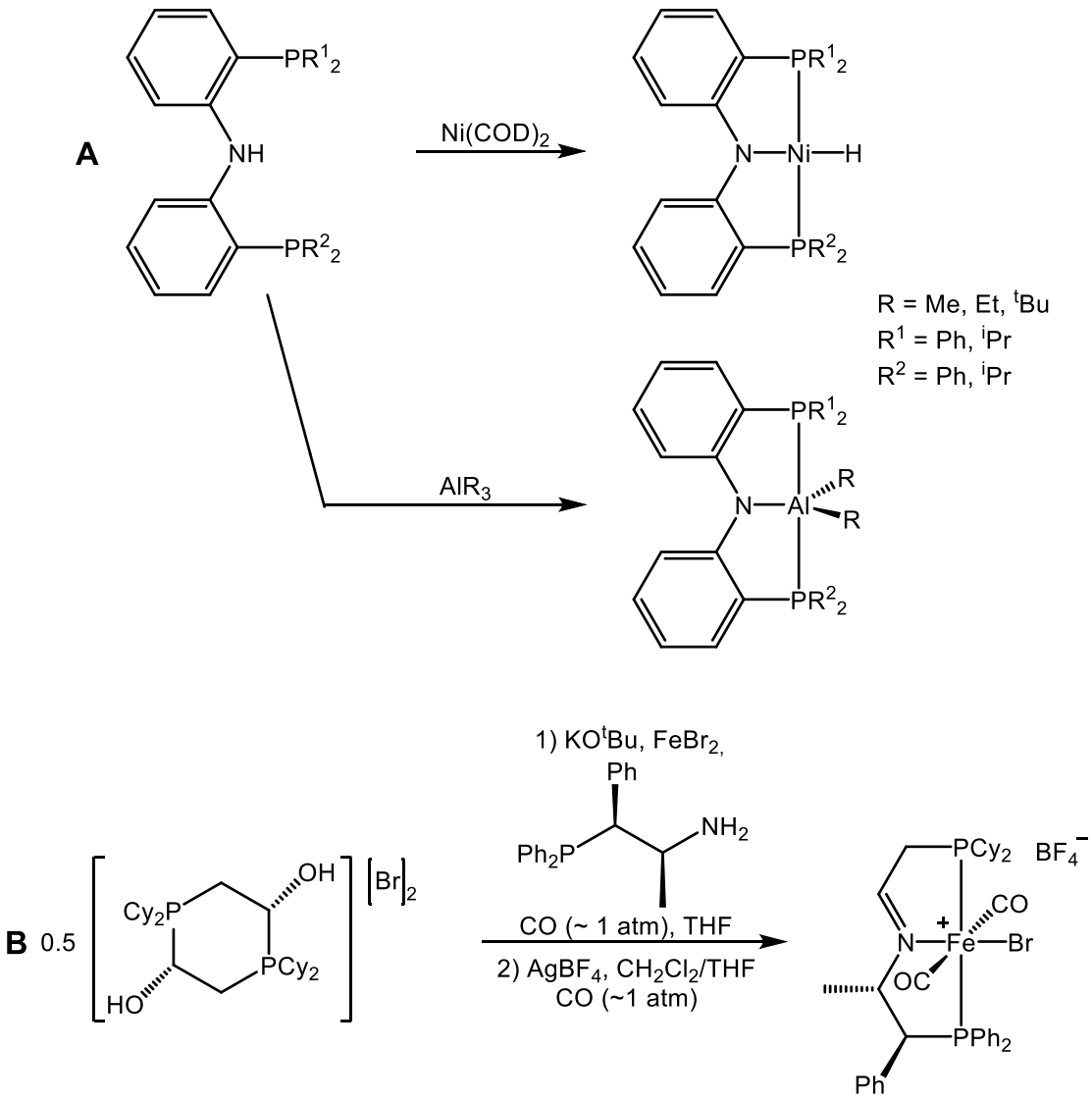

Scheme 2-1. Synthesis of pincer complexes supported by unsymmetrical PNP' pincer ligands.

Although there is not a wide body of literature on the synthesis of "unsymmetrical" PXP' pincer species, this area of investigation appears to be attracting increasing attention in recent years, as evidenced by the reports on PNP' ligation cited above. Where the synthesis of such species is feasible, the mixed phosphorus donor approach appears to confer added control over the steric and electronic features of metal pincer complexes, which can result in more active and more selective metal catalysts. In

this regard, this chapter details the synthesis of a series of PSiP' ligands and their coordination chemistry with Group 10 metals.

2.2 Results and Discussion

2.2.1 Ligand synthesis

Tertiary bis(phosphino)silanes are effective as pro-ligands for the synthesis of PSiP silyl pincer complexes, as oxidative addition of the Si-H bond to late metal centers occurs readily to form the targeted pincer complexes.[68] In an effort to prepare "unsymmetrical" tertiary bis(phosphino)silanes that feature two different types of phosphino donors, the synthetic strategy employed for the synthesis of related mixed donor (PSiN)H ligands was utilized (Scheme 2-2).[111,112] It was found that (phosphinoaryl)chlorosilane species (**2-1** and **2-2**) could be readily prepared by lithiation of the corresponding 2-bromoaryl phosphine with one equiv. of ^{n}BuLi in cold (-78 °C) hexanes, followed by treatment with one equiv. of $MeHSiCl_2$. Subsequent treatment of such (phosphinoaryl)chlorosilanes with a litihium salt of choice, be it $^{i}Pr_2PCH_2Li$ or *o*-$Ph_2PC_6H_4Li$, led to the synthesis of the desired "unsymmetrical" tertiary bis(phosphino)silanes **2-3** - **2-5** (**2-3** = (Cy-PSiP'-Ph)H, **2-4** = (Ph-PSiP*-^{i}Pr)H, **2-5** = (Cy-PSiP*-^{i}Pr)H, which were isolated in high yields. As expected, all three compounds feature two $^{31}P\{^{1}H\}$ NMR resonances (for **2-3**: -7.6, -11.1 ppm; for **2-4**: -2.6, -9.6 ppm; for **2-5**: -1.4, -7.1 ppm). The ^{1}H NMR spectra (benzene-d_6) of the tertiary silanes also feature a resonance attributable to the Si-*H* proton at 6.09, 5.11, and 5.18 ppm, respectively, for **2-3**, **2-4**, and **2-5**. In turn, the ^{29}Si NMR spectra of the three pro-ligands

feature a single resonance that exhibits one-bond Si-H coupling: -23.0 ppm, $^{1}J_{SiH}$ = 40 Hz for **2-3**, -16.6 ppm, $^{1}J_{SiH}$ = 38 Hz for **2-4**, -14.3 ppm, $^{1}J_{SiH}$ = 39 Hz for **2-5**.

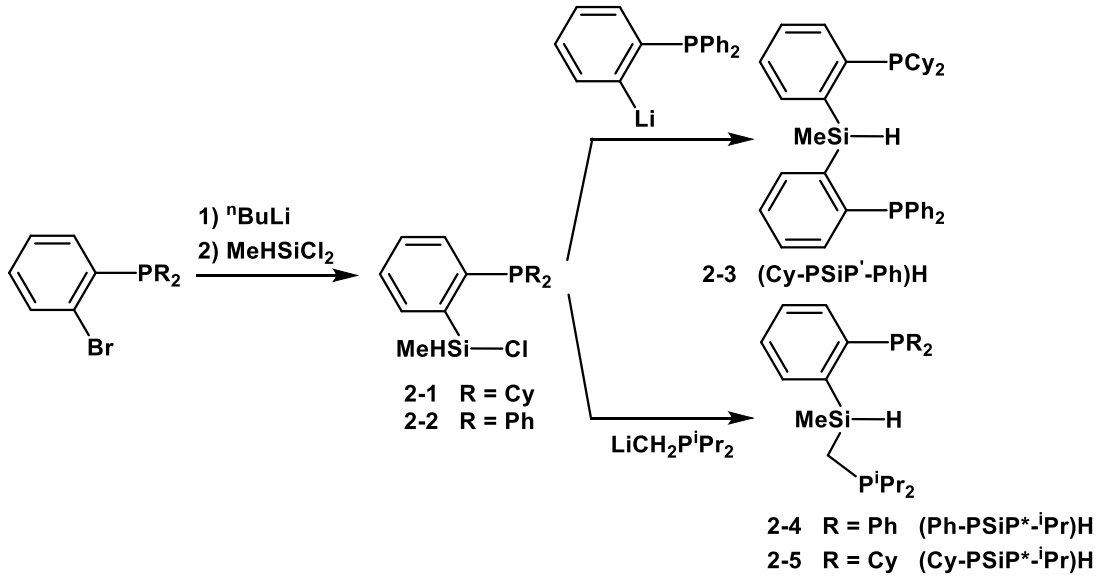

Scheme 2-2. Synthesis of (PSiP')H ligands.

2.2.2 Synthesis and characterization of (Cy-PSiP'-Ph)MCl (M = Ni, Pd, Pt) complexes

A logical starting point for access to Group 10 metal silyl pincer chemistry is the synthesis of M^{II} chloride species of the type (PSiP')MCl (M = Ni, Pd, Pt) as they can be used as precursors to various complexes such as alkyl and hydride species. In this regard, the synthesis of Group 10 metal complexes of the type (Cy-PSiP'-Ph)MCl was targeted initially (Scheme 2-3).

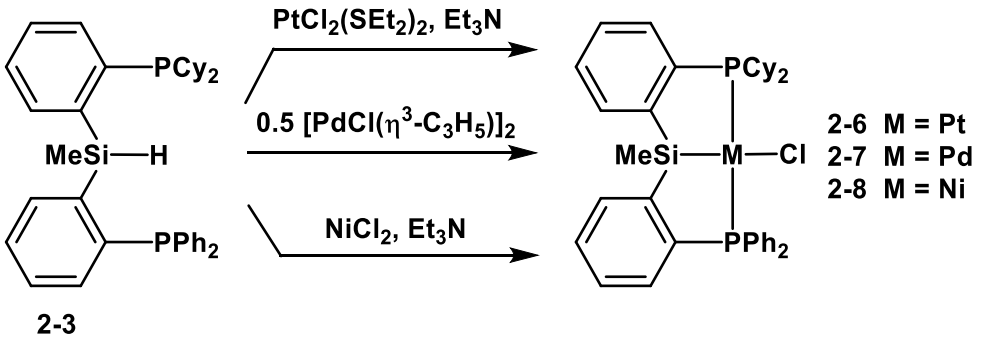

Scheme 2-3. Synthesis of group 10 metal complexes supported by Cy-PsiP'-Ph.

The treatment of $PtCl_2(Et_2S)_2$ with one equiv. of the tertiary silane **2-3** in the presence of one equiv. of Et_3N resulted in the formation of (Cy-PSiP'-Ph)PtCl (**2-6**) upon mixing at room temperature (Scheme 2-3). Complex **2-6** was isolated in 89% yield as a pale yellow solid. The solution $^{31}P\{^1H\}$ NMR spectroscopic data for **2-6** (benzene-d_6) are consistent with the formation of a new Pt complex (Table 2-1). However upon close examination the spectrum appears to be second order. Iterative simulation of the experimentally obtained $^{31}P\{^1H\}$ NMR spectrum of **2-6** revealed an AB spin system ($^2J_{PP}$ = -373 Hz) with ^{195}Pt satellites ($^1J_{PPt}$ = 3090 and 2945 Hz), with the chemical shifts of the phosphorous nuclei determined to be 62.8 and 51.2 ppm, respectively (Figure 2-1). These data support the assignment of **2-6** as a C_1-symmetric square-planar complex of Cy-PSiP'-Ph, with both phosphino donors bound to the Pt center in a *trans* fashion. The ^{29}Si NMR spectrum of **2-6** features a resonance at 35.0 ppm, which is consistent with a metal silyl species, thereby confirming κ^3-coordination of Cy-PSiP'-Ph to the metal center (Table 2-1). Complex **2-6** exhibited high thermal stability in benzene solution, as no reaction was observed upon heating a benzene solution of **2-6** and Et_3N at 90 – 100 °C over the course of several days.

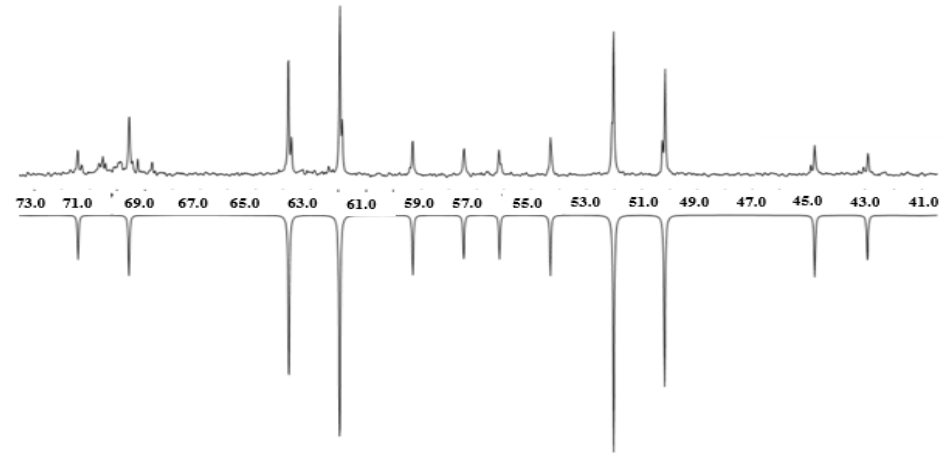

Figure 2-1. Experimental (top; benzene-d_6) and simulated (inverted) $^{31}P\{^1H\}$ NMR spectrum of **2-6** (202.46 MHz).

In an effort to prepare a Pd analogue of **2-6**, a benzene solution of **2-3** was treated with 0.5 equiv. of $[PdCl(\eta^3\text{-}C_3H_5)]_2$. Monitoring of the reaction progress by use of $^{31}P\{^1H\}$ NMR spectroscopy indicated quantitative conversion to the desired (Cy-PSiP'-Ph]PdCl (**2-7**) upon mixing at room temperature (Scheme 2-3). Complex **2-7** was isolated as a yellow solid in 90% yield. Solution NMR spectroscopic data for **2-7** (benzene-d_6; Table 2-1) are consistent with a C_1-symmetric structure where both phosphino donors are bound to the Pd center, as evidenced by the presence of two doublets in the $^{31}P\{^1H\}$ NMR spectrum at 63.1 and 42.4 ppm ($^2J_{PP}$ = 348 Hz) that arise from the two inequivalent phosphorous donors. The observation of a relatively large $^2J_{PP}$ coupling constant for **2-7** is consistent with *trans*-disposed phosphino donors, as would be anticipated for a square planar (Cy-PSiP'-Ph)Pd^{II} pincer complex. The ^{29}Si NMR spectrum of **2-7** features a resonance at 57.0 ppm, which is consistent with a Pd silyl species and confirms κ^3-coordination of the silyl pincer ligand.

The Ni derivative (Cy-PSiP'-Ph)NiCl (**2-8**) was also readily prepared by the reaction of **2-3** with $NiCl_2$ in the presence of one equiv. of Et_3N. Heating of the reaction mixture at 65 °C in benzene solution for 24 h afforded **2-8** as an orange solid in 90% yield following workup. As in the case of **2-7**, solution NMR spectroscopic data for **2-8** (benzene-d_6; Table 2-1) are consistent with a C_1-symmetric structure where both phosphino donors are bound to the Ni center, as indicated by the presence of two doublets in the $^{31}P\{^1H\}$ NMR spectrum at 60.4 and 41.6 ppm ($^2J_{PP}$ = 261 Hz) corresponding to the two inequivalent phosphorous nuclei. The observed $^2J_{PP}$ coupling constant for **2-8** is also evidence for a square planar (Cy-PSiP'-Ph)Ni^{II} pincer species with *trans*-disposed phosphino donors. The ^{29}Si NMR spectrum of **2-8** features a resonance at 58.7 ppm, which is consistent with a Ni silyl species and confirms κ^3-coordination of the pincer ligand.

Compound	$^{31}P\{^1H\}$ NMR	^{29}Si NMR
2-3	-7.6, -11.1	-23.0
2-6	62.8, 51.2 ($^2J_{PP}$ = -373 Hz)	35.0
2-7	63.1, 42.4 ($^2J_{PP}$ = 348 Hz)	57.0
2-8	60.4, 41.6 ($^2J_{PP}$ = 261 Hz)	58.7
2-9	62.7, 51.3 ($^2J_{PP}$ = -373 Hz)	37.7
2-10	65.3, 43.2 ($^2J_{PP}$ = 360 Hz)	NA
2-11	66.0, 54.5 ($^2J_{PP}$ = 269 Hz)	NA
2-12	65.2, 51.2 ($^2J_{PP}$ = 359 Hz)	NA
2-13	62.6, 51.6 ($^2J_{PP}$ = 248 Hz)	68.2

Table 2-1. Selected NMR spectroscopic data (ppm) for compounds **2-3** and **2-6** – **2-13** (benzene-d_6); ^1H-^{29}Si HMBC.

The solid state structures of **2-7** and **2-8** were determined using single crystal X-ray diffraction techniques (Figure 2-2; Table 2-2). Both complexes exhibit the anticipated distorted square planar coordination geometry in the solid state, with κ^3-coordination of

the Cy-PSiP'-Ph ligand and chloride bound in the remaining coordination site *trans* to Si. The structure of **2-8** is comparable to that of (Cy-PSiP)NiCl, which also exhibits distorted square planar coordination geometry at the Ni center.[88]

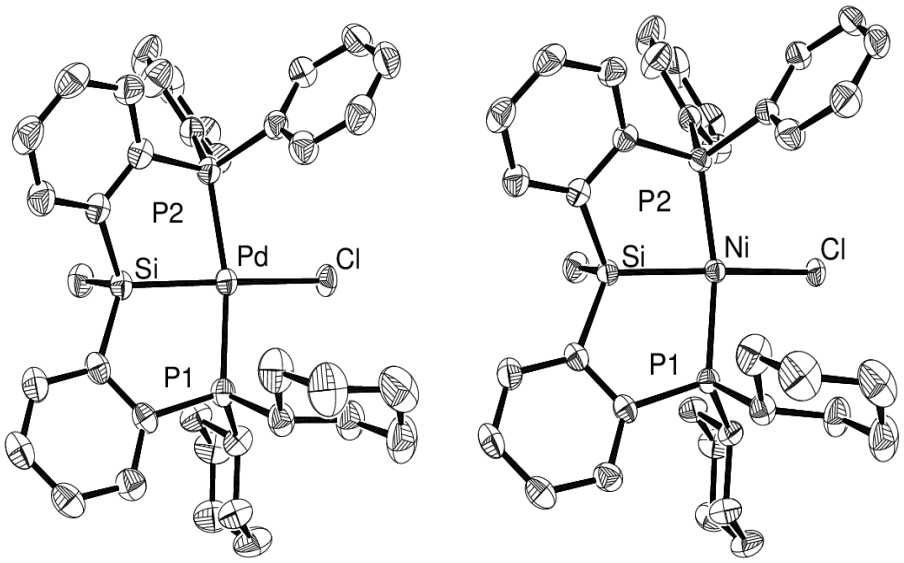

Figure 2-2. The crystallographically determined structure of **2-7** (left) and **2-8** (right), shown with 50% displacement ellipsoids. All H atoms have been omitted for clarity.

Bond Lengths (Å)			
2-7		**2-8**	
Pd-P1	2.2897(8)	Ni-P1	2.1777(5)
Pd-P2	2.2932(8)	Ni-P2	2.1780(5)
Pd-Si	2.2731(8)	Ni-Si	2.2144(6)
Pd-Cl	2.4409(6)	Ni-Cl	2.2544(5)
Bond Angles (°)			
2-7		**2-8**	
P1-Pd-P2	158.42(3)	P1-Ni-P2	158.12(2)
Si-Pd-Cl	164.69(3)	Si-Ni-Cl	162.86(2)

Table 2-2. Selected interatomic distances (Å) and angles (°) for **2-7** and **2-8.**

2.2.3 Synthesis and reactivity of (Cy-PSiP'-Ph)MR (M = Ni, Pd, Pt; R = alkyl or aryl) complexes

The synthesis of alkyl platinum derivatives of the chloride complexes **2-6** - **2-8** was pursued as the resulting M^{II} complexes were anticipated to be good candidates for the study of E-H (E = main group element, e.g. C, N, Si, B) bond activation chemistry. Thus, treatment of **2-6** - **2-8** with one equiv. of MeMgBr (3.0 M in THF) in benzene solution led to formation of the corresponding methyl complexes (Cy-PSiP'-Ph)MMe (M = Pt, **2-9**; M = Pd, **2-10**; M = Ni, **2-11**), which were isolated in 83 - 91% yield (Scheme 2-4). As in the case of **2-6**, the ^{1}H NMR spectroscopic data (benzene-d_6) for **2-9** proved somewhat challenging to interpret, as the alkyl region of the spectrum is obscured by overlapping resonances due to the P*Cy* substituents. The Pt*Me* resonance can be identified in the ^{1}H spectrum of **2-9** as a peak at 0.54 ppm by the presence of platinum satellites ($^{2}J_{HPt}$). The solution ^{31}P{^{1}H} NMR data for **2-10** and **2-11** are consistent with C_1-symmetric square-planar structures with chemically inequivalent phosphino donors bound to the metal center in a *trans* fashion, as indicated by the presence of two doublets at 65.3 and 43.2 ppm for **2-10** ($^{2}J_{PP}$ = 360 Hz), and 66.04 and 54.51 ppm for **2-11** ($^{2}J_{PP}$ = 268 Hz). Upon close examination, the ^{31}P{^{1}H} NMR spectrum of **2-9** is more complicated than a simple first order spectrum. Iterative simulation of the experimentally obtained ^{31}P{^{1}H} NMR spectrum of **2-9** revealed an AB spin system ($^{2}J_{PP}$ = -373 Hz) with ^{195}Pt satellites ($^{1}J_{PPt}$ = 3076 and 2921 Hz), with the chemical shifts of the phosphorous nuclei determined to be 62.7 and 51.3 ppm, respectively (Figure 2-3). These data are consistent with a C_1 symmetric square-planar (Cy-PSiP'-Ph)Pt complex that

features *trans*-disposed, chemically inequivalent phosphino donors. Complex **2-9** also gave rise to a ^{29}Si NMR resonance at 37.7 ppm that is shifted relative to the starting (Cy-PSiP'-Ph)MCl complex indicating that the chloride ligand has been exchanged for a methyl group (Table 2-1).

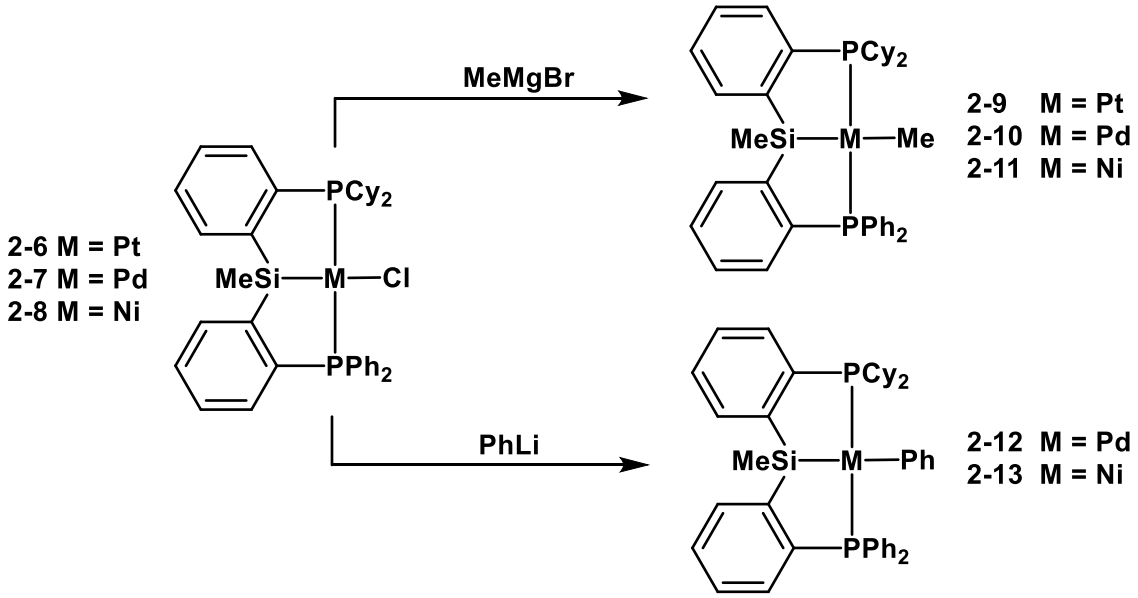

Scheme 2-4. Synthesis of (Cy-PSiP'-Ph)M(alkyl) (M = Pt, Pd, Ni) complexes.

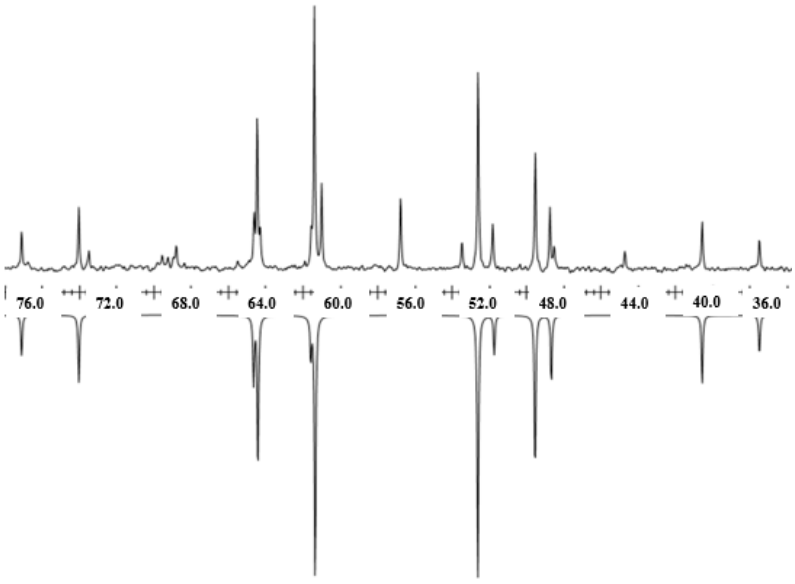

Figure 2-3. Experimental (top; benzene-d_6) and simulated (inverted) ^{31}P{^{1}H} NMR spectrum of **2-9** (202.46 MHz).

While attempts to prepare a Pt phenyl complex of the type (Cy-PSiP'-Ph)PtPh by treatment of **2-6** with PhLi were not successful, the corresponding Pd (**2-12**) and Ni (**2-13**) complexes proved isolable (Scheme 2-4). As in the case of the analogous methyl complexes **2-10** and **2-11**, the solution $^{31}P\{^{1}H\}$ NMR spectroscopic data (benzene-d_6; Table 2-1) for **2-12** and **2-13** are consistent with C_1-symmetric square planar complexes, as indicated by the observation of two doublets corresponding to the phosphino donors of the metal-bound Cy-PSiP'-Ph ligand (65.2 and 51.2 ppm, $^{2}J_{PP}$ = 359 Hz for **2-12**; 62.6 and 51.6 ppm, $^{2}J_{PP}$ = 248 Hz for **2-13**). Complexes **2-13** also gave rise to a ^{29}Si NMR resonance at 68.2 ppm that is shifted relative to the starting (Cy-PSiP'-Ph)NiCl complex, which is consistent with exchange of the chloride ligand for a phenyl group.

The relatively facile isolation of Pd and Ni alkyl and aryl complexes supported by Cy-PSiP'-Ph ligation proved surprising in light of previous observations involving related complexes supported by Cy-PSiP ligation. Namely, complexes of the type (Cy-PSiP)MMe (M = Pd, Ni) were previously shown to undergo rearrangement processes involving Si-C(sp^2) bond cleavage in the ligand backbone to form four membered M-C-C-P metallacycles and transfer a methyl group to Si, as shown in Scheme 2-5. While analogous complexes of the type (Ph-PSiP)MMe (M = Pd, Ni; Ph-PSiP = κ3-(2-Ph2*P*C6H4)2*Si*Me−) are unknown, (Ph-PSiP)PdEt is moderately stable in 1,4-dioxane solution where it undergoes β-H elimination to form an η2-(Si-H)Pd0 species.[121] While (Cy-PSiP)PdMe could be isolated as the kinetic product that subsequently underwent facile rearrangement, the analogous terminal nickel methyl complex was not isolable, as

it readily formed an equilibrium mixture containing the rearranged Ni species. This rearrangement was proposed to occur via a M^0 intermediate of the type [(Cy-PSiP)Me]M^0, that formed via a formal Si-Me reductive elimination process (Scheme 2-5).[88, 122] In the case of (Cy-PSiP'-Ph)MR (M = Ni, Pd; R = Me, Ph) no spectroscopic evidence was observed for such a rearrangement process at room temperature. With regards to this rearrangement process occurring at elevated temperatures as was seen with (Cy-PSiP)Pd-Me,[123] no rearrangement or decomposition was observed upon heating **2-10**, **2-11** and **2-13** at 65 °C in benzene solution for one day. Upon heating **2-12** in benzene solution at 65°C for one day the complex decomposed to form multiple unidentified products (^{31}P NMR). Thus, it appears that Cy-PSiP'-Ph ligation offers an electronic balance between the two phosphino donors, allowing for the isolation of the square planar κ^3-PSiP terminal methyl and phenyl complexes.

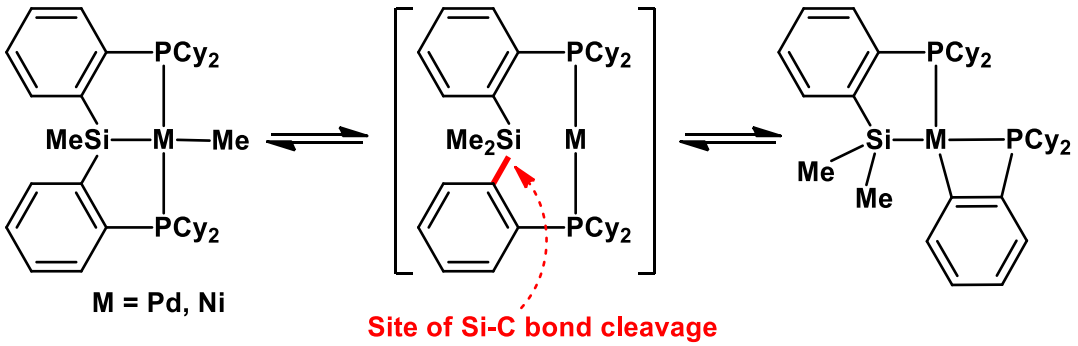

Scheme 2-5. Rearrangement of (Cy-PSiP)MMe (M = Pd, Ni) complexes by Si-C(sp^2) bond cleavage in the pincer ligand backbone.

In an effort to begin to assess the reactivity of such (Cy-PSiP'-Ph)MR (M = Pt, Pd, Ni; R = alkyl or aryl) complexes in E-H bond activation processes, their reactivity with hydrosilanes was probed. In this regard, complex **2-9** was reacted with various silanes including $PhSiH_3$, $^{i}Pr_2SiHCl$, Ph_2SiHCl and Ph_2SiH_2 (1 - 10 equiv., benzene-d_6).

Surprisingly, none of these hydrosilanes seemed to react with **2-9**, even upon heating of the reaction mixtures at 80 °C over the course of several days. This lack of reactivity is unusual, as analogous complexes of the type (R'-PSiP)PtR (R' = Cy, Ph) reacted readily with these and other hydrosilanes to afford isolable platinum silyl products with the concommitant loss of RH.[124] Much like the Pt analogue, compounds **2-10** and **2-11** did not react with hydrosilanes.[88]

2.2.4 Synthesis and reactivity of (Cy-PSiP'-Ph)M(NHR) (M = Ni, Pd, Pt; R = H or Ph) complexes

The chemistry of Group 10 terminal amido complexes remains relatively unexplored in comparison to that of related metal alkyl derivatives. Such late transition metal amido complexes that feature a high d-electron count at the metal centre are proposed to be highly nucleophilic and basic at the amido N due to disruption of ligand-to-metal π-bonding.[125-127] As a result of this, as well as the polar nature of the metal-heteroatom bond, such complexes are anticipated to be highly reactive,[125,127,128] and examples of stoichiometric C-H bond activation involving net C-H bond addition across a late metal amido bond have been demonstrated for Ru^{II} amido and anilido complexes.[129-131] Although examples of complexes that could be isolated are scarce, Group 10 metal amido complexes have been proposed as intermediates in a number of important catalytic processes,[132-134] including Pd-catalyzed C-N cross-coupling. As such, an understanding of the structural and reactivity features of such complexes may prove useful in the further development of amination catalysis.

In this context, the synthesis of Group 10 metal amido and anilido complexes supported by Cy-PSiP'-Ph ligation was targeted (Scheme 2-6). Previous work in the Turculet group involving the synthesis of related complexes supported by Cy-PSiP ligation demonstrated that although Pt amido and anilido complexes of the type (Cy-PSiP)Pt(NHR) (R = ^{t}Bu, aryl) are readily isolable, analogous Pd and Ni terminal anilido complexes readily rearrange in solution via Si-C(sp^2) bond cleavage processes in the PSiP ligand backbone (Scheme 2-7).[123] In accordance with these previous observations, treatment of **2-6** with either 10 equiv. of $LiNH_2$ or 5 equiv. of LiNHPh afforded the corresponding Pt terminal amido complexes (Cy-PSiP'-Ph)Pt(NH_2) (**2-14**) and (Cy-PSiP'-Ph)Pt(NHPh) (**2-15**) in good yields (Scheme 2-6). As in the case of **2-6** and **2-9**, the $^{31}P\{^{1}H\}$ NMR spectra of **2-14** and **2-15** revealed an AB spin system with ^{195}Pt satellites in each case after simulation of the experimentally obtained data (Figure 2-4; for **2-14** : $^{2}J_{PP}$ = -394 Hz, $^{1}J_{PPt}$ = 3108 and 2984 Hz ; for **2-15** : $^{2}J_{PP}$ = -398 Hz, $^{1}J_{PPt}$ = 3200 and 2878 Hz).

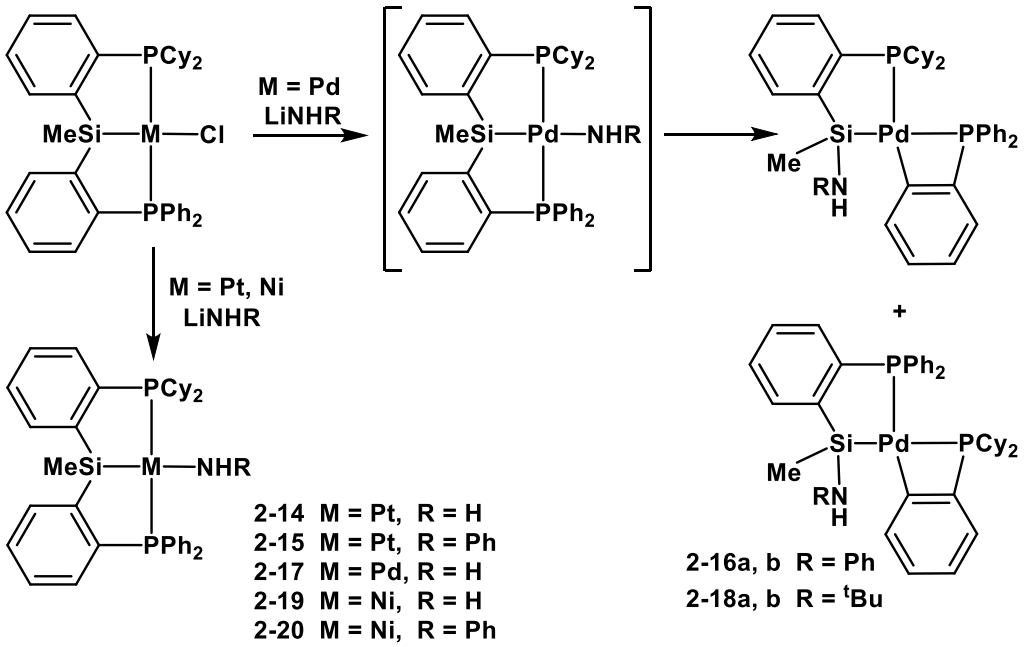

Scheme 2-6. Synthesis of (Cy-PSiP'-Ph)M(NHR) (M = Pt, Ni; R = H, Ph) amido complexes and rearrangement of related Pd species by Si-C(sp^2) bond cleavage in the pincer ligand backbone.

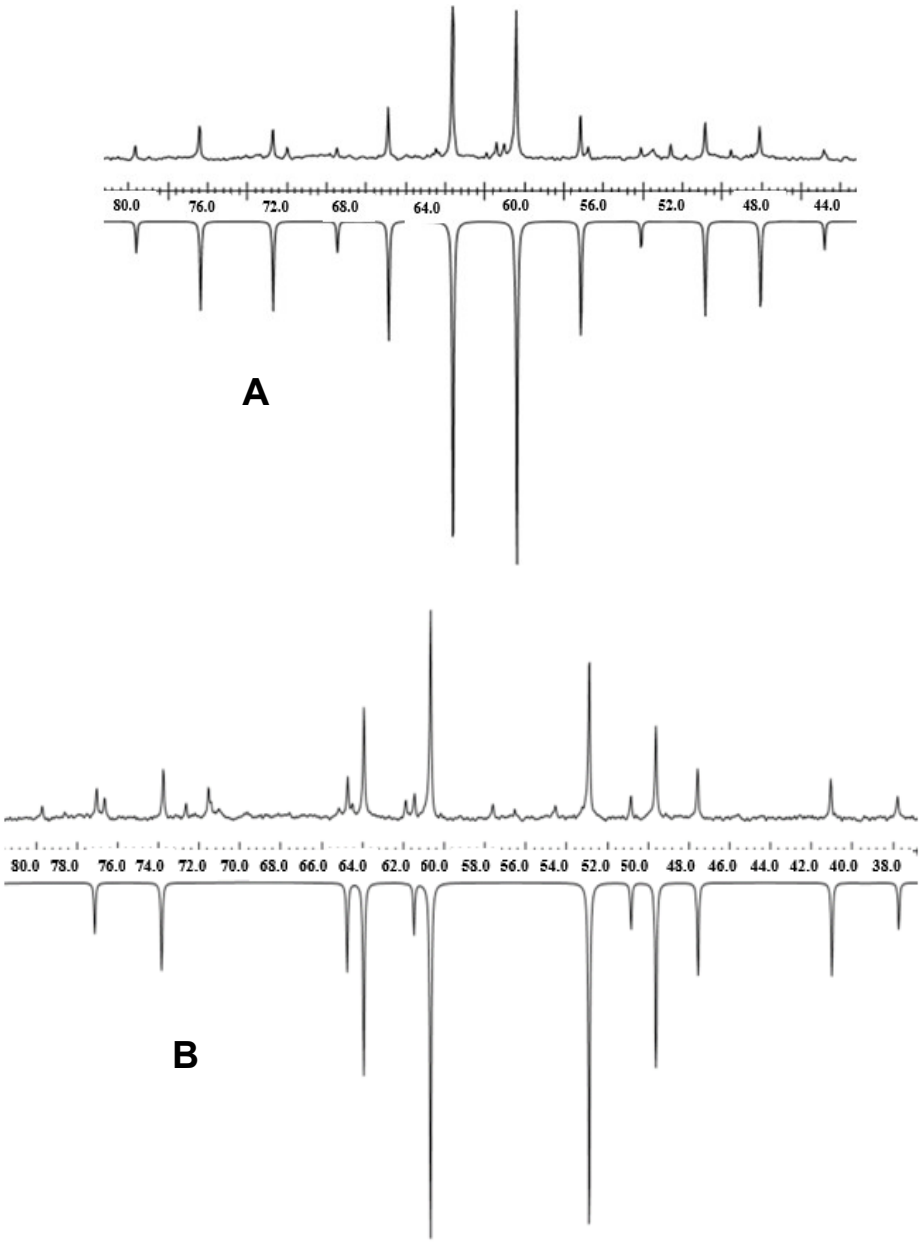

Figure 2-4. Experimental (top; benzene-d_6) and simulated (inverted) $^{31}P\{^{1}H\}$ NMR spectrum (202.46 Hz) of **2-14** (**A**) and **2-15** (**B**).

A related reaction of (Cy-PSiP'-Ph)PdCl (**2-7**) with LiNHPh did not afford the terminal anilido complex observed for Pt (Scheme 2-6). Rather, treatment of **2-7** with 5 equiv of LiNHPh led to the formation of a 1:1 mixture (according to analysis of ^{31}P NMR spectra) of isomeric metallacycles (**2-16a**, **b**) where Si-C(sp^2) bond cleavage has occurred

in the PSiP' ligand backbone and the anilido ligand has been transferred to Si. The formation of isomers results from cleavage of either of the two Si-C(sp^2) bonds in the PSiP' ligand (closest to either the Ph_2P donor or closest to the Cy_2P donor), and there does not appear to be a preference for the formation of one isomer over the other. Each isomer of **2-16** gives rise to a characteristic pair of doublets in the $^{31}P\{^1H\}$ NMR spectrum of the mixture (at 72.5 and -45.1 ppm, $^2J_{PP}$ = 21 Hz; and at 58.9 and -34.5 ppm, $^2J_{PP}$ = 21 Hz), where the relatively small $^2J_{PP}$ coupling observed is indicative of *cis*-disposed phosphino donors. The chemical shift of these ^{31}P NMR resonances is comparable to the data obtained for the analogous Pd complexes [κ^2-(2-$Cy_2PC_6H_4$)*Si*Me(NHPh)]Pd[(κ^2-(2-$Cy_2PC_6H_4$)] (69.2 (d) and -39.6 (d) ppm, $^2J_{PPcis}$ = 20 Hz) and [(κ^2–$Cy_2PC_6H_4SiMe_2$)Pd(κ^2–$Cy_2PC_6H_4$)] (68.3 (d) and -39.2 (d) ppm, $^2J_{PPcis}$ = 19 Hz).[88, 123] Surprisingly, treatment of **2-7** with 10 equiv. of $LiNH_2$ does appear to lead to the formation of a terminal parent amido complex of the type (Cy-PSiP-Ph)Pd(NH_2) (**2-17**), as evidenced by the drastically different $^{31}P\{^1H\}$ NMR spectrum of this product which features two doublets at 63.1 and 42.4 ppm ($^2J_{PP}$ = 350 Hz). These data are more in line with the NMR features of the related C_1-symmetric Pd species **2-7**, **2-10**, and **2-12**, wherein the PSiP' ligand framework is intact. Complex **2-17** was isolated in 75% yield. Heating of **2-17** in benzene solution (65 °C, 24 h) showed that the complex decomposed by forming a mixture of unidentified products (^{31}P NMR).

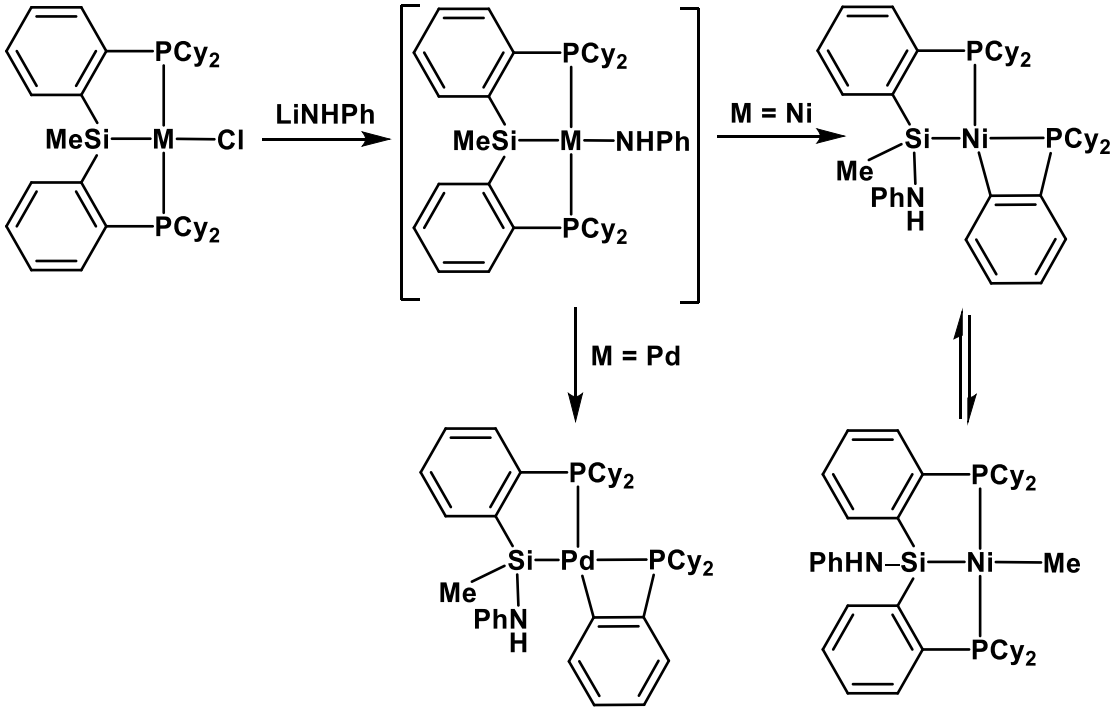

Scheme 2-7. Rearrangement of (Cy-PSiP)M(NHPh) (M = Pd, Ni) amido complexes by Si-C(sp^2) bond cleavage in the pincer ligand backbone.

The stability of the Pd parent amido complex **2-17** relative to the related (unobserved) anilido derivative can be attributed to either steric or electronic factors, as the parent amido ligand is clearly less sterically encumbering and more electron-rich than the anilido donor. In an effort to determine whether the electronic properties of the amido ligand influence the stability of the ensuing terminal amido Pd complex, the synthesis of a Pd amido complex featuring a more electron-rich amido ligand was attempted. The reaction of **2-7** with LiNH^{t}Bu resulted in the formation of a mixture of isomers (**2-18a**, **b**, 2:1; $^{31}P\{^1H\}$ NMR: 69.2 and -45.9 ppm, $^2J_{PP}$ = 22 Hz and 56.5 and -36.1 ppm, $^2J_{PP}$ = 21 Hz) analogous to that observed for **2-16a**, **b**. This observation suggests that the factors that govern the stability of terminal Pd amido species in this system are likely rather complex.

In an effort to determine if chemical exchange occurs between isomers such as **2-16a**, **b** and **2-18a**, **b** saturation transfer NMR experiments were carried out (^{31}P NMR, 50 °C). Such a chemical exchange process would involve an equilibrium between the observed rearranged complexes and a possible Pd^0 intermediate (Scheme 2-8). Attempts to observe chemical exchange processes in these compounds were complicated by the fact that they are unstable at elevated temperatures over short periods of time (ca. 30 mins at 50 °C) and even at room temperature over longer periods of time, decomposing to form complex mixtures of unidentified products (^{31}P NMR). This complicated the saturation transfer experiments, as the experiment entails evaluating the increase in the intensity of one NMR resonance versus another as evidence of chemical exchange. While this phenomenon was indeed observed for these complexes it was difficult to determine if the decrease in intensity was due to exchange or from the fact that the decomposition products became more prominent as the experiments were run. As such, it cannot conclusively be determined on the basis of these results if the Si-C(sp^2) bond cleavage leading to the formation of **2-16a**, **b** and **2-18a**, **b** is a reversible process under the conditions examined.

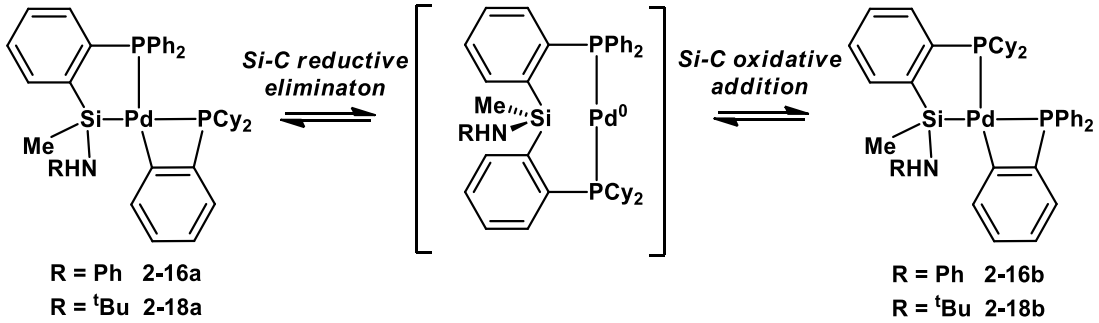

Scheme 2-8. Proposed mechanism for chemical exchange between isomers of the type **2-16a**, **b** and **2-18a**, **b** via reversible Si-C(sp^2) bond cleavage.

Interestingly, while Ni terminal amido complexes proved elusive in the case of Cy-PSiP ligation, related (Cy-PSiP'-Ph)Ni amido species were readily isolated. Treatment of **2-8** with either 10 equiv. of $LiNH_2$ or 5 equiv. of LiNHPh resulted in formation of the corresponding amido complexes (Cy-PSiP'-Ph)Ni(NH_2) (**2-19**) and (Cy-PSiP'-Ph)Ni(NHPh) (**2-20**), respectively (Scheme 2-6). Both complexes **2-19** and **2-20** were readily isolated in good yield (73 and 78%, respectively). Solution NMR spectroscopic data (benzene-d_6) for these compounds are similar to the data obtained for **2-8**, **2-11** and **2-13** and are consistent with C_1-symmetric square planar complexes where the Cy-PSiP'-Ph phosphino donors are coordinated in a *trans* fashion, as indicated by the presence of two doublets in the $^{31}P\{^1H\}$ NMR spectra at 60.4 and 41.6 ppm for **2-19** ($^2J_{PP}$ = 262 Hz) and 57.5 and 41.2 ppm for **2-20** ($^2J_{PP}$ = 285 Hz). Given that complexes of the type (Cy-PSiP)Ni(NHR) have not been observed directly,[123] the observed stability of such (Cy-PSiP'-Ph)Ni terminal amido complexes once again highlights the complexity of the factors that govern Si-C bond cleavage processes in such PSiP ligated species.

Preliminary reactivity studies utilizing the Pt, Pd and Ni terminal amido complexes reported herein indicate that such complexes are relatively unreactive, as little to no reactivity was observed with unsaturated substrates such as phenyl acetylene, cyclohexyl allene and xylyl isocyanide.

2.2.5 Metalation of alternative PSiP' ligands with Group 10 metals

The metalation of the related pincer ligands (Ph-PSiP*-^{i}Pr)H (**2-4**, Figure 2-4) and (Cy-PSiP*-^{i}Pr)H (**2-5**, Figure 2-4) with Group 10 metals was also investigated. As previously (*vide supra*), the synthesis of (PSiP*)MCl species (M = Pt, Pd, Ni) was

targeted as an appealing entry into the coordination chemistry of such mixed donor pincer ligands. Treatment of a benzene solution of **2-4** with one equiv. of (COD)PtBnCl (COD = 1,5-cyclohexadiene) resulted in the formation of a new complex, tentatively formulated as (Ph-PSiP*-^{i}Pr)PtCl (**2-21**, Scheme 2-9), which was isolated in 85% yield. The $^{31}P\{^{1}H\}$ NMR spectrum of **2-21** contains two doublets at 54.1 and -3.8 ppm ($^{1}J_{PP}$ = 411 Hz) with ^{195}Pt satellites ($^{1}J_{PPt}$ = 1542 and 1346 Hz, respectively), which is consistent with a C_1-symmetric structure for the complex in which the ligand phosphino donors are *trans*-disposed (on the basis of the relatively large $^{1}J_{PP}$ coupling constant) and are both coordinated to Pt. Although X-ray quality crystals of **2-21** have thus far proven elusive, the structure of this complex can be speculated upon by comparing ^{31}P NMR data for **2-21** to that of complexes such as **2-16**, **2-18**, [κ^2-(2-Cy$_2$*P*C$_6$H$_4$)*Si*Me(NHPh)]Pd[(κ^2-(2-Cy$_2$*PC*$_6$H$_4$)],[124] and [(κ^2-Cy$_2$*P*C$_6$H$_4$*Si*Me$_2$)Pd(κ^2-Cy$_2$*PC*$_6$H$_4$)],[124] all of which feature a four-membered Pd-C-C-P metallacycle. All four of the latter complexes feature a significantly upfield shifted ^{31}P NMR resonance (*vide infra*) that corresponds to the phosphino donor in the constrained four-membered palladacycle. As such, the ^{31}P NMR data obtained for **2-21** is in agreement with the formation of a comparable Pt-Si-C-P metallacycle, where the resonance corresponding ^{i}Pr$_2$P donor is similarly upfield shifted. Attempts to prepare analogous Pd and Ni chloride complexes by treating a benzene solution of **2-4** with either [Pd(η^3-C$_3$H$_5$)Cl]$_2$, NiCl$_2$ or NiCl$_2$(DME) (DME = 1,2-dimethoxyethane) did not lead to formation of the desired Ph-PSiP*-^{i}Pr complexes.

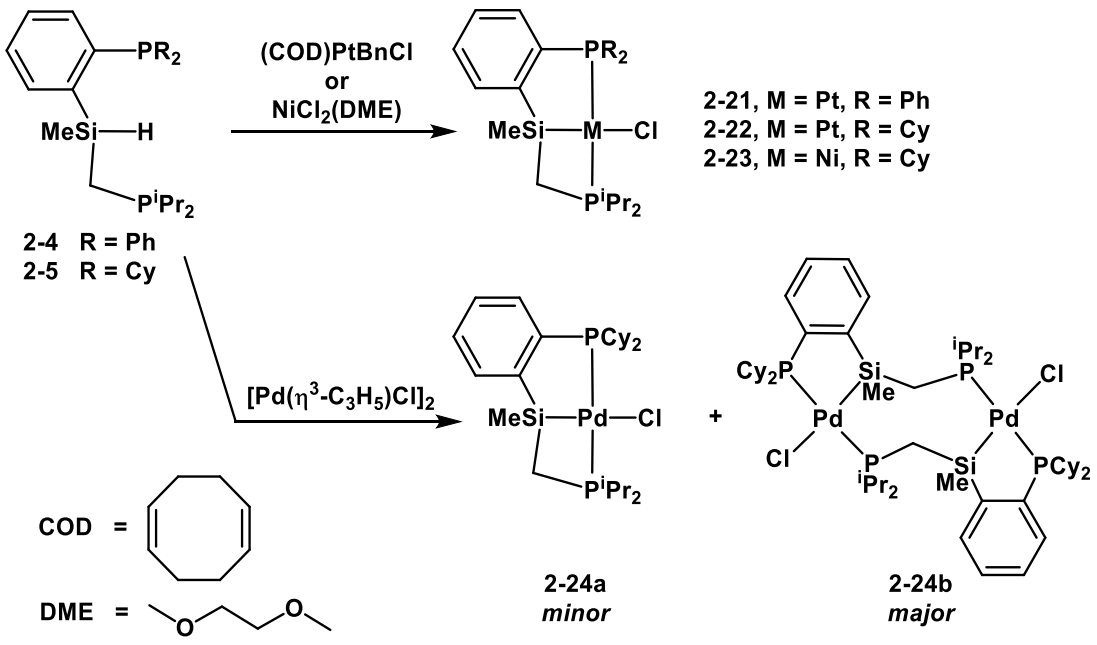

Scheme 2-9. Synthesis of Group 10 metal complexes supported by Ph-PSiP*-^{i}Pr and Cy-PSiP*-^{i}Pr ligation.

A related Pt complex featuring Cy-PSiP*-^{i}Pr ligation was also synthesized by treatment of a benzene solution of **2-5** with one equiv. of (COD)PtBnCl to obtain (Cy-PSiP*-^{i}Pr)PtCl (**2-22**, Scheme 2-9), which was isolated as an orange solid in 82% yield. The $^{31}P\{^{1}H\}$ NMR spectrum of **2-22** features two doublets at 64.1 and -3.0 ppm ($^{2}J_{PP}$ = 390 Hz) with ^{195}Pt satellites ($^{1}J_{PPt}$ = 1561 and 1286 Hz, respectively), which is consistent with a C_1-symmetric structure for the complex in which the ligand phosphino donors are *trans*-disposed and are both coordinated to Pt. As in the case of **2-21**, this complex also gives rise to a significantly upfield shifted ^{31}P NMR resonance, which lends support to the formulation of **2-22** as a mononuclear complex that contains a four-membered Pt-Si-C-P metallacycle (Scheme 2-9). An analogous Ni complex was also synthesized by treating a benzene solution of **2-5** with one equiv. of $NiCl_2$(DME) to obtain (Cy-PSiP*-^{i}Pr)NiCl (**2-23**, Scheme 2-9), which was isolated as an orange solid in 88% yield. The

$^{31}P\{^{1}H\}$ NMR spectrum of **2-23** contains two doublets at 51.9 and -21.1 ppm ($^{2}J_{PP}$ = 278 Hz), which is consistent with κ^3-(Cy-PSiP*-^{i}Pr) coordination to Ni analogous to that proposed for **2-22**.

Interestingly, attempts to prepare an analogous complex of the type (Cy-PSiP*-^{i}Pr)PdCl by treating a benzene solution of **2-5** with 0.5 equiv. of $[Pd(\eta^3\text{-}C_3H_5)Cl]_2$ resulted in the formation of a mixture of products, **2-24a, b** (1:5 ratio of **a**:**b** on the basis of ^{31}P NMR). The minor product **2-24a** gives rise to two doublets in the $^{31}P\{^{1}H\}$ NMR spectrum of the mixture at 60.2 and -23.6 ppm ($^{2}J_{PP}$ = 378 Hz), which, by analogy with **2-21** - **2-23**, is consistent with a mononuclear complex that contains a four-membered Pd-Si-C-P metallacycle. In contrast, the major product **2-24b** features two $^{31}P\{^{1}H\}$ NMR resonances at 69.6 (d) and 30.7 ppm (d, $^{2}J_{PP}$ = 342 Hz). X-ray quality crystals of **2-24** were obtained, and the resulting structure (Figure 2-5) revealed a binuclear Pd complex with the formulation $[(Cy\text{-}PSiP^*\text{-}^{i}Pr)PdCl]_2$ in which the $CH_2P^{i}Pr_2$ ligand arms bridge between the two Pd centers to form an eight-membered Pd-Si-C-P-Pd-Si-C-P ring. Each Pd center features approximate square planar coordination geometry with *trans*-disposed phosphino donors, each of which originates from a different PSiP ligand. This solid state structure is consistent with complex **2-24b**, as it features *trans*-disposed phosphino donors without formation of a four-membered metallacycle of the type that would be anticipated for a mononuclear κ^3-(Cy-PSiP*-^{i}Pr)Pd complex. In solution, **2-24b** is anticipated to have C_2-symmetry, resulting in the observation of chemically equivalent PCy_2 and $P^{i}Pr_2$ donors, respectively (^{31}P NMR). The formation of this dinuclear complex is not surprising, given the anticipated strain that might be associated with the formation of a κ^3-(R-PSiP*-^{i}Pr)Pd complex.

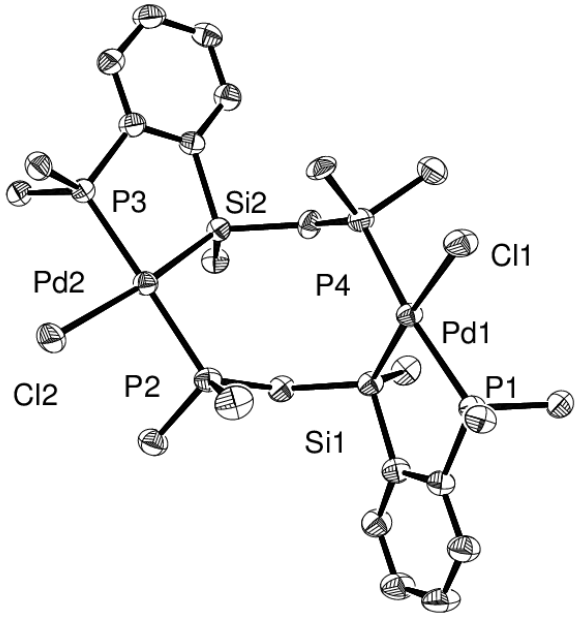

Figure 2-5. The crystallographically determined structure of **2-24b**, shown with 50% displacement ellipsoids. All H atoms and selected C atoms have been omitted for clarity.

Bond Lengths (Å)			
Pd1-P1	2.3051(8)	Pd2-P2	2.3560(8)
Pd1-P4	2.3360(8)	Pd2-P3	2.3129(8)
Pd1-Si1	2.3036(9)	Pd2-Si2	2.2994(8)
Pd1-Cl1	2.4583(8)	Pd2-Cl2	2.4486(8)
Bond Angles (°)			
P1-Pd1-P4	172.19(3)	P2-Pd2-P3	178.40(3)
Si1-Pd1-Cl1	175.60(3)	Si2-Pd2-Cl2	171.44(3)
P2-C40-Si1	128.52(17)	P4-C80-Si2	130.14(18)

Table 2-3. Selected interatomic distances (Å) and angles (°) for **2-24b**.

2.3 Conclusions

The methodology developed for the synthesis of mixed donor PSiN pincer ligands has been successfully extended to the synthesis of new PSiP' ligands that feature two different phosphino donors. A series of Group 10 metal complexes featuring such "unsymmetrical" PSiP' ligands have been prepared and characterized, including examples of Ni, Pd and Pt chloride, alkyl, aryl, anilido, and rare examples of late metal parent amido complexes. Throughout these studies Cy-PSiP'-Ph ligation has proved to be an effective platform for the synthesis of a variety of square planar complexes that feature strongly electron-donating ligands, such as alkyl, aryl and amido, coordinated trans to Si. In particular, unlike the related (Cy-PSiP)MX (M = Ni, Pd; X = alkyl, amido) analogues, which underwent spontaneous rearrangement processes resulting in Si-C(sp^2) bond cleavage in the ligand backbone and transfer of the X ligand to Si, complexes of the type (Cy-PSiP'-Ph)MX proved isolable in most cases, with the exception of the Pd amido species (Cy-PSiP'-Ph)Pd(NHPh) and (Cy-PSiP'-Ph)Pd(NH^{t}Bu), which did undergo a related ligand rearrangement. Unfortunately, at this point it is not possible to firmly conclude what factors (steric or electronic) govern such rearrangements, as no obvious pattern governing which square planar PSiP complexes will undergo such Si-C(sp^2) bond cleavage processes could be discerned. While (Cy-PSiP'-Ph)MMe species were readily isolated, such complexes proved to be surprisingly unreactive towards Si-H bonds in silanes. Similarly, complexes of the type (Cy-PSiP'-Ph)M(NH_2) (M = Ni, Pd, Pt) did not undergo insertion reactions with unsaturated substrates such as alkynes, allenes, and isocyanides.

Group 10 metal chloride complexes supported by the related PSiP' ligands Ph-PSiP*-^{i}Pr and Cy-PSiP*-^{i}Pr were also synthesized and characterized. While such ligands are anticipated to form a relatively strained four-membered metallacycle upon complexation to a metal center in a κ^3-manner, spectroscopic evidence is consistent with the formation of κ^3-(R-PSiP*-^{i}Pr) complexes, with only one exception in the case of Pd, in which case a dinuclear complex with bridging $CH_2P^{i}Pr_2$ ligand arms was obtained. These preliminary studies suggest that R-PSiP*-^{i}Pr ligation is viable for the synthesis of pincer complexes.

2.4 Experimental Section

2.4.1 General considerations

All experiments were conducted under nitrogen in an MBraun glovebox or using standard Schlenk techniques. Dry, oxygen-free solvents were used unless otherwise indicated. Pentane, benzene, and toluene were deoxygenated and dried by sparging with nitrogen and subsequent passage through a double-column (one activated alumina column and one column packed with activated Q-5) solvent purification system purchased from MBraun Inc. Tetrahydrofuran and diethyl ether were purified by distillation from Na/benzophenone under N_2. All purified solvents were stored over 4 Å molecular sieves. All deuterated solvents were degassed via three freeze-pump-thaw cycles and stored over 4 Å molecular sieves. The compounds $PtCl_2(SEt_2)_2$, $[PdCl(\eta^3\text{-}C_3H_5)]_2$, and $NiCl_2$(DME) were purchased from Strem Chemicals and used as received. Triethylamine was sparged with nitrogen and subsequently distilled from CaH_2. Silanes were purchased from Gelest. The compounds $(2\text{-}BrC_6H_4)PCy_2$,[135] $(2\text{-}BrC_6H_4)PPh_2$,[136] and

$LiCH_2PiPr_2$[137] were prepared using literature methods. All other reagents were purchased from Aldrich and used without further purification. Unless otherwise stated, ^1H, ^{13}C, ^{31}P, and ^{29}Si NMR characterization data were collected at 300K on a Bruker AV-500 spectrometer operating at 500.1, 125.8, 202.5, and 99.4 MHz (respectively) with chemical shifts reported in parts per million downfield of $SiMe_4$ (for ^1H, ^{13}C, and ^{29}Si) or 85% H_3PO_4 in D_2O (for ^{31}P). Variable- temperature NMR data were collected on a Bruker AV-300 spectrometer. ^1H and ^{13}C NMR chemical shift assignments are based on data obtained from ^{13}C-DEPTQ, ^1H-^1H COSY, ^1H-^{13}C HSQC, and ^1H-^{13}C HMBC NMR experiments. ^{29}Si NMR assignments are based on ^1H-^{29}Si HMQC and ^1H-^{29}Si HMBC experiments. ^1H-^{29}Si coupling constants were determined by the use of ^1H-coupled ^1H-^{29} HMQC and ^1H-^{29}Si HMBC experiments. Infrared spectra were recorded as thin films between NaCl plates using a Bruker VECTOR 22 FT-IR spectrometer at a resolution of 4 cm^{-1}. ESI Mass spec was performed on a VG/Micromass Quattro Mass Spectrometer at the Dalhousie University Mass Spectrometry Laboratory. Chemical shift values and coupling constants for the ^{31}P NMR of **2-6** and **2-9** were obtained via simulations ran by Dr. Mike Lumsden of the NMR[3] facilities at Dalhousie University.

2.4.2 Synthetic detail and characterization data

$(2\text{-}Cy_2PC_6H_4)SiMeHCl$ (2-1). A cold (-78 °C) solution of $(2\text{-}BrC_6H_4)PCy_2$ (4.16 g, 11.7 mmol) in ca. 30 mL of hexanes was treated with ^{n}BuLi (1.6 M in hexanes, 7.30 mL, 11.7 mmol). The reaction mixture was allowed to stir at -78 °C for 30 minutes, and was subsequently treated with Cl_2MeSiH (1.20 mL, 11.7 mmol). The resulting yellow solution was allowed to warm to room temperature over the course of 1 h, at which point

the volatile components of the reaction mixture were removed under vacuum. The remaining residue was extracted with ca. 50 mL of benzene, and the benzene extract was filtered through Celite. The filtrate solution was collected and the volatile components were removed under vacuum. The remaining residue was washed with 3 × 5 mL cold (-30 °C) pentane to afford **2-1** as a yellow solid (2.50 g, 60% yield). ^{1}H NMR (500 MHz, benzene-d_6): δ 8.11 (d, 1 H, H_{arom}, J = 7 Hz), 7.34 (d, 1 H, H_{arom}, J = 7 Hz), 7.20 (m, 2 H, H_{arom}), 6.13 (m, 1 H, Si*H*), 2.15-0.89 (overlapping resonances, 22 H, P*Cy*), 0.89 (t, 3 H, Si*Me*, $^{3}J_{HH}$ = 3.5 Hz). ^{13}C{^{1}H} NMR (125.8 MHz, benzene-d_6): δ 136.3 (C_{arom}), 136.19 (C_{arom}) 132.9 (CH$_{arom}$), 130.8 (CH$_{arom}$), 129.9 (CH$_{arom}$), 129.1 (CH$_{arom}$), 35.7 (d, CH$_{2Cy}$, J = 11 Hz), 31.4 (d, CH$_{2Cy}$, J = 15 Hz), 30.4-25.2 (P*Cy*), 4.3 (Si*Me*). ^{31}P{^{1}H} NMR (202.5 MHz, benzene-d_6): δ -8.5. ^{29}Si NMR (99.4 MHz, benzene-d_6): δ -6.2. IR (cm^{-1}): 2185 (br, Si-H).

(2-Ph$_2$PC$_6$H$_4$)SiMeHCl (2-2). A cold (-78 °C) solution of (2-BrC$_6$H$_4$)PPh$_2$ (2.30 g, 6.73 mmol) in ca. 20 mL of hexanes was treated with ^{n}BuLi (2.5 M in hexanes, 2.70 mL, 6.73 mmol). The reaction mixture was allowed to stir at -78 °C for 45 minutes, and was subsequently treated with Cl$_2$MeSiH (1.65 mL, 14.4 mmol) . The resulting yellow solution was allowed to warm to room temperature over the course of 1 h, at which point the volatile components of the reaction mixture were removed under vacuum. The remaining residue was extracted with ca. 50 mL of benzene, and the benzene extract was filtered through Celite. The filtrate solution was collected and the volatile components were removed under vacuum. The remaining residue was washed with 3 × 5 mL cold (-30 °C) pentane to afford **2-2** as a white solid (0.64 g, 28% yield). ^{1}H NMR (500 MHz, benzene-d_6): δ 7.95 (d, 1 H, H_{arom}, J = 8 Hz), 7.40-7.20 (m, 5 H, H_{arom}), 7.08 (t, 1 H,

H_{arom}, J = 8 Hz), 7.07 – 6.98 (9 H, H_{arom}), 6.00 (m, 1 H, Si*H*), 0.70 (t, 3 H, Si*Me*, $^{3}J_{HH}$ = 6 Hz). $^{13}C\{^{1}H\}$ NMR (125.8 MHz, benzene-d_6): δ 136.4 (C_{arom}), 136.3 (C_{arom}), 135.1 (C_{arom}), 134.4 (CH_{arom}), 134.3 (CH_{arom}), 134.2 (CH_{arom}), 134.1 (CH_{arom}), 131.7 (CH_{arom}), 129.9 (CH_{arom}), 129.4 (CH_{arom}), 129.3 (CH_{arom}), 3.2 (Si*Me*). $^{31}P\{^{1}H\}$ NMR (202.5 MHz, benzene-d_6): δ -12.0. ^{29}Si NMR (99.4 MHz, benzene-d_6): δ -2.3. IR (cm^{-1}): 2186 (br, Si-H).

(Cy-PSiP'-Ph)H (2-3). A pre-cooled (-30 °C) solution of **2-1** (1.69 g, 4.79 mmol) in ca. 4 mL of THF was treated with a pre-cooled (-30 °C) solution of (2-LiC_6H_4)PPh_2·$Et_2O_{(0.7)}$ (1.53 g, 4.79 mmol) in ca. 4 mL of THF. The resulting reaction mixture was allowed to stand at room temperature for 20 h and was subsequently filtered through Celite. The filtrate solution was collected and dried under vacuum. The remaining residue was washed with 2 × 3 mL of cold pentane and dried in vacuo to obtain **2-3** as a tan powder (1.30 g, 85 % yield). ^{1}H NMR (500 MHz, benzene-d_6): δ 7.84 (d, 1 H, H_{arom}, J = 7 Hz), 7.80 (d, 1 H, H_{arom}, J = 8 Hz), 7.45 (d, 1 H, H_{arom}, J = 8 Hz), 7.37 – 7.28 (m, 4 H, H_{arom}), 7.19 (t, 1 H, H_{arom}, J = 7 Hz), 7.14 (m, 2 H, H_{arom}), 7.10 – 6.90 (m, 8 H, H_{arom}), 6.09 (m, 1 H, Si*H*), 1.90-0.99 (overlapping resonances, 22 H, P*Cy*), 0.90 (d, 3 H, Si*Me*, $^{3}J_{HH}$ = 4 Hz). $^{13}C\{^{1}H\}$ NMR (125.8 MHz, benzene-d_6): δ 137.8 (C_{arom}), 137.7 (C_{arom}), 137.6 (C_{arom}), 134.7 (CH_{arom}), 134.3 (CH_{arom}), 134.2 (CH_{arom}), 134.1 (CH_{arom}), 134.0 (CH_{arom}), 132.6 (CH_{arom}), 129.9 (CH_{arom}), 129.0 (CH_{arom}), 128.8 (CH_{arom}), 128.6 (CH_{arom}), 35.9 (d, Cy_{CH}, J = 14 Hz), 35.7 (d, Cy_{CH}, J = 14 Hz) 31.2-26.9 (P*Cy*), -1.6 (Si*Me*). $^{31}P\{^{1}H\}$ NMR (202.5 MHz, benzene-d_6): δ -7.60 (s), -11.1 (s). ^{29}Si NMR (99.4 MHz, benzene-d_6): δ -23.0. IR (cm^{-1}): 2360 (br, Si-H). HRMS (ESI): $[M + H]^+$ calcd for $C_{37}H_{44}P_2Si$ 578.2605, found 579.2760.

(Ph-PSiP*-^{i}Pr)H (2-4). A pre cooled (-30 °C) solution of **2-2** (0.078 g, 0.23 mmol) in ca. 3 mL of THF was added to a pre-cooled (-30 °C) solution of $LiCH_2P^iPr_2$ (0.032 g, 0.23 mmol) in ca. 3 mL of THF. The resulting reaction mixture was allowed to stand at room temperature for 18 h and was subsequently filtered through Celite. The filtrate solution was collected and dried under vacuum. The remaining residue was washed with 2 × 3 mL of cold pentane and dried in vacuo to obtain **2-4** as a yellow oil (0.069 g, 89% yield). ^{1}H NMR (500 MHz, benzene-d_6): δ 7.81 (d, 1 H, H_{arom}, J = 7 Hz), 7.42 (t, 2 H, H_{arom}, J = 7 Hz), 7.36 (m, 4 H, H_{arom}), 7.04 (m, 7 H, H_{arom}), 5.11 (m, 1 H, Si*H*), 1.36 (d, PCH_2, 1 H, J = 4 Hz), 1.33 (d, PCH_2, 1 H, J = 4 Hz), 1.14-1.01 (22 H, PCy), 0.97-0.87 (overlapping resonances, 14 H, PC*H*Me$_2$ + PCH*Me*$_2$), 0.81 (d, 3 H, Si*Me*, $^3J_{HH}$ = 4 Hz). ^{13}C{^{1}H} NMR (125.8 MHz, benzene-d_6): δ 136.9 (C_{arom}), 136.7 (C_{arom}), 136.6 (C_{arom}), 134.6 (CH$_{arom}$), 134.5 (CH$_{arom}$), 130.2 (CH$_{arom}$), 129.3 (CH$_{arom}$), 129.2 (CH$_{arom}$), 129.1 (CH$_{arom}$), 25.8 (CH$_2$P), 20.5 (P*C*HMe$_2$), 19.8 (PCH*Me*$_2$), 9.1 (Si*Me*). ^{31}P{^{1}H} NMR (202.5 MHz, benzene-d_6): -2.6 (s), -9.6 (s). ^{29}Si NMR (99.4 MHz, benzene-d_6): δ -13.6. IR (cm^{-1}): 2123 (br, Si-H). HRMS (ESI): $[M + H]^+$ calcd for $C_{26}H_{34}P_2Si$ 436.1828, found 437.1995.

(Cy-PSiP*-^{i}Pr)H (2-5). A pre-cooled (-30 °C) solution of **2-1** (1.15 g, 3.27mmol) in ca. 3 mL of THF was added to a pre-cooled (-30 °C) solution of $LiCH_2P^iPr_2$ (0.45 g, 3.27 mmol) in ca. 3 mL of THF. The resulting reaction mixture was allowed to stand at room temperature for 24 h and was subsequently filtered through Celite. The filtrate solution was collected and dried under vacuum. The remaining residue was washed with 2 × 3 mL of cold pentane and dried in vacuo to obtain **2-5** as an amber oil (1.12 g, 97% yield). ^{1}H NMR (500 MHz, benzene-d_6): δ 7.74 (d, 1 H, H_{arom}, J = 7 Hz), 7.46 (d, 1 H,

*H*arom, *J* = 7 Hz), 7.19 (m, 2 H, *H*arom), 5.18 (m, 1 H, Si*H*), 2.00-1.51 (22 H, P*Cy*), 1.38 – 1.00 (overlapping resonances, 14 H, PC*H*Me$_2$ + PCH*Me*$_2$), 0.77 (d, 3 H, Si*Me*, $^3J_{HH}$ = 4 Hz). $^{13}C\{^1H\}$ NMR (125.8 MHz, benzene-d_6): δ 136.3 (*C*H$_{arom}$), 136.2 (*C*H$_{arom}$), 132.9 (*C*H$_{arom}$), 129.2 (*C*$_{arom}$), 128.7 (*C*$_{arom}$), 36.1 (d, *C*H$_{Cy}$, *J* = 14 Hz), 35.9 (d, *C*H$_{Cy}$, *J* = 14 Hz), 31.6-26.9 (*C*H$_{2Cy}$), 25.5 (*C*HMe$_2$), 25.1 (*C*HMe$_2$), 20.4 (CH*Me*$_2$), 20.2 (CH*Me*$_2$), 19.6 (CH*Me*$_2$), 19.0 (CH*Me*$_2$), -1.9 (Si*Me*). $^{31}P\{^1H\}$ NMR (202.5 MHz, benzene-d_6): δ -1.4 (s), -7.1 (s). ^{29}Si NMR (99.4 MHz, benzene-d_6): δ -14.3. IR (cm^{-1}): 2116 (s, Si-H). HRMS (ESI): $[M + H]^+$ calcd for $C_{26}H_{46}P_2Si$ 448.2788, found 449.2932.

(Cy-PSiP'-Ph)PtCl (2-6). A room temperature solution of **2-1** (0.24 g, 0.43 mmol) in ca. 3 mL of benzene was added to a solution of $PtCl_2(Et_2S)_2$ (0.19 g, 0.43 mmol) in ca. 3 mL of benzene. Neat Et_3N (60 μL, 0.43 mmol) was added to the solution. The reaction mixture was allowed to stand at room temperature for 45 min., at which point the volatile components were removed under vacuum. The remaining residue was extracted into ca. 4 mL of benzene. The solution was filtered through Celite and the filtrate solution was collected. The volatile components of the filtrate solution were removed under vacuum. The remaining residue was washed with 2 × 3 mL of cold (-30 °C) pentane and dried in vacuo to afford **2-6** (0.22 g, 89% yield) as a yellow solid. ^{1}H NMR (500 MHz, benzene-d_6): δ 8.04 (m, 2 H, *H*$_{arom}$), 7.77 (m, 1 H, *H*$_{arom}$), 7.68 (m, 2 H, *H*$_{arom}$), 7.63 (m, 1 H, *H*$_{arom}$), 7.45 (m, 2 H, *H*$_{arom}$), 7.32 (m, 1 H, *H*$_{arom}$), 7.30 (m, 1 H, *H*$_{arom}$), 7.18 (m, 2 H, *H*$_{arom}$), 7.06 (m, 2 H, *H*$_{arom}$), 6.98 (m, 4 H, *H*$_{arom}$), 3.18-0.77 (22 H, P*Cy*), 0.57 (s, 3 H, Si*Me*). $^{13}C\{^1H\}$ NMR (125.8 MHz, benzene-d_6): δ 136.0 (*C*$_{arom}$), 135.9 (*C*$_{arom}$), 135.0 (*C*$_{arom}$), 134.9 (*C*$_{arom}$), 134.8 (*C*$_{arom}$), 134.7 (*C*$_{arom}$), 134.2 (*C*H$_{arom}$), 134.0 (*C*H$_{arom}$), 133.8 (*C*H$_{arom}$), 132.0 (*C*H$_{arom}$), 131.6 (*C*H$_{arom}$), 131.1 (*C*H$_{arom}$), 131.0

(CH$_{arom}$), 130.0 (CH$_{arom}$), 129.9 (CH$_{arom}$), 129.7 (CH$_{arom}$), 129.6 (CH$_{arom}$), 129.5 (CH$_{arom}$), 129.4 (CH$_{arom}$), 37.5 (d, CH$_{Cy}$, J = 13 Hz), 37.2 (d, CH$_{Cy}$, J = 13 Hz), 32.1-26.5 (PCy), 7.2 (SiMe). ^{31}P{^{1}H} NMR (202.5 MHz, benzene-d_6): AB spin system; δ A = 62.8 ppm ($^{1}J_{PPt}$ = 3090 Hz), δ B = 51.2 ppm ($^{1}J_{PPt}$ = 2945 Hz), $^{2}J_{PP}$ = -373 Hz. ^{29}Si NMR (99.4 MHz, benzene-d_6): δ 35.0.

(Cy-PSiP'-Ph)PdCl (2-7). A room temperature solution of **2-1** (0.15 g, 0.33 mmol) in ca. 3 mL of benzene was added to a solution of [Pd(η^3-C_3H_5)Cl]$_2$ (0.061 g 0.17 mmol) in ca. 3 mL of benzene. The resulting reaction mixture was allowed to stand at room temperature for 18 h, at which point the solution was filtered through Celite. The filtrate was collected and the volatile components were removed under vacuum. The remaining residue was washed with 2 × 3 mL cold (-30 °C) pentane and dried in vacuo to obtain **2-7** (0.14 g, 90% yield) as a yellow solid. ^{1}H NMR (500 MHz, benzene-d_6): δ 8.08 (m, 2 H, H_{arom}), 8.01 (d, 1 H, H_{arom}, J = 7 Hz), 7.96 (d, 1 H, H_{arom}, J = 7 Hz), 7.70 (m, 2 H, H_{arom}), 7.43 (m, 1 H, H_{arom}), 7.39, (m, 2 H, H_{arom}), 7.32 (m, 1 H, H_{arom}), 7.20 (m, 2 H, H_{arom}), 7.11-6.6 (8 H, H_{arom}) 2.43 - 0.17 (22 H, PCy), 0.13 (s, 3 H, SiMe). ^{13}C{^{1}H} NMR (125.8 MHz, benzene-d_6): δ 133.7 (C_{arom}), 133.6 (C_{arom}), 133.2 (C_{arom}), 132.9 (CH$_{arom}$), 132.7 (CH$_{arom}$), 132.5 (CH$_{arom}$), 132.3 (CH$_{arom}$), 130.1 (CH$_{arom}$), 129.9 (CH$_{arom}$), 129.5 (CH$_{arom}$), 129.2 (CH$_{arom}$), 129.1 (CH$_{arom}$), 127.8 (CH$_{arom}$), 127.7 (CH$_{arom}$), 36.3 (d, CH$_{Cy}$, J = 20 Hz), 35.6 (d, CH$_{Cy}$, J = 18 Hz), 29.3-25.4 (CH$_{2Cy}$), 7.3 (SiMe). ^{31}P{^{1}H} NMR (202.5 MHz, benzene-d_6): δ 63.1 (d, 1 P, $^{2}J_{PP}$ = 348 Hz), 42.4 (d, 1 P, $^{2}J_{PP}$ = 348 Hz). ^{29}Si NMR (99.4 MHz, benzene-d_6): δ 57.0.

(Cy-PSiP'-Ph)NiCl (2-8). A room temperature solution of **2-1** (0.23 g, 0.40 mmol) in ca. 5 mL of benzene was added to a solution of $NiCl_2$ (0.052 g, 0.40 mmol) in

ca. 5 mL of benzene. Neat Et_3N (60 μL, 0.40 mmol) was added to the reaction mixture. The resulting solution was allowed to heat at 65 °C temperature for 20 h. The reaction mixture was subsequently filtered through Celite. The filtrate solution was collected and the volatile components were removed under vacuum. The remaining residue was washed with cold (-30 °C) pentane (2 × 3 mL) and dried *in vacuo* to obtain **2-8** (0.21 g, 90% yield) as an orange solid. ^{1}H NMR (500 MHz, benzene-d_6): δ 8.19 (m, 2 H, H_{arom}), 7.94 (m, 2 H, H_{arom}), 7.64 (m, 2 H, H_{arom}), 7.42 (m, 2 H, H_{arom}), 7.31 (m, 2 H, H_{arom}), 7.21 (m, 2 H, H_{arom}), 7.09-6.98 (6 H, H_{arom}), 1.75 – 0.87 (22 H, P*Cy*), 0.64 (s, 3 H, Si*Me*). ^{13}C{^{1}H} NMR (125.8 MHz, benzene-d_6): δ 132.7 (C_{arom}), 132.6 (C_{arom}), 131.8 (C_{arom}), 131.7 (C_{arom}), 130.8 (CH_{arom}), 130.5 (CH_{arom}), 130.3 (CH_{arom}), 130.1 (CH_{arom}), 127.5 (CH_{arom}), 127.4 (CH_{arom}), 127.3 (CH_{arom}), 127.0 (CH_{arom}), 126.9 (CH_{arom}), 126.8 (CH_{arom}), 126.7 (CH_{arom}), 126.3 (CH_{arom}), 126.2 (CH_{arom}), 126.1 (CH_{arom}), 34.5 (d, CH_{Cy}, J = 20 Hz), 32.8 (d, CH_{Cy}, J = 18 Hz), 28.3-24.3 (CH_{2Cy}), 4.3 (Si*Me*). ^{31}P{^{1}H} NMR (202.5 MHz, benzene-d_6): δ 60.4 (d, 1 P, $^2J_{PP}$ = 261 Hz), 41.6 (d, 1 P, $^2J_{PP}$ = 261 Hz). ^{29}Si NMR (99.4 MHz, benzene-d_6): δ 58.7.

(Cy-PSiP'-Ph)PtMe (2-9). A solution of **2-6** (0.19 g, 0.24 mmol) in ca. 3 mL of benzene was treated with MeMgBr (3.0 M in THF, 80 μL, 0.24 mmol). The reaction mixture was allowed to stand at room temperature for 45 min, and was subsequently filtered through Celite. The filtrate solution was collected and the volatile components were removed under vacuum. The remaining residue was washed with cold (-30 °C) pentane (2 × 3 mL) and dried *in vacuo* to obtain **2-9** (0.18 g, 91% yield) as a brown solid. ^{1}H NMR (500 MHz, benzene-d_6): 8.22 (m, 1 H, H_{arom}), 8.11-8.01 (4 H, H_{arom}), 7.61 (m, 3 H, H_{arom}), 7.48 (m, 2 H, H_{arom}), 7.32 (m, 3 H, H_{arom}), 7,06-6.10 (5 H, H_{arom}), 1.80-0.91 (22

H, P*Cy*), 0.54 (s with Pt satellites, 3 H, Pt*Me*, $^{2}J_{HPt}$ = 21 Hz), 0.14 (s, 3 H, Si*Me*). $^{13}C\{^{1}H\}$ NMR (125.8 MHz, benzene-d_6): 155.2 (C_{arom}), 144.0 (C_{arom}), 134.9 (CH_{arom}), 134.3 (CH_{arom}), 133.2 (CH_{arom}), 132.1 (CH_{arom}), 131.2 (CH_{arom}), 130.1 (CH_{arom}), 129.7 (CH_{arom}), 38.2 (d, CH_{Cy}, J = 34 Hz), 37.8 (d, CH_{Cy}, J = 28 Hz), 30.4-26.0 (CH_{2Cy}), 7.3 (Pt*Me*), 1.2 (Si*Me*). $^{31}P\{^{1}H\}$ NMR (202.5 MHz, benzene-d_6): AB spin system; δ A = 62.7 ($^{1}J_{P\text{-}Pt}$ = 3076 Hz), δ B 51.3 ($^{1}J_{P\text{-}Pt}$ = 2921 Hz), $^{2}J_{PP}$ = -373 Hz. ^{29}Si NMR (99.4 MHz, benzene-d_6): δ 37.7.

(Cy-PSiP'-Ph)PdMe (2-10). A solution of **2-7** (0.055 g, 0.076 mmol) in ca. 2 mL of benzene was treated with MeMgBr (3.0 M in THF, 25 μL, 0.076 mmol). The reaction mixture was allowed to stand at room temperature for 45 min, and was subsequently filtered through Celite. The filtrate solution was collected and the volatile components were removed under vacuum. The remaining residue was washed with cold (-30 °C) pentane (2 × 3 mL) and dried *in vacuo* to obtain **2-10** (0.046 g, 83% yield) as a brown solid. $^{31}P\{^{1}H\}$ NMR (202.5 MHz, benzene-d_6): δ 65.3 (d, 1 P, ^{2}J = 360 Hz), 43.2 (d, 1 P, ^{2}J = 360 Hz).

(Cy-PSiP'-Ph)NiMe (2-11). A solution of **2-8** (0.044 g, 0.065 mmol) in ca. 2 mL of benzene was treated with MeMgBr (3.0 M in THF, 22 μL, 0.065 mmol). The reaction mixture was allowed to stand at room temperature for 45 min, and was subsequently filtered through Celite. The filtrate solution was collected and the volatile components were removed under vacuum. The remaining residue was washed with cold (-30 °C) pentane (2 × 3 mL) and dried *in vacuo* to obtain **2-11** (0.038 g, 86% yield) as a light brown solid. ^{1}H NMR (500 MHz, benzene-d_6): δ 8.21 (m, 2 H, H_{arom}), 7.30 (m, 2 H, H_{arom}), 7.62 (m, 2 H, H_{arom}), 7.40 (m, 3 H, H_{arom}), 7.33 (m, 2 H, H_{arom}), 7.10-6.80 (7 H,

*H*arom), 2.85-1.47 (22 H, P*Cy*), 1.26 (s, 3 H, Ni*Me*), 0.56 (s, 3 H, Si*Me*). $^{13}C\{^{1}H\}$ NMR (125.8 MHz, benzene-d_6): δ 134.8 (*C*arom), 134.6 (*C*arom), 133.6 (*C*arom), 133.5 (*C*arom), 132.6 (*C*Harom), 132.5 (*C*Harom), 132.3 (*C*Harom), 132.0 (*C*Harom), 131.7 (*C*Harom), 130.8 (*C*Harom), 130.1 (*C*Harom), 129.3 (*C*Harom), 129.1 (*C*Harom), 36.4 (d, *C*HCy, J = 34 Hz), 34.8 (d, *C*HCy, J = 33 Hz), 30.2-24.8 (*C*H2Cy), 7.8 (Ni*Me*), 2.6 (Si*Me*). $^{31}P\{^{1}H\}$ NMR (202.5 MHz, benzene-d_6): δ 66.0 (d, 1 P, $^{2}J_{PP}$ = 268 Hz), 54.5 (d, 1 P, $^{2}J_{PP}$ = 268 Hz).

(Cy-PSiP'-Ph)PdPh (2-12). A solution of **2-7** (0.10 g, 0.14 mmol) in ca. 3 mL of benzene was treated with PhLi (1.8 M in $^{n}Bu_2O$, 78 μL, 0.14 mmol). The reaction mixture was allowed to stand at room temperature for 45 min, and was subsequently filtered through Celite. The filtrate solution was collected and the volatile components were removed under vacuum. The remaining residue was washed with cold (-30 °C) pentane (2 × 3 mL) and dried *in vacuo* to obtain **2-12** (0.090 g, 89% yield) as a brown solid. $^{31}P\{^{1}H\}$ NMR (202.5 MHz, benzene-d_6): δ 65.2 (d, 1 P, $^{2}J_{PP}$ = 359 Hz), 51.2 (d, 1 P, $^{2}J_{PP}$ = 359 Hz).

(Cy-PSiP'-Ph)NiPh (2-13). A solution of **2-8** (0.076 g, 0.11 mmol) in ca. 3 mL of benzene was treated with PhLi (1.8 M in $^{n}Bu_2O$, 63 μL, 0.11 mmol). The reaction mixture was allowed to stand at room temperature for 45 min, and was subsequently filtered through Celite. The filtrate solution was collected and the volatile components were removed under vacuum. The remaining residue was washed with cold (-30 °C) pentane (2 × 3 mL) and dried *in vacuo* to obtain **2-13** (0.068 g, 89% yield) as a brown solid. ^{1}H NMR (500 MHz, benzene-d_6): δ 8.15 (m, 2 H, *H*arom), 7.71 (m, 2 H, *H*arom), 7.50 (m, 2 H, *H*arom), 7.45 (br d, 1 H, J = 8 Hz, *H*arom), 7.39 (m, 2 H, *H*arom), 7.26 (m, 2 H, *H*arom), 7.19 (m, 2 H, *H*arom), 7.05 (m, 3 H, *H*arom), 6.98 (m, 2 H, *H*arom), 2.33-0.84 (22 H,

P*Cy*), 0.63 (s, 3 H, Si*Me*). $^{13}C\{^{1}H\}$ NMR (125.8 MHz, benzene-d_6): δ 135.0 (C_{arom}), 134.9 (C_{arom}), 133.7 (C_{arom}), 133.5 (C_{arom}), 133.4 (CH_{arom}), 133.1 (CH_{arom}), 131.5 (CH_{arom}), 130.6 (CH_{arom}), 130.5 (CH_{arom}), 129.6 (CH_{arom}), 129.5 (CH_{arom}), 129.2 (CH_{arom}), 129.1 (CH_{arom}), 126.3 (CH_{arom}), 121.9 (CH_{arom}), 36.0 (d, CH_{Cy}, J = 21 Hz), 33.0-26.9 (CH_{2Cy}), 7.0 (Si*Me*). $^{31}P\{^{1}H\}$ NMR (202.5 MHz, benzene-d_6): δ 62.6 (d, 1 P, $^{2}J_{PP}$ = 248 Hz), 51.6 (d, 1 P, $^{2}J_{PP}$ = 248 Hz). ^{29}Si NMR (99.4 MHz, benzene-d_6): δ 68.2.

(Cy-PSiP'-Ph)Pt(NH_2) (2-14). A solution of **2-6** (0.15 g, 0.19 mmol) in ca. 3 mL of benzene was treated with a suspension of $LiNH_2$ (0.022 g, 0.95 mmol) in ca. 3 mL of benzene. The resulting solution was allowed to stir for 18 h at room temperature. The reaction mixture was subsequently filtered through Celite. The filtrate solution was collected and the volatile components were removed under vacuum. The remaining residue was washed with cold (-30 °C) pentane (2 × 3 mL) and dried *in vacuo* to obtain **2-14** (0.13 g, 82% yield) as a yellow solid. ^{1}H NMR (500 MHz, benzene-d_6): δ 8.01 (m, 4 H, H_{arom}), 7.69 (m, 2 H, H_{arom}), 7.49 (m, 2 H, H_{arom}), 7.3 (m, 4 H, H_{arom}), 7.22-7.18 (2 H, H_{arom}), 7.13-6.88 (9 H, H_{arom}), 2.56 (m, 2 H, NH_2), 2.34-0.91 (22 H, P*Cy*), 0.57 (s with Pt satellites, 3 H, Si*Me,* $^{2}J_{HPt}$ = 21 Hz). $^{13}C\{^{1}H\}$ NMR (125.8 MHz, benzene-d_6): δ 134.3 (C_{arom}), 134.1 (C_{arom}), 134.0 (C_{arom}), 133.5 (C_{arom}), 133.3 (CH_{arom}), 133.1 (CH_{arom}), 132.8 (CH_{arom}), 132.5 (CH_{arom}), 131.3 (CH_{arom}), 130.2 (CH_{arom}), 129.2 (CH_{arom}), 129.0 (CH_{arom}), 128.2 (CH_{arom}), 128.1 (CH_{arom}), 127.9 (CH_{arom}), 36.7 (d, CH_{Cy}, J = 40 Hz), 29.5-22.6 (CH_{2Cy}), 7.5 (Si*Me*). $^{31}P\{^{1}H\}$ NMR (202.5 MHz, benzene-d_6): AB spin system; δ A = 64.8 ($^{1}J_{PPt}$ = 3108 Hz), δ B = 59.2 ($^{1}J_{PPt}$ = 2984 Hz), $^{2}J_{PP}$ = -394 Hz. ^{29}Si NMR (99.4 MHz, benzene-d_6): δ 35.7.

(Cy-PSiP'-Ph)Pt(NHPh) (2-15). A solution of **2-6** (0.024 g, 0.029 mmol) in ca. 2 mL of benzene was treated with a slurry of LiNHPh (0.014 g, 0.15 mmol) in ca. 2 mL of benzene. The reaction mixture was allowed to stand at room temperature for 20 h, after which the solution was dark orange in color. The reaction mixture was filtered through Celite. The filtered solution was collected and the volatile components were removed under vacuum. The remaining residue was washed with cold (-30 °C) pentane (2 × 3 mL) and dried *in vacuo* to obtain **2-15** (0.019 g, 79% yield) as a yellow solid. ^{1}H NMR (500 MHz, benzene-d_6): δ 8.10 – 8.03 (3 H, H_{arom}), 7.67 (m, 2 H, H_{arom}), 7.46 (m, 2 H, H_{arom}), 7.34 (m, 1 H, H_{arom}), 7.30 (m, 1 H, H_{arom}), 7.18 (m, 2 H, H_{arom}), 7.07 (m, 2 H, H_{arom}), 7.03-6.93 (6 H, H_{arom}), 6.71 (m, 2 H, H_{arom}), 6.36 (d, 2 H, H_{arom}, J = 8 Hz), 3.17 (m, 1 H, N*H*), 1.68-0.87 (22 H, P*Cy*), 0.57 (s with Pt satellites, 3 H, Si*Me*, $^{2}J_{HPt}$ = 11 Hz). ^{13}C{^{1}H} NMR (125.8 MHz, benzene-d_6): δ 135.0 (C_{arom}), 134.9 (C_{arom}), 134.8 (C_{arom}), 134.7 (C_{arom}), 134.2 (C_{arom}), 134.1 (C_{arom}), 134.0 (CH_{arom}), 133.8 (CH_{arom}), 133.4 (CH_{arom}), 133.3 (CH_{arom}), 133.2 (CH_{arom}), 133.1 (CH_{arom}), 132.0 (CH_{arom}), 131.1 (CH_{arom}), 131.0 (CH_{arom}), 130.9 (CH_{arom}), 130.0 (CH_{arom}), 129.9 (CH_{arom}), 129.7 (CH_{arom}), 129.6 (CH_{arom}), 129.5 (CH_{arom}), 129.4 (CH_{arom}), 37.6 (d, CH_{Cy}, J = 24 Hz), 37.3 (d, CH_{Cy}, J = 24 Hz), 30.2-26.5 (CH_{2Cy}), 7.2 (Si*Me*). ^{31}P{^{1}H} NMR (202.5 MHz, benzene-d_6): AB spin system; δ A = 62.1 ($^{1}J_{PPt}$ = 3200 Hz), δ B = 51.5 ($^{1}J_{PPt}$ = 2878 Hz), $^{2}J_{PP}$ = -398 Hz. ^{29}Si NMR (99.4 MHz, benzene-d_6): δ 39.9. ^{15}N NMR (50.7 MHz, benzene-d_6): δ -325.7.

[κ^2-(2-Cy$_2$*P*C$_6$H$_4$)*Si*Me(NHPh)]Pd[(κ^2-(2-Ph$_2$*PC*$_6$H$_4$)] + [κ^2-(2-Ph$_2$*P*C$_6$H$_4$)*Si*Me(NH-Ph)]Pd[(κ^2-(2-Cy$_2$*PC*$_6$H$_4$)] (2-16a,b). A solution of **2-7** (0.014 g, 0.020 mmol) in ca. 2 mL of benzene was treated with a slurry of LiNHPh (0.010 g, 0.099 mmol) in ca. 2 mL of benzene. The reaction mixture was allowed to stand at room

temperature for 45 minutes, after which it was filtered through Celite. The filtrate solution was collected and the volatile components were removed under vacuum. The remaining residue was washed with cold (-30 °C) pentane (2 × 3 mL) and dried *in vacuo* to obtain **2-16a**,**b** (0.013 g, 87% yield) as a brown solid. NMR analysis of **2-16** was consistent with the formation of a 1:1 mixture of isomers, **2-16a** and **2-16b**, resulting from Si-C(sp^2) cleavage in the PSiP' ligand backbone. ^{1}H NMR (500 MHz, benzene-d_6): δ 8.39-8.29 (H_{arom}), 7.87-7.25 (H_{arom}), 7.09-6.60 (H_{arom}), 4.25 (N*H*) 3.20 (N*H*), 2.18-0.89 (P*Cy*), 0.76 (s, Si*Me*), 0.74 (s, Si*Me*). ^{13}C{^{1}H} NMR (125.8 MHz, benzene-d_6): δ 134.2 (C_{arom}), 134.0 (C_{arom}), 133.8 (C_{arom}), 133.6 (C_{arom}), 133.5 (CH_{arom}), 133.2 (CH_{arom}, 133.04 (CH_{arom}), 130.4 (CH_{arom}), 129.8 (CH_{arom}), 129.4 (CH_{arom}), 117.8 (CH_{arom}), 117.5 (CH_{arom}), 117.2 (CH_{arom}), 116.9 (CH_{arom}), 106.0 (CH_{arom}), 29.8-26.1 (CH_{2Cy}), 5.1 (Si*Me*), 4.8 (Si*Me*). ^{31}P{^{1}H} NMR (202.5 MHz, benzene-d_6): δ 72.5 (d, 1 P, $^2J_{PP}$ = 21 Hz), -45.1 (d, 1 P, $^2J_{PP}$ = 21 Hz), 58.9 (d, 1 P, $^2J_{PP}$ = 21 Hz), -34.5 (d, 1 P, $^2J_{PP}$ = 21 Hz). ^{29}Si NMR (99.4 MHz, benzene-d_6): δ 32.5, 37.6.

(Cy-PSiP'-Ph)Pd(NH_2) (2-17). A solution of **2-7** (0.021 g, 0.029 mmol) in ca. 3 mL of benzene was treated with a slurry of $LiNH_2$ (0.007 g, 0.29 mmol) in ca. 3 mL of benzene. The reaction mixture was allowed to stand at room temperature for 18 h, after which it was filtered through Celite. The filtrate solution was collected and the volatile components were removed under vacuum. The remaining residue was washed with cold (-30 °C) pentane (2 × 3 mL) and dried *in vacuo* to obtain **2-17** (0.018 g, 84% yield) as a brown solid. ^{1}H NMR (500 MHz, benzene-d_6): δ 8.08 (m, 2 H, H_{arom}), 8.00 (d, 1 H, H_{arom}, J = 7 Hz), 7.95 (d, 1 H, H_{arom}, J = 7 Hz), 7.77-7.67 (3 H, H_{arom}), 7.44 (m, 1 H, H_{arom}), 7.39 (m, 1 H, H_{arom}), 7.31 (m, 1 H, H_{arom}), 7.19 (m, 3 H, H_{arom}), 7.10-6.76 (5 H, H_{arom}), 4.46

(m, 2 H, N*H*), 2.5-0.85 (22 H, P*Cy*), 0.56 (s, 3 H, Si*Me*). $^{13}C\{^{1}H\}$ NMR (125.8 MHz, benzene-d_6): δ 135.2 (C_{arom}), 135.1 (C_{arom}), 134.8 (C_{arom}), 134.7 (C_{arom}), 134.3 (CH_{arom}), 134.0 (CH_{arom}), 133.8 (CH_{arom}), 133.6 (CH_{arom}), 133.4 (CH_{arom}), 132.2 (CH_{arom}), 131.2 (CH_{arom}), 131.0 (CH_{arom}), 130.6 (CH_{arom}), 130.2 (CH_{arom}), 129.9 (CH_{arom}), 129.6 (CH_{arom}), 129.2 (CH_{arom}), 37.6 (d, CH_{Cy}, J = 57 Hz), 36.6 (d, CH_{Cy}, J = 57 Hz), 30.5-23.2 (CH_{2Cy}), 8.4 (Si*Me*). $^{31}P\{^{1}H\}$ NMR (202.5 MHz, benzene-d_6): δ 63.1 (d, 1 P, $^{2}J_{PP}$ = 350 Hz), 42.4 (d, 1 P, $^{2}J_{PP}$ = 350 Hz). ^{29}Si NMR (99.4 MHz, benzene-d_6): δ 55.8.

[κ²-(2-Cy₂*P*C₆H₄)*Si*Me(NH^{t}Bu)]Pd[(κ²-(2-Ph₂*P*C₆H₄)] + [κ²-(2-Ph₂*P*C₆H₄)*Si*Me(NH-^{t}Bu)]Pd[(κ²-(2-Cy₂*P*C₆H₄)] (2-18a,b). A solution of **2-7** (0.011 g, 0.017 mmol) in ca. 2 mL of benzene was treated with a slurry of LiNH^{t}Bu (0.007 g, 0.085 mmol) in ca. 2 mL of benzene. The reaction mixture was allowed to stand at room temperature for 45 minutes, after which it was filtered through Celite. The filtrate solution was collected and the volatile components were removed under vacuum. The remaining residue was washed with cold (-30 °C) pentane (2 × 3 mL) and dried *in vacuo* to obtain **2-18a**,**b** (0.010 g, 86% yield) as a brown solid. NMR analysis of **2-18** was consistent with the formation of a 1:1 mixture of isomers, **2-18a** and **2-18b**, resulting from Si-C(sp^2) cleavage in the PSiP' ligand backbone. ^{1}H NMR (500 MHz, benzene-d_6): δ 8.50-8.35 (H_{arom}), 8.08 (m, H_{arom}), 7.80-7.66 (H_{arom}), 7.54-7.18 (H_{arom}), 7.14-6.97 (H_{arom}), 2.31-1.4 (P*Cy*), 1.37-1.22 (CMe_3), 0.97 (s, Si*Me*), 0.81 (s, Si*Me*). $^{13}C\{^{1}H\}$ NMR (125.8 MHz, benzene-d_6): δ 136.1 (C_{arom}), 135.7 (C_{arom}), 135.3 (C_{arom}), 134.4 (C_{arom}), 134.3 (CH_{arom}), 134.1 (CH_{arom}), 133.9 (CH_{arom}), 133.6 (CH_{arom}), 133.4 (CH_{arom}), 133.2 (CH_{arom}), 132.9 (CH_{arom}), 131.5 (CH_{arom}), 129.9 (CH_{arom}), 129.4 (CH_{arom}), 125.5 (CH_{arom}), 124.4 (CH_{arom}), 37.7 (CMe_3), 36.8 (d, CH_{Cy}, J = 29 Hz), 34.7-34.1 (CH_{Cy}), 32.3 (d, CH_{Cy},

J = 43 Hz), 31.2-26.1 (*C*H$_{2Cy}$) ^{31}P{^{1}H} NMR (202.5 MHz, benzene-d$_6$): δ 69.2 (d, 1 P, $^{2}J_{PP}$ = 22 Hz, **2-18a**), -45.9 (d, 1 P, $^{2}J_{PP}$ = 22 Hz, **2-18a**), 55.5 (d, 1 P, $^{2}J_{PP}$ = 21 Hz, **2-18b**), -36.1 (d, 1 P, $^{2}J_{PP}$ = 21 Hz, **2-18b**). ^{29}Si NMR (99.4 MHz, benzene-*d*$_6$): δ 30.1, 29.8.

(Cy-PSiP'-Ph)Ni(NH$_2$) (2-19). A solution of **2-8** (0.022 g, 0.033 mmol) in ca. 2 mL of benzene was treated with a slurry of LiNH$_2$ (0.008 g, 0.33 mmol) in ca. 3 mL of benzene. The resulting reaction mixture was allowed to stand at room temperature for 20 h, after which it was filtered through Celite. The filtrate solution was collected and the volatile components were removed under vacuum. The remaining residue was washed with cold (-30 °C) pentane (2 × 3 mL) and dried *in vacuo* to obtain **2-19** (0.016 g, 73% yield) as an orange solid. ^{1}H NMR (500 MHz, benzene-*d*$_6$): δ 8.19 (m ,2 H, *H*$_{arom}$), 7.94 (t, 2 H, *H*$_{arom,}$ *J* = 7 Hz), 7.64 (m, 2 H, *H*$_{arom}$), 7.43 (t, 2 H, *H*$_{arom,}$ *J* = 7 Hz), 7.30 (m, 2 H, *H*$_{arom}$), 7.20 (m, 2 H, *H*$_{arom}$), 7.13-6.98 (6 H, *H*$_{arom}$), 2.65 (m, 2 H, N*H*$_2$), 2.45-0.87 (22 H, P*Cy*), 0.65 (s, 3 H, Si*Me*). ^{13}C{^{1}H} NMR (125.8 MHz, benzene-*d*$_6$): δ 135.3 (*C*$_{arom}$), 135.2 (*C*$_{arom}$), 134.3 (*C*$_{arom}$), 134.2 (*C*$_{arom}$), 133.5 (*C*H$_{arom}$), 133.1 (*C*H$_{arom}$), 132.9 (*C*H$_{arom}$), 132.7 (*C*H$_{arom}$), 131.7 (*C*H$_{arom}$), 131.3 (*C*H$_{arom}$), 130.9 (*C*H$_{arom}$), 130.2 (*C*H$_{arom}$), 130.1 (*C*H$_{arom}$), 130.0 (*C*H$_{arom}$), 129.6 (*C*H$_{arom}$), 129.6 (*C*H$_{arom}$), 129.4 (*C*H$_{arom}$), 129.3 (*C*H$_{arom}$), 37.1 (d, *C*H$_{Cy,}$ *J* = 26 Hz), 35.3 (d, *C*H$_{Cy,}$ *J* = 26 Hz) 30.9-26.9 (P*Cy*), 6.9 (Si*Me*). ^{31}P{^{1}H} NMR (202.5 MHz, benzene-*d*$_6$): δ 60.4 (d, 1 P, $^{2}J_{PP}$ = 262 Hz), 41.6 (d, 1 P, $^{2}J_{PP}$ = 262 Hz). ^{29}Si NMR (99.4 MHz, benzene-*d*$_6$): δ 59.6.

(Cy-PSiP'-Ph]Ni(NHPh) (2-20). A solution of **2-8** (0.025 g, 0.038 mmol) in ca. 3 mL of benzene was treated with a slurry of LiNHPh (0.008 g, 0.33 mmol) in ca. 3 mL of benzene. The reaction mixture was allowed to stand at room temperature for 4 h, after

which it was filtered through Celite. The filtrate solution was collected and the volatile components were removed under vacuum. The remaining residue was washed with cold (-30 °C) pentane (2 × 3 mL) and dried *in vacuo* to obtain **2-20** (0.020 g, 78 % yield) as a dark red solid. ^{1}H NMR (500 MHz, benzene-d_6): δ 8.09 (m, 1 H, H_{arom}), 7.97 (d, 1 H, H_{arom}, J = 7 Hz), 7.41 (m, 2 H, H_{arom}), 7.34 (m, 2 H, H_{arom}), 7.20 (m, 2 H, H_{arom}), 7.12-6.98 (10 H, H_{arom}), 6.84 (d, 1 H, $H_{arom,}$ J = 8 Hz), 6.56 (m, 2 H, H_{arom}), 6.35 (m, 2 H H_{arom}), 2.76 (br s, 1 H, N*H*), 2.34-0.86 (22 H, P*Cy*), 0.62 (s, 3 H, Si*Me*). ^{13}C{^{1}H} NMR (125.8 MHz, benzene-d_6): δ 135.1 (C_{arom}), 134.9 (C_{arom}), 133.3 (C_{arom}), 133.2 (C_{arom}), 133.1 (C_{arom}), 133.0 (C_{arom}),132. 9 (C_{arom}). 131.1 (CH$_{arom}$), 131.0 (CH$_{arom}$), 130.9 (CH$_{arom}$), 130.5 (CH$_{arom}$), 130.1 (CH$_{arom}$), 130.0 (CH$_{arom}$), 129.9 (CH$_{arom}$), 129.5 (CH$_{arom}$), 129.4 (CH$_{arom}$), 129.2 (CH$_{arom}$), 117.6 (CH$_{arom}$), 115.6 (CH$_{arom}$), 111.0 (CH$_{arom}$), 36.9 (d, CH$_{Cy}$, J = 11 Hz), 36.8 (d, CH$_{Cy}$, J = 11 Hz) 30.7-27.0 (CH$_{2Cy}$), 6.0 (Si*Me*). ^{31}P{^{1}H} NMR (202.5 MHz, benzene-d_6): δ 57.5 (d, 1 P, $^{2}J_{PP}$ = 285 Hz), 41.2 (d, 1 P, $^{2}J_{PP}$ = 285 Hz. ^{29}Si NMR (99.4 MHz, benzene-d_6): δ 58.0. ^{15}N NMR (50.7 MHz, benzene-d_6): δ -317.0.

(Ph-PSiP*-^{i}Pr)PtCl (2-21). A room temperature solution of **2-4** (0.14 g, 0.31 mmol) in ca. 2 mL of benzene was treated with a solution of (COD)PtBnCl (0.14 g, 0.31 mmol) in ca. 2 mL of benzene. The reaction mixture was allowed to stand at room temperature for 18 h, after which the volatile components were removed under vacuum and the remaining residue was washed with cold (-30 °C) pentane (2 × 3 mL) and dried *in vacuo* to obtain **2-21** (0.12 g, 84% yield) as a yellow solid. ^{1}H NMR (500 MHz, benzene-d_6): δ 7.90-7.78 (overlapping resonances, 3 H, H_{arom}), 7.77-7.57 (overlapping resonances, 3 H, H_{arom}), 7.50 (d, 2 H, H_{arom}, J = 7 Hz), 7.31-7.23 (overlapping resonances, 3 H,

H_{arom}), 6.90 (overlapping resonances, 3 H, H_{arom}), 2.20 (s, 2 H, PCH_2), 1.41 (d, 3 H, CHMe_2, J = 7 Hz), 1.34 (d, 3 H, CHMe_2, J = 7 Hz), 1.19 (d, 3 H, CHMe_2, J = 7 Hz), 1.14 (d, 3 H, CHMe_2, J = 7 Hz), 1.03-0.90 (m, 2 H, CHMe$_2$), 0.34 (s with Pt satellites, 3 H, SiMe, $^3J_{HPt}$ = 13 Hz). $^{13}C\{^1H\}$ NMR (125.8 MHz, benzene-d_6): δ 139.0 (C_{arom}), 138.0 (C_{arom}), 137.0 (C_{arom}), 136.0 (C_{arom}), 134.6 (CH$_{arom}$), 134.4 (CH$_{arom}$), 133.6 (CH$_{arom}$), 133.5 (CH$_{arom}$), 132.9 (CH$_{arom}$), 132.8 (CH$_{arom}$), 130.41 (CH$_{arom}$), 130.0 (CH$_{arom}$), 28.1 (PCH$_2$), 26.8 (CHMe_3), 26.6 (CHMe_3), 26.2 (CHMe_3), 26.0 (CHMe_3), 18.5 (CHMe$_3$), 8.5 (SiMe). $^{31}P\{^1H\}$ NMR (202.5 MHz, benzene-d_6): δ 54.1 (d with Pt satellites, 1 P, $^1J_{PPt}$ = 1542 Hz, $^2J_{PP}$ = 411 Hz), -3.8 (d with Pt satellites, 1 P, $^1J_{PPt}$ = 1346 Hz, $^2J_{PP}$ = 411 Hz). ^{29}Si NMR (99.4 MHz, benzene-d_6): -30.5 (s with Pt satellites, $^1J_{SiPt}$ = 1250 Hz)

(Cy-PSiP*-^{i}Pr)PtCl (2-22). A room temperature solution of **2-5** (0.11 g, 0.24 mmol) in ca. 3 mL of benzene was treated with a solution of (COD)PtBnCl (0.10 g, 024 mmol) in ca. 3 mL of benzene. The reaction mixture was allowed to stand at room temperature for 24 h, after which the volatile components were removed under vacuum and the remaining residue was washed with cold (-30 °C) pentane (2 × 3 mL) and dried *in vacuo* to obtain **2-22** (0.091 g, 84% yield) as an orange solid. ^{1}H NMR (500 MHz, benzene-d_6): δ 7.53 (d, 1 H, H_{arom}, J = 7 Hz), 7.39 (t, 1 H, H_{arom}, J = 7 Hz), 7.09 (m, 1 H, H_{arom}), 6.99 (m, 1 H, H_{arom}), 2.33 (m, 2 H, PCH_2), 1.83-1.35 (22 H, PCy), 1.32 (d, 3 H, CHMe_2, J = 7 Hz), 1.28 (d, 3 H, CHMe_2, J = 7 Hz), 1.17-1.15 (overlapping resonances, 2 H, CHMe$_2$), 0.96 (d, 3 H, CHMe_2, J = 7 Hz), 0.93 (d, 3 H, CHMe_2, J = 7 Hz), 0.60 (s, 3 H, SiMe). $^{13}C\{^1H\}$ NMR (125.8 MHz, benzene-d_6): δ 132.3 (C_{arom}), 132.2 (C_{arom}), 131.6 (CH$_{arom}$), 130.5 (CH$_{arom}$), 129.5 (CH$_{arom}$), 129.4 (CH$_{arom}$), 30.8 (PCH$_2$), 30.1-26.6 (PCy), 19.8 (CHMe_2), 19.1 (CHMe_2), 18.1 (CHMe_2), 4.2 (SiMe). $^{31}P\{^1H\}$ NMR (202.5 MHz,

benzene-d_6): δ 64.1 (d with Pt satellites, 1 P, $^1J_{PPt}$ = 1561 Hz, $^2J_{PP}$ = 390 Hz), -3.0 (d with Pt satellites, 1 P, $^1J_{PPt}$ = 1286 Hz, $^2J_{PP}$ = 390 Hz). ^{29}Si NMR (99.4 MHz, benzene-d_6): δ -29.8 (with Pt satellites, $^1J_{SiPt}$ = 1352 Hz).

(Cy-PSiP*-^{i}Pr)NiCl (2-23). A room temperature solution of **2-5** (0.11 g, 0.24 mmol) in ca. 3 mL of benzene was treated with a solution of $NiCl_2$(DME) (0.055 g, 0.24 mmol) in ca. 3 mL of benzene. Neat Et_3N (35 μL, 0.25 mmol) was added to the reaction mixture. The reaction mixture was allowed to stand at room temperature for 18 h, after which the solution was filtered through Celite. The filtrate solution was retained and the volatile components were removed under vacuum. The remaining residue was washed with cold (-30 °C) pentane (2 × 3 mL) and dried *in vacuo* to obtain **2-23** (0.099 g, 88% yield) as a yellow solid. ^{1}H NMR (500 MHz, benzene-d_6): δ 7.43 (d, 1 H, H_{arom}, J = 14 Hz), 7.37 (m, 1 H, H_{arom}), 7.31 (s, 1 H, H_{arom}), 7.00 (m, 1 H, H_{arom}), 2.65 (m, 2 H, PCH_2), 2.29-1.45 (22 H, P*Cy*), 1.42-1.20 (12 H, CH*Me*$_2$), 1.10-1.03 (2 H, C*H*Me$_2$), 0.54 (s, 3 H, Si*Me*). ^{13}C{^{1}H} NMR (125.8 MHz, benzene-d_6): δ 131.5 (C_{arom}), 131.4 (C_{arom}), 131.1 (CH$_{arom}$), 130.8 (CH$_{arom}$), 130.4 (CH$_{arom}$), 129.7 (CH$_{arom}$), 35.0 (PCH$_2$), 30.8-26.8 (P*Cy*), 23.2 (CH*Me*$_2$), 14.8 (C*H*Me$_2$), 9.1 (Si*Me*). ^{31}P{^{1}H} NMR (202.5 MHz, benzene-d_6): δ 51.9 (d, 1 P, $^2J_{PP}$ = 278 Hz), -21.1 (d, 1 P, $^2J_{PP}$ = 278 Hz). ^{29}Si NMR (99.4 MHz, benzene-d_6): δ -2.3.

[(Cy-PSiP*-^{i}Pr)PdCl]$_n$ (2-24a, n = 1; b, n = 2). A room temperature solution of **2-5** (0.13 g, 0.28 mmol) in ca. 3 mL of benzene was treated with a solution of [Pd(η^3-C_3H_5)Cl]$_2$ (0.052 g, 0.14 mmol) in ca. 3 mL of benzene. The resulting reaction mixture was allowed to stand at room temperature for 24 h. The volatile components of the reaction mixture were subsequently removed under vacuum and the remaining residue

was washed with cold (-30 °C) pentane (2 × 3 mL) and dried *in vacuo* to obtain **2-24** an orange solid (0.11 g). NMR analysis of **2-24** indicated that this compound is formed as a 1:5 mixture of the monomeric complex **2-24a** and the dimer **2-24b**. Crystallization of the crude material from Et_2O at -30 °C afforded pure **2-24b** (0.060 g, 45%). NMR data are reported for the mixture. ^{1}H NMR (500 MHz, benzene-d_6): δ 7.60 (d, H_{arom}, J = 7 Hz), 7.42 (m, H_{arom}), 7.35 (br m, H_{arom}), 7.31 (m, H_{arom}), 7.23 (m, H_{arom}) 7.14-7.09 (H_{arom}), 6.99 (s, H_{arom}), 3.11 (m, PCH_2), 2.87 (m, CHMe$_2$), 2.77 (m, CHMe$_2$), 2.57 (m, CHMe$_2$), 2.40 (br m, PCH$_2$), 2.05 – 0.92 (PCy + CHMe_2), 0.74 (s, SiMe), 0.57 (s, SiMe). ^{13}C{^{1}H} NMR (125.8 MHz, benzene-d_6): δ 133.4 (C_{arom}), 133.2 (C_{arom}), 133.2 (C_{arom}), 131.5 (CH$_{arom}$), 131.3 (CH$_{arom}$), 129.7 (CH$_{arom}$), 129.6 (CH$_{arom}$), 37.8 (d, CH$_{Cy}$, J = 21 Hz), 36.5 (d, CH$_{Cy}$, J = 21 Hz), 31.4-27.14 (CH$_{2Cy}$) 24.0 (CHMe$_2$), 23.2 (PCH$_2$), 23.2 (CHMe$_2$), 22.4 (CHMe$_2$), 20.1 (CHMe$_2$), 14.8 (SiMe), 11.2 (SiMe). ^{31}P{^{1}H} NMR (202.5 MHz, benzene-d_6): δ 69.6 (d, $^2J_{PP}$ = 342 Hz, **2-24b**), 30.7 (d, $^2J_{PP}$ = 342 Hz, **2-24b**), 60.2 (d, $^2J_{PP}$ = 378 Hz, **2-24a**), -23.6 (d, $^2J_{PP}$ = 378 Hz, **2-24a**). ^{29}Si NMR (99.4 MHz, benzene-d_6): δ 32.1.

2.4.3: Crystallographic solution and refinement details

Crystallographic data for **2-7** were obtained at 173(±2) K on a Bruker D8/APEX II CCD diffractometer, while for **2-8** and **2-24b** data were obtained at 173(±2) K on a Bruker PLATFORM/APEX II CCD diffractometer. For all three structures graphite-monochromated Mo Kα (λ = 0.71073 Å) radiation was utilized, employing a sample that was mounted in inert oil and transferred to a cold gas stream on the diffractometer. Programs for diffractometer operation, data collection, and data reduction (including

SAINT) were supplied by Bruker. Gaussian integration (face-indexed) was employed as the absorption correction method in each case. All structures were solved by use of the Patterson search/structure expansion and were refined by use of full-matrix least-squares procedures (on F^2) with R_1 based on $F_0^2 \geq 2\sigma(F_0^2)$ and wR_2 based on $F_0^2 \geq -3\sigma(F_0^2)$. For **2-7** and **2-8** anisotropic displacement parameters were employed for all non-hydrogen atoms. For **2-24b**, disorder involving the ^{i}Pr substituents on P4 (C81-C83, C85 and C86) was noted during the solution and refinement process. This disorder was modeled in a satisfactory manner by refining the carbon atoms in question over two positions A and B, with 65 and 35% occupancy, respectively. Two disordered molecules of diethyl ether solvent were also located in the asymmetric unit. The disordered solvent molecules were modeled isotropically over two positions: for O1S and C1S-C4S over two positions A and B with 70 and 30% occupancy, respectively; for O2S and C5S-C8S over two positions A and B with 55 and 45% occupancy, respectively. Distances within the disordered solvent diethyl ether molecules were given idealized target values during refinement: d(O1SA–C1SA) = d(O1SA–C3SA) = d(O1SB–C1SB) = d(O1SB–C3SB) = d(O2SA–C5SA) = d(O2SA–C7SA) = d(O2SB–C5SB) = d(O2SB–C7SB) = 1.46(1) Å; d(C1SA–C2SA) = d(C3SA–C4SA) = d(C1SB–C2SB) = d(C3SB–C4SB) = d(C5SA–C6SA) = d(C7SA–C8SA) = d(C5SB–C6SB) = d(C7SB–C8SB) = 1.54(1) Å; d(O1SA…C2SA) = d(O1SA…C4SA) = d(O1SB…C2SB) = d(O1SB…C4SB) = d(O2SA…C6SA) = d(O2SA…C8SA) = d(O2SB…C6SB) = d(O2SB…C8SB) = 2.43(1) Å; d(C1SA…C3SA) = d(C1SB…C3SB) = d(C5SA…C7SA) = d(C5SB…C7SB) = 2.38(1) Å. Hydrogen atoms were added at calculated positions throughout and refined by use of a riding model employing isotropic displacement parameters based on the isotropic

displacement parameters of the attached atoms. Additional crystallographic information is provided in Appendix A.

Chapter 3 Group 8 and 9 Metal Complexes Supported by Mixed Donor PSiP' Silyl Pincer Ligation

3.1 Introduction

Much like mixed donor pincer complexes of Group 10 metals, Group 8 and 9 metal complexes of this type are also quite prevalent in the literature as was discussed in detail in Chapter 1. Arguably the most notable examples of such mixed donor complexes are the (PNN)Ru species reported by Milstein and coworkers that catalyze various transformations including the dehydrogenative coupling of alcohols and amines and the hydrogenation of organic carbonates, carbamates and formates.[9] As was also discussed in Chapter 1, work in the Turculet group with Group 8 and 9 metal complexes supported by PSiP ligation has led to the isolation of 14-electron trigonal pyramidal (PSiP)Ru^{II} species[138] as well as (PSiP)Ir complexes that undergo facile C-H and N-H bond oxidative addition.[10] In light of the promising reactivity observed for such PSiP ligated metal complexes, the synthesis of Group 8 and 9 metal complexes supported by PSiP' ligands featuring two different types of phosphino donors was pursued. Such "unsymmetrical" PSiP' ligation offers an additional means by which the steric and electronic features of the metal pincer complex can be tuned and may lead to new or possibly enhanced reactivity in group 8 and 9 metal pincer species. Preliminary results toward the synthesis of such complexes are detailed herein.

3.2 Results and Discussion

3.2.1 Attempted synthesis of Ru complexes supported by PSiP' ligation

Given the structural similarities between Cy-PSiP and Cy-PSiP'-Ph ligation, the synthesis of Ru complexes supported by the latter was initially attempted by using the same synthetic route developed for preparing [(Cy-PSiP)RuCl]$_2$.[138] In accordance with this protocol, a solution of [(*p*-cymene)RuCl$_2$]$_2$ was treated with two equiv. of PCy$_3$ to effectively break up the Ru dimer, and the resulting mixture was subsequently treated with (Cy-PSiP'-Ph)H (**2-3**) and Et$_3$N. However, no clean formation of a (Cy-PSiP'-Ph)Ru species was attained by this route. Variations of this reaction where PCy$_3$ and/or Et$_3$N were omitted were similarly unsuccessful, and no isolable Ru species was detected by ^{31}P NMR analysis of the resulting reaction mixtures. Attempts to metalate **2-3** by reaction with a different Ru starting material, (COD)Ru(2-methylallyl)$_2$ were also unsuccessful. Similar reactions utilizing (Ph-PSiP*-^{i}Pr)H (**2-4**) also failed to provide evidence for an isolable Ru complex supported by PSiP' ligation. By comparison, treatment of (Cy-PSiP*-^{i}Pr)H (**2-5**) with (COD)Ru(2-methylallyl)$_2$ in benzene solution (70 °C for 24 h) did lead to the clean (by ^{31}P NMR) formation of a new Ru complex (**3-1**) that gives rise to two ^{31}P{^{1}H} NMR resonances at 82.2 (singlet) and 23.3 ppm (singlet). The observation that the ^{31}P{^{1}H} NMR resonances appear as singlets suggest that only one ligand arm is coordinated to the metal center in **3-1**. While not definitive, it can be speculated that the dicyclohexyl phosphino donor is coordinating to Ru as it would form a more stable five-membered metallacycle as opposed to the four-membered metallacycle that would be

result from coordination of the diisopropyl phosphino group to the metal. The ^{1}H NMR spectrum of the reaction mixture does not contain resonances that can be attributed to free COD, which suggests that the final complex may have COD coordinated to the Ru center. Unfortunately, efforts to purify **3-1** and fully characterize it have thus far proven unsuccessful, and as such a definitive formulation for this complex remains elusive.

3.2.2: Attempted synthesis of Rh and Ir complexes supported by PSiP' ligation

While Ru complexes supported by PSiP' ligation proved relatively elusive, somewhat more success was had at synthesizing Group 9 metal complexes of this type. Treatment of a benzene solution of **2-3** with 0.5 equiv. of $[Rh(COE)_2Cl]_2$ led to the formation of a new Rh-containing product that is tentatively formulated as (Cy-PSiP'-Ph)Rh(H)Cl (**3-2**; Scheme 3-1) on the basis of NMR data. Complex **3-2** was obtained as an orange solid in 84% yield and features a characteristic Rh-*H* resonance at -18.72 ppm (m) in the ^{1}H NMR spectrum (benzene-d_6) of the isolated complex. The presence of a Rh-*H* is consistent with Si-H oxidative addition of **2-3** to the metal center. The ^{31}P{^{1}H} NMR spectrum of **3-2** features two doublets of doublets at 63.7 ($^{1}J_{PRh}$ = 120 Hz, $^{2}J_{PP}$ = 356 Hz) and 42.8 ppm ($^{1}J_{PRh}$ = 120 Hz, $^{2}J_{PP}$ = 356 Hz), consistent with metalation of **2-3** to the Rh center to form a C_1-symmetric complex with chemically inequivalent phosphino donors bound to the metal center in a *trans* fashion.

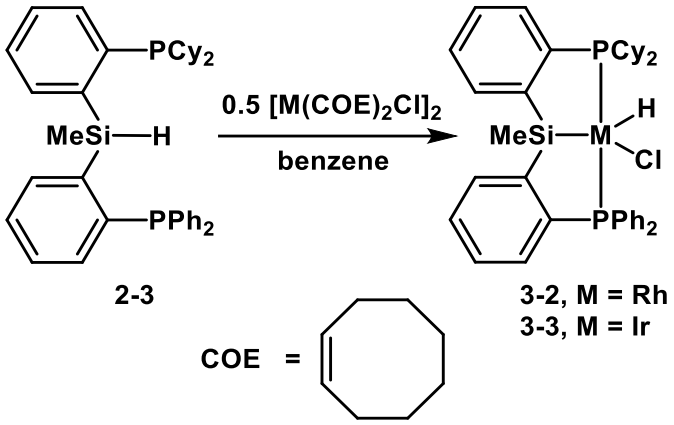

Scheme 3-1. Synthesis of (Cy-PSiP'-Ph)M(H)Cl (M = Rh, Ir).

An analogous Ir complex was also synthesized by treating a benzene solution of **2-3** with 0.5 equiv. of $[Ir(COE)_2Cl]_2$ to obtain (Cy-PSiP'-Ph)Ir(H)Cl (**3-3**; Scheme 3-1), which was isolated as an orange solid in 76% yield (Scheme 3-1). The $^{31}P\{^1H\}$ NMR spectrum of **3-3** contains two doublets at 60.2 and 47.5 ppm ($^2J_{PP}$ = 335 Hz), which is consistent with the formation of a C_1-symmetric Ir complex of Cy-PSiP'-Ph that features chemically inequivalent phosphino donors bound to the metal center in a *trans* fashion. The ^1H NMR spectrum of **3-3** features an Ir-*H* resonance at -23.99 ppm (apparent triplet), which is consistent with Si-H bond oxidative addition of **2-3** to the Ir center.

Attempts to synthesize Group 9 metal complexes supported by R-PSiP*-^{i}Pr ligation (R = Ph, Cy) by an analogous route were met with mixed success. Thus, while the reaction of **2-4** with half an equiv. of $[Rh(COE)_2Cl]_2$ led to the formation of an intractable reaction mixture from which no pure material could be isolated, the analogous reaction with **2-5** led to the clean formation of a new Rh complex that is tentatively formulated as (Cy-PSiP*-^{i}Pr)Rh(H)Cl (**3-4**; Scheme 3-2) on the basis of NMR spectroscopic data. Complex **3-4** was isolated as a dark red solid in 84% yield. The $^{31}P\{^1H\}$ NMR spectrum of **3-4** contains two doublets of doublets at 66.5 ($^1J_{PRh}$ = 117 Hz,

$^2J_{PP}$ = 330 Hz) and 39.0 ppm ($^1J_{PRh}$ = 111 Hz , $^2J_{PP}$ = 330 Hz), which is consistent with a in which the Cy-PSiP*-^{i}Pr ligand is bound to Rh with *trans*-disposed, chemically inequivalent phosphino donors. The ^{1}H NMR spectrum of **3-4** (benzene-d_6) features a Rh-*H* resonance at -17.02 ppm (m), which indicates that Si-H bond oxidative addition of **2-5** has occurred. Given the relatively up-field ^{31}P NMR resonances observed for **3-4**, it is possible that this complex is not a mononuclear species, but rather a dimer analogous to **2-24b** (*cf.* ^{31}P{^{1}H} NMR data for **2-24b**: 69.6 (d, $^2J_{PP}$ = 342 Hz) and 30.7 ppm (d, $^2J_{PP}$ = 342 Hz); Scheme 3-2). Unfortunately X-ray quality crystals of **3-4** have thus far proven elusive.

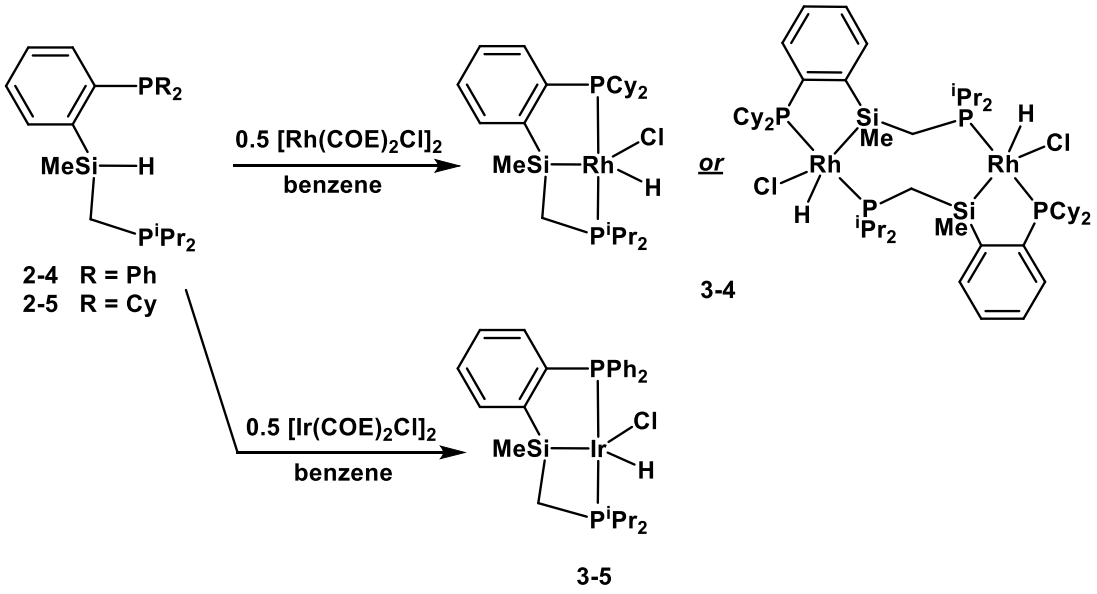

Scheme 3-2. Synthesis of (R-PSiP*-^{i}Pr)M(H)Cl (R = Ph, Cy; M = Rh, Ir) complexes.

Treatment of a benzene solution of **2-4** with 0.5 equiv. of $[Ir(COE)_2Cl]_2$ led to the clean (by ^{31}P NMR) formation of a new Ir complex that is tentatively formulated as (Ph-PSiP*-^{i}Pr)Ir(H)Cl (**3-5**) and was isolated as an orange solid in 83% yield (Scheme 3-2). The ^{31}P{^{1}H} NMR spectrum of **3-5** contains two doublets at 37.8 and -2.3 ppm ($^2J_{PP}$ = 364 Hz), which is consistent with a C_1-symmetric complex featuring chemically

inequivalent phosphino donors bound to the Ir center in a *trans* fashion. The presence of a significantly up-field shifted ^{31}P NMR resonance for **3-5** is unlike the observed data for **3-4**, and lends some support for the formulation of **3-5** as a mononuclear complex featuring a four membered Ir-Si-C-P metallacycle (Scheme 3-2). The ^{1}H NMR spectrum of **3-5** (benzene-d_6) features an Ir-*H* resonance at -22.15 ppm (apparent triplet), which is consistent with Si-H bond oxidative addition of **2-4**. By comparison, an analogous reaction utilizing **2-5** proved unsuccessful.

3.3: Conclusions

Preliminary investigations have indicated that Group 8 and 9 metal complexes supported by PSiP' ligation are synthetically accessible. While the synthesis of Ru complexes proved challenging, the reaction of **2-5** with (COD)Ru(2-methylallyl)$_2$ led to the apparent formation of a (Cy-PSiP*-^{i}Pr)Ru species that remains to be further characterized. More success was attained in the synthesis of Group 9 complexes, where both Cy-PSiP'-Ph and R-PSiP*-^{i}Pr (R = Ph, Cy) ligated species were isolated for Rh and Ir. In the absence of crystallographic data, the formulation of complexes supported by the latter R-PSiP*-^{i}Pr ligand as either mononuclear or dinuclear is tentative, and solution NMR data suggests that while (Ph-PSiP*-^{i}Pr)Ir(H)Cl is monomeric, (Cy-PSiP*-^{i}Pr)Rh(H)Cl is possibly a dimeric species.

Given the proposed structural similarities between complexes of the type (PSiP')M(H)Cl (M = Rh, Ir) and analogous Cy-PSiP species, the reactivity of the former in E-H bond activation reactions is likely to be promising. As such, further characterization and investigation of these complexes is certainly warranted.

3.4: Experimental Section

3.4.1: General considerations

All experiments were conducted under nitrogen in an MBraun glovebox or using standard Schlenk techniques. Dry, oxygen-free solvents were used unless otherwise indicated. Pentane, benzene, and toluene were deoxygenated and dried by sparging with nitrogen and subsequent passage through a double-column solvent purification system (one activated alumina column and one column packed with activated Q-5) purchased from MBraun Inc. Tetrahydrofuran and diethyl ether were purified by distillation from Na/benzophenone under nitrogen. All purified solvents were stored over 4 Å molecular sieves. All deuterated solvents were degassed via three freeze-pump-thaw cycles and stored over 4 Å molecular sieves. The complexes $[M(COE)_2Cl]_2$ (M = Rh, Ir), [(*p*-cymene)$RuCl_2]_2$ and (COD)Ru(2-methylallyl)$_2$ were purchased from Strem Chemicals and used as received. Triethylamine was deoxygenated and dried by sparging with nitrogen and subsequent distillation from CaH_2. All other reagents were purchased from Aldrich and used without further purification. Unless otherwise stated, ^{1}H, ^{13}C, ^{31}P, and ^{29}Si NMR characterization data were collected at 300K on a Bruker AV-500 spectrometer operating at 500.1, 125.8., 202.5, and 99.4 MHz (respectively) with chemical shifts reported in parts per million downfield of $SiMe_4$ (for ^{1}H, ^{13}C, and ^{29}Si) or 85% H_3PO_4 in D_2O (for ^{31}P). ^{1}H and ^{13}C NMR chemical shift assignments are based on data obtained from ^{13}C-DEPTQ, ^{1}H-^{1}H COSY, ^{1}H-^{13}C HSQC, and ^{1}H-^{13}C HMBC NMR experiments. ^{29}Si NMR assignments are based on ^{1}H-^{29}Si HMBC experiments.

3.4.2: Synthetic detail and characterization data

(Cy-PSiP*-^{i}Pr)Ru(2-methylallyl) (3-1). A room temperature solution of **2-5** (0.12 g, 0.27 mmol) in ca. 3 mL of benzene was mixed with a room temperature solution of (COD)Ru(2-methylallyl)$_2$ (0.087 g, 0.27 mmol) in ca. 3 mL of benzene. The reaction mixture was heated at 70 °C for 24 h, following which the volatile components of the mixture were removed under vacuum and the remaining residue was washed with 2 × 3 mL of cold (-30 °C) pentane and dried *in vacuo* to obtain **3-1** (0.11 g, 90% yield) as an orange solid. ^{31}P{^{1}H} NMR (202.5 MHz, benzene-d_6): δ 82.2 (s), 23.3 (s). ^{29}Si NMR (99.4 MHz, benzene-d_6): δ 24.5.

(Cy-PSiP'-Ph)Rh(H)Cl (3-2). A room temperature solution of **2-3** (0.066 g, 0.12 mmol) in ca. 3 mL of benzene was mixed with a room temperature solution of [Rh(COE)$_2$Cl]$_2$ (0.041 g, 0.057 mmol) in ca. 3 mL of benzene. The resulting reaction mixture was allowed to stand at room temperature for 24 h. The volatile components of the reaction mixture were subsequently removed under vacuum and the remaining residue was washed with 2 × 3 mL of cold (-30 °C) pentane and dried *in vacuo* to obtain **3-2** (0.097 g, 84% yield) as an orange solid. ^{1}H NMR (500 MHz, benzene-d_6): δ 8.24 (m, 1 H, H_{arom}), 8.05 (m, 1 H, H_{arom}), 7.94 (d, 1 H, H_{arom}, J = 7 Hz), 7.66 (m, 2 H, H_{arom}), 7.49 (m, 1 H, H_{arom}), 7.36 (m, 2 H, H_{arom}), 7.25 (m, 2 H, H_{arom}), 7.05 (4 H, H_{arom}), 2.06-0.90 (22 H, P*Cy*), 0.76 (s, 3 H, Si*Me*), -18.72 (m, 1 H, Rh*H*). ^{13}C{^{1}H} NMR (125.8 MHz, benzene-d_6): δ 145.2 (C_{arom}), 144.8 (C_{arom}), 142.6 (C_{arom}), 135.0 (d, CH_{arom}, J = 18 Hz), 133.6 (d, CH_{arom}, J = 21 Hz), 132.5 (CH_{arom}), 132.2 (CH_{arom}), 131.7 (CH_{arom}), 131.5 (CH_{arom}), 130.7 (CH_{arom}), 130.2 (CH_{arom}), 129.8 (CH_{arom}), 129.5 (CH_{arom}), 128.6 (CH_{arom}), 34.1-25.6 (P*Cy*), 7.7 (Si*Me*). ^{31}P{^{1}H} NMR (202.5 MHz, benzene-d_6): δ 63.7 (dd, $^{1}J_{PRh}$ =

120 Hz, $^{2}J_{PP}$ = 356 Hz), 42.8 (dd, $^{1}J_{PRh}$ = 120 Hz, $^{2}J_{PP}$ = 356 Hz). ^{29}Si NMR (99.4 MHz, benzene-d_6): 43.4 .

(Cy-PSiP'-Ph)Ir(H)Cl (3-3). A room temperature solution of **2-3** (0.040 g, 0.070 mmol) in ca. 3 mL of benzene was mixed with a room temperature solution of $[Ir(COE)_2Cl]_2$ (0.035 g, 0.031 mmol) in ca. 3 mL of benzene. The resulting reaction mixture was allowed to stand at room temperature for 24 h. The volatile components of the reaction mixture were subsequently removed under vacuum and the remaining residue was washed with 2 × 3 mL of cold (-30 °C) pentane and dried *in vacuo* to obtain **3-3** (0.031, 76% yield) as an orange solid. $^{31}P\{^{1}H\}$ NMR (202.5 MHz, benzene-d_6): δ 60.2 (d, $^{2}J_{PP}$ = 335 Hz), 47.5 (d, $^{2}J_{PP}$ = 335 Hz). ^{29}Si NMR (99.4 MHz, benzene-d_6): δ 97.5.

(Cy-PSiP*-^{i}Pr)Rh(H)Cl (3-4). A room temperature solution of **2-5** (0.036 g, 0.077 mmol) in ca. 3 mL of benzene was mixed with a room temperature solution of $[Rh(COE)_2Cl]_2$ (0.028 g, 0.039 mmol) in ca. 3 mL of benzene. The resulting reaction mixture was allowed to stand at room temperature for 24 h. The volatile components of the reaction mixture were subsequently removed under vacuum and the remaining residue was washed with 2 × 3 mL of cold (-30 °C) pentane and dried *in vacuo* to obtain **3-4** (0.031 g, 84% yield) as a dark red solid. ^{1}H NMR (500 MHz, benzene-d_6): δ 7.63 (d, 1 H, H_{arom}, J = 11 Hz), 7.27 (m, 1 H, H_{arom}), 7.10 (m, 1 H, H_{arom}), 7.08 (m, 1 H, H_{arom}), 3.68 (s, 2 H, PCH_2), 2.41-1.05 (30 H, PCy + CHMe$_2$), 0.87 (s, 3 H, SiMe), -17.01 (m, 1 H, RhH). $^{13}C\{^{1}H\}$ NMR (125.8 MHz, benzene-d_6):δ 139.5 (C_{arom}), 139.1 (C_{arom}), 133.1 (CH$_{arom}$), 132.9 (CH$_{arom}$), 130.5 (CH$_{arom}$), 129.7 (CH$_{arom}$), 33.4 (d, CH$_{Cy}$, J = 24 Hz), 30.9 (d, CH$_{Cy}$, J = Hz), 29.8 – 27.0 (CH$_{2Cy}$), 26.7 (PCH$_2$), 22.3 (CHMe$_2$), 22.1 (CHMe$_2$), 20.4

(*C*HMe$_2$), 19.2 (*C*HMe$_2$), 1.5 (Si*Me*). ^{31}P{^{1}H} NMR (202.5 MHz, benzene-d_6): δ 66.5 (dd, $^1J_{PRh}$ = 117 Hz, $^2J_{PP}$ = 330 Hz), 39.0 (dd, $^1J_{PRh}$ = 111 Hz , $^2J_{PP}$ = 330 Hz). ^{29}Si NMR (99.4 MHz, benzene-d$_6$): δ 34.4.

(Ph-PSiP*-^{i}Pr)Ir(H)Cl (3-5). A room temperature solution of **3-2** (0.023 g, 0.054 mmol) in ca. 3 mL of benzene was mixed with a room temperature solution of [Ir(COE)$_2$Cl]$_2$ (0.024 g, 0.027 mmol) in ca. 3 mL of benzene. The resulting reaction mixture was allowed to stand at room temperature for 24 h. The volatile components of the reaction mixture were subsequently removed under vacuum and the remaining residue was washed with 2 × 3 mL of cold (-30 °C) pentane and dried *in vacuo* to obtain **3-5** (0.0194 g, 83% yield) as a dark orange solid. ^{1}H NMR (500 MHz, benzene-d_6): δ 7.88 (m, 1 H, *H*$_{arom}$), 7.74 (m, 1 H, *H*$_{arom}$), 7.58 (d, 1 H, *H*$_{arom}$, *J* = 7 Hz), 7.27 (m, 1 H, *H*$_{arom}$), 7.06-6.80 (21 H, *H*$_{arom}$), 2.08 (m, 2 H, CH$_2$P), 1.60 (m, 1 H, C*H*Me$_2$), 1.16 (d, 3 H, C*H*Me$_2$, *J* = 8 Hz), 1.12 (d, 3 H, C*H*Me$_2$, *J* = 7 Hz), 1.03 (d, 3 H, C*H*Me$_2$, *J* = 8 Hz), 1.01 (d, 3 H, C*H*Me$_2$, *J* = 7 Hz), 0.32 (s, 3 H, Si*Me*), -22.15 (m, 1 H, Ir*H*). ^{13}C{^{1}H} NMR (125.8 MHz, benzene-d_6): δ 157.0 (*C*$_{arom}$), 135.1 (*C*H$_{arom}$), 134.9 (*C*H$_{arom}$), 134.8 (*C*H$_{arom}$), 134.7 (*C*H$_{arom}$), 134.1 (*C*H$_{arom}$), 133.7 (*C*H$_{arom}$), 131.8 (*C*H$_{arom}$), 131.7 (*C*H$_{arom}$), 130.5 (*C*H$_{arom}$), 130.3 (*C*H$_{arom}$), 129.9 (*C*H$_{arom}$), 129.6 (*C*H$_{arom}$), 129.5 (*C*H$_{arom}$), 128.9 (*C*H$_{arom}$), 30.1 (*C*HMe$_2$), 26.5 (*C*HMe$_2$), 25.8 (*C*HMe$_2$), 20.3 (*C*HMe$_2$), 19.5 (*C*HMe$_2$), 19.1 (*C*HMe$_2$), 18.9 (*C*HMe$_2$), 14.3 (Si*Me*). ^{31}P{^{1}H} NMR (202.5 MHz, benzene-d_6): δ 37.8 (d, $^2J_{PP}$ = 364 Hz), -2.3 (d, $^2J_{PP}$ = 364 Hz). ^{29}Si NMR (99.4 MHz, benzene-d_6): δ 40.5.

Chapter 4: Conclusions

4.1 Summary and Conclusions

The synthesis of Group 10 (Ni, Pd, and Pt) metal complexes supported by "unsymmetrical" PSiP' ligands that feature two different phosphino donors has been detailed in this thesis, as well as preliminary reactivity studies targeting the synthesis of Group 8 and 9 metal complexes of this type. In Chapter 2, the synthesis and reactivity of (Cy-PSiP'-Ph)MCl (M = Pt, Pd, Ni) complexes was described (Scheme 4-1). Such chloride complexes represent a convenient and versatile entry point for exploring the reaction chemistry of such Group 10 metal species. Terminal square planar alkyl and aryl derivatives were obtained via salt metathesis reactions of (Cy-PSiP'-Ph)MCl (M = Pt, Pd, Ni) with the corresponding lithium alkyl and aryl reagents (Scheme 4-1). These complexes were tested for their reactivity toward Si-H bonds by attempted reactions with a variety of hydrosilanes. However, surprisingly little reactivity was observed. This is unlike previous observations involving related (R-PSiP)M(alkyl) (R = Ph, Cy) complexes.[123, 88] In the case of (R-PSiP)MMe (R = Ph, M = Pt; R = Cy, M = Pt, Pd), facile reactivity with hydrosilanes occurred to provide the corresponding metal silyl complexes, while the related (Cy-PSiP)NiMe complex (as well as the Pd derivative, over time) underwent a reversible ligand rearrangement process involving Si-C(sp^2) and Si-C(sp^3) bond cleavage steps. By comparison (Cy-PSiP'-Ph)MMe did not appear to react with hydrosilanes and the Ni and Pd derivatives proved stable toward ligand

rearrangement processes. These reactivity differences likely reflect differences in the electronic character of the metal center in such "unsymmetrical" silyl pincer species.

The synthesis of terminal amido complexes of the type (Cy-PSiP'-Ph)M(NHR) (M = Ni, Pd, Pt; R = H or Ph) was also targeted (Scheme 4-1). Indeed, treatment of (Cy-PSiP'-Ph)MCl species with an appropriate LiNHR reagent led to the corresponding amido and anilido complexes. Such Group 10 metal amido species were generally isolated as stable square planar complexes that failed to undergo insertion reactions with xylyl isocyanide and alkynes. Interestingly, while the parent palladium amido complex (Cy-PSiP'-Ph)Pd(NH_2) proved isolable, related complexes of the type (Cy-PSiP'-Ph)Pd(NHR) (R = Ph, ^{t}Bu) were shown to undergo rearrangement processes involving Si-C(sp^2) bond cleavage of the ligand backbone. It is unclear at this point what factors govern such rearrangement processes, as both electron rich (NH^tBu) and relatively electron poor (NHPh) amido ligands seemed to facilitate the rearrangement process. Although steric factors might play a role, this has not previously been observed to be the case in related Cy-PSiP Ni and Pd chemistry.[123, 88]

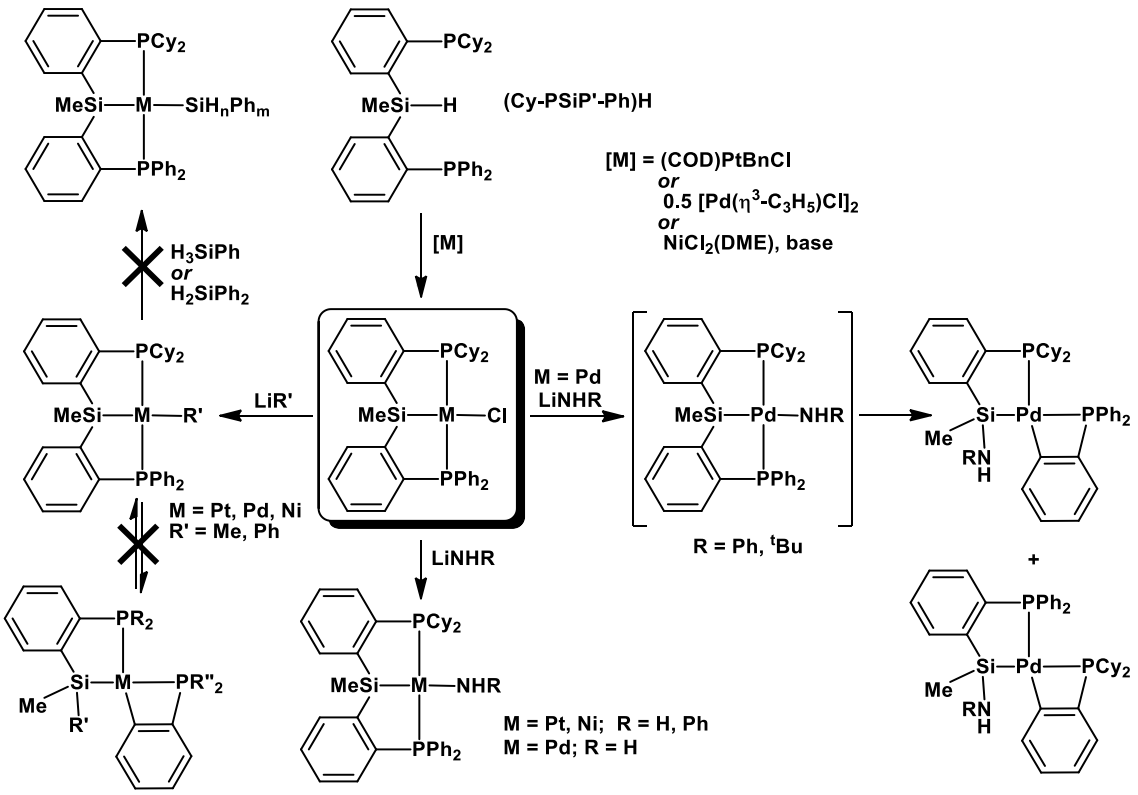

Scheme 4-1. Summary of Group 10 metal complexes supported by Cy-PSiP'-Ph ligation.

Chapter 2 also detailed the synthesis of Group 10 complexes supported by alternative PSiP' ligands, Ph-PSiP*-^{i}Pr and Cy-PSiP*-^{i}Pr, that feature an alkyl phosphino donor arm that is anticipated to form a constrained four-membered chelate ring upon k^3-coordination to a single metal center (Scheme 4-2). Platinum complexes of the type (R-PSiP*-^{i}Pr)PtCl (R = Ph, Cy) were synthesized by reacting the corresponding tertiary silane ligand precursor with (COD)PtBnCl. Primarily on the basis of ^{31}P NMR data, these ligands are proposed to indeed form mononuclear Pt complexes that contain a four-membered metalacycle. A related Ni complex was also successfully synthesized by the reaction of (Cy-PSiP*-^{i}Pr)H with $NiCl_2$(DME) in the presence of base. As in the case of the Pt derivative, ^{31}P NMR data for this compound are consistent with the formation of a mononuclear (Cy-PSiP*-^{i}Pr)NiCl species. By comparison, attempts to prepare a related

Pd complex by the reaction of (Cy-PSiP*-^{i}Pr)H with [Pd(η^3-C_3H_5)Cl]$_2$ led to the formation of a mixture of monomeric and dimeric complexes, where the dinuclear complex [(Cy-PSiP*-^{i}Pr)PdCl]$_2$ is the major product formed in solution. The latter complex was crystallographically characterized and shown to contain two square planar Pd centers that are bridged by $CH_2P^{i}Pr_2$ ligand arms.

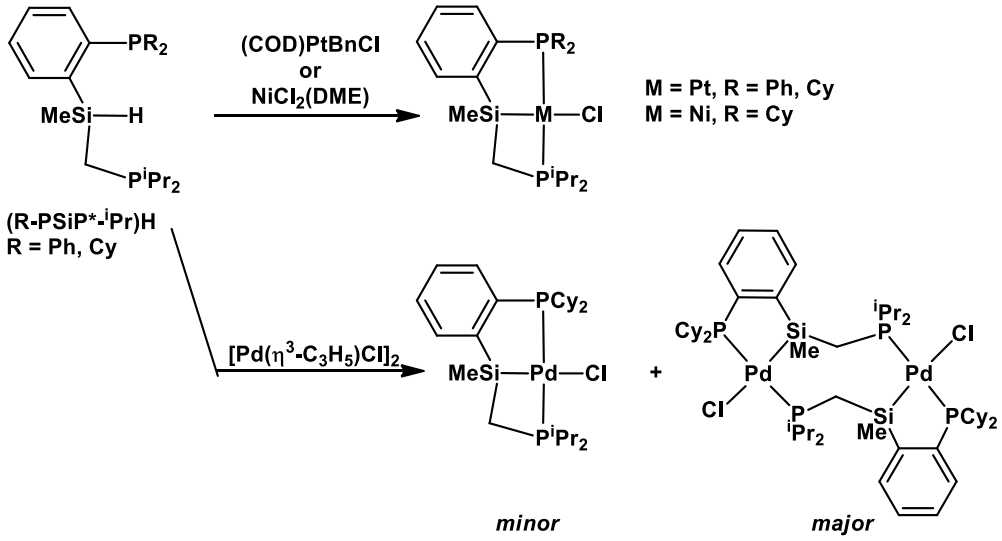

Scheme 4-2. Summary of Group 10 metal complexes supported by R-PSiP*-^{i}Pr (R = Ph, Cy) ligation.

Chapter 3 detailed preliminary results involving the synthesis of Group 8 and 9 metal complexes supported by PSiP' ligation (Scheme 4-3). While Ru complexes proved challenging to prepare, Rh and Ir species of the type (PSiP')M(H)Cl were more readily accessed by the reaction of the tertiary silane ligand precursors with [M(COE)$_2$Cl]$_2$ (M = Rh, Ir). Complexes of the type (Cy-PSiP'-Ph)M(H)Cl are anticipated to be structurally similar to related Cy-PSiP species. In the absence of crystallographic data, the formulation of complexes supported by R-PSiP*-^{i}Pr (R = Ph, Cy) as either mononuclear

or dinuclear is tentative, and solution NMR data suggests that while (Ph-PSiP*-^{i}Pr)Ir(H)Cl is monomeric, (Cy-PSiP*-^{i}Pr)Rh(H)Cl is possibly a dimeric species.

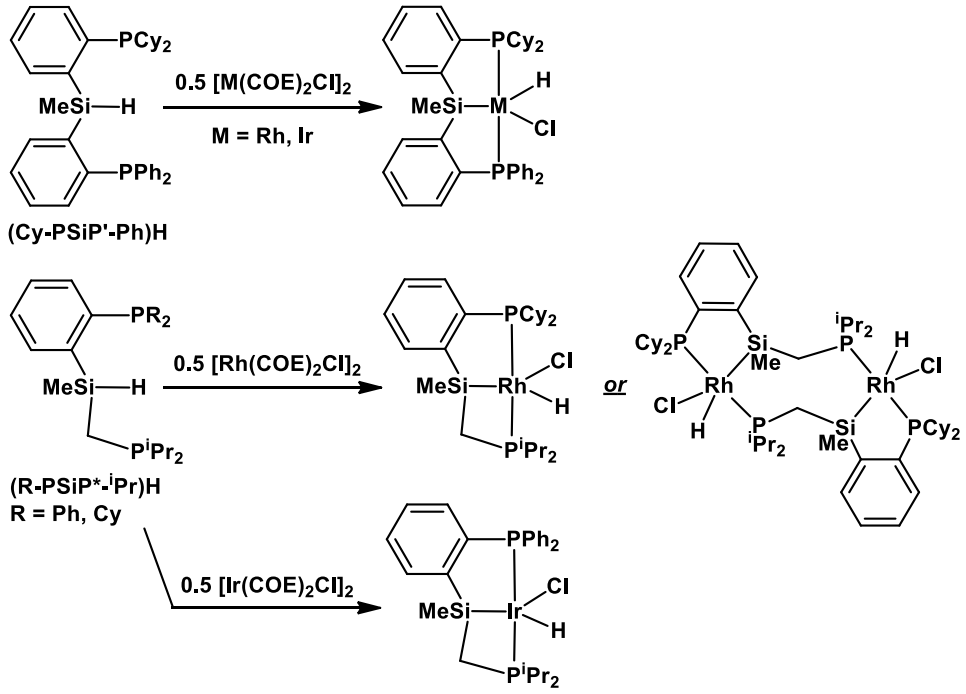

Scheme 4-3. Summary of Group 9 metal complexes supported by PSiP' ligation.

4.2 Future Work

Having established that platinum group metal complexes supported by PSiP' ligation are indeed synthetically accessible, further characterization, including X-ray crystallographic studies, of such complexes is necessary. As well, the further elaboration of the reactivity of such Group 8, 9 and 10 metal complexes remains to be explored. In particular, the bond activation chemistry of complexes of the type (PSiP')M(H)Cl (M = Rh, Ir) is an interesting avenue to explore (Scheme 4-4), as related (Cy-PSiP)Ir(H)Cl complexes have been shown to serve as precursors to highly reactive Ir^{I} species of the type (Cy-PSiP)Ir^{I} that can undergo C-H and N-H bond cleavage chemistry.[10, 106, 139] In this regard, the synthesis of complexes of the type (PSiP')M(H)(NHR) (M = Rh, Ir; R =

H, alkyl or aryl) via salt metathesis routes utilizing LiNHR reagents is of interest, as it can help determine the relative stability of such amido hydride complexes as might result from N-H bond oxidative addition of H_2NR to a putative (PSiP')M^I source. The generation of coordinatively unsaturated (PSiP')M^I, either via dehydrohalogenation of (PSiP')M(H)Cl or by H_2 elimination from (PSiP')$M(H)_2$, is also of interest, as such (PSiP')M^I species can then be utilized in E-H bond activation studies (E = main group element), such as the activation of N-H bonds in H_2NR to generate the corresponding amido hydride complexes. The effects of variations in the silyl pincer structure on E-H bond activation chemistry can thus be elucidated, with the goal of accessing Group 9 metal complexes that are highly reactive towards E-H bond oxidative addition, and that may undergo subsequent insertion chemistry into the M-E bond in order to facilitate a possible catalytic process. With respect to the effects of silyl pincer ligand structure on the E-H bond activation aptitude of the ensuing metal complexes, the relative strain associated with mononuclear complexes supported by R-PSiP*-^{i}Pr ligation may lead to exceptional reactivity, as the four-membered chelate ring may leave the metal center relatively open and accessible to incoming substrates. The $^i Pr_2P$ donor in such complexes may also exhibit some hemilability, which could also lead to enhanced reactivity.

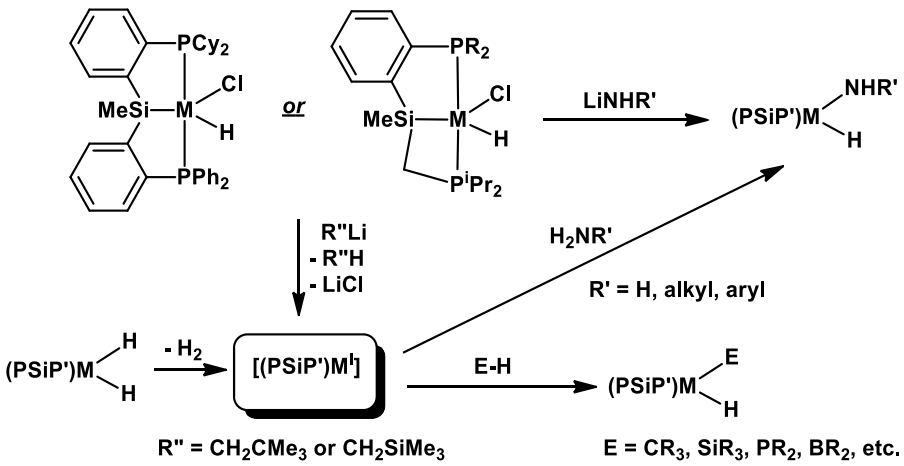

Scheme 4-4. Proposed studies of E-H bond activation by Group 9 metal complexes supported by PSiP' ligation.

References

1. W. S. Knowles, *Adv. Synth. Catal.,* **2003**, *345,* 1-13.
2. R. Noyori, *Adv. Synth. Catal.,* **2003**, *345,* 15-32.
3. B. K. Sharpless, *Angew. Chem. Int. Ed.,* **2002**, *41,* 2024-2032.
4. R. H. Grubbs, *Adv. Synth. Catal.,* **2007**, *349,* 34-40.
5. R. R. Schrock, *Adv. Synth. Catal.,* **2007**, *349,* 41-53.
6. Y. Chauvin, *Adv. Sytnh. Catal.,* **2007**, *349,* 27-33.
7. E. Negishi, *Angew. Chem. Int. Ed.,* **2011**, *50,* 6738-6764.
8. A. Suzuki, *Angew. Chem. Int. Ed.,* **2011**, *50,* 6723-6737.
9. E. Balaraman, C. Gunanathan, J. Zhang, L. J. W. Shimon and D. Milstein, *Nat. Chem.,* **2011**, *3,* 609-614.
10. E. Morgan, D. F. MacLean, R. McDonald and L. Turculet, *J. Am. Chem. Soc.,* **2009**, *131,* 14234-14236.
11. S. J. Mitton and L. Turculet, *Chem. Eur. J.,* **2012**, *18,* 15258-15262.
12. E. Balaraman, B. Gnanaprakasam, L. J. W. Shimon and D. Milstein, *J. Am. Chem. Soc.,* **2010**, *132,* 16756-16758.
13. M. Gandelman, B. Rybtchinski, N. Ashkenazi, R. M. Gauvin and D. Milstein, *J. Am. Chem. Soc.,* **2001**, *123,* 5372-5373.
14. M. Gandelman, A. Vigalok, L. J. W. Shimon and D. Milstein, *Organometallics,* **1997**, *16,* 3981-3986.
15. M. Gandelman, A. Vigalok, L. Konstantinovski and D. Milstein, *J. Am. Chem. Soc.,* **2000**, *122,* 9848-9849.
16. M. E. van der Boom and D. Milstein, *Chem. Rev.,* **2003**, *103,* 1759-1792.
17. M. Albrecht and G. van Koten, *Angew. Chem. Int. Ed.,* **2001**, *40,* 3750-3781.
18. J. Choi, A. H. R. MacArthur, M. Brookhart and A. S. Goldman, *Chem. Rev.,* **2011**, *111,* 1761–1779.
19. C. J. Moulton and B. L. Shaw, *J. Chem. Soc., Dalton Trans.,* **1976**, *11,* 1020-1024.
20. N. A. Al-Salem, H. D. Empsall, R. Markham, B. L. Shaw and B. Weeks, *J. Chem. Soc., Dalton Trans.,* **1979**, *12,* 1972-1982.

21. H. D. Empsall, E. M. Hyde, E. Mentzer and B. L. Shaw, *J. Chem. Soc., Dalton Trans*., **1977**, *22,* 2285-2291.

22. C. Crocker, R. J. Errington, W. S. McDonald, K. J. Odell and B. L. Shaw, *J. Chem. Soc., Chem. Commun.,* **1979**, *11,* 498-499.

23. C. Crocker, R. J. Errington, R. Markham, C. J. Moulton, K. J. Odell and B. L. Shaw, *J. Am. Chem. Soc.,* **1980**, *102,* 4373-4379.

24. R. A. Gossage, G. D. McLennan, and S. R. Stobart, *Inorg. Chem.,* **1996**, *35*, 1729-1732.

25. M. J. Auburn, R. D. Holmes-Smith, S. R. Stobart, P. K. Bakshi and T. S. Cameron, *Organometallics*, **1996**, *15*, 3032-3036.

26. R. D. Brost, G. C. Bruce, F. L. Joslin and S. R. Stobart, *Organometallics,* **1997**, *16,* 5669-5680.

27. M. Gupta, C. Hagen, R. J. Flesher, W. C. Kaska and C. M. Jensen, *Chem. Commun.,* **1996***, 17,* 2083-2084.

28. C. Gunanathan and D. Milstein, *Chem. Rev.,* **2014**, *114,* 12024-12087.

29. K. J. Szabo, *Top. Organomet. Chem.,* **2013***, 40,* 203-242.

30. K. E. Allen, D. M. Heinekey, A. S. Goldman and K. I. Goldberg, *Organometallics,* **2013**, *32,* 1579-1582.

31. M. C. Haibach, S. Kundu, M. Brookhart, and A. S. Goldman, *Acc. Chem. Res.,* **2012**, *45,* 947-958.

32. a) B. A. Arndsten, R. G. Bergman, T. A. Mobley, and T. H. Peters, *Acc. Chem. Res.,* **1995**, *28,* 154-162. b) A. E. Shilov and G. B. Shul'pin, *Chem. Rev.,* **1997**, *97,* 2879−2932. c) R. H. Crabtree, *J. Chem. Soc., Dalton Trans.,* **2001**, *17,* 2437–2450. d) J. A. Labinger, J. E. Bercaw, *Nature,* **2002**, *417,* 507.

33. a) H. A. Zhong, J. A. Labinger and J. E. Bercaw, *J. Am. Chem. Soc.,* **2002**, *124,* 1378-1399. b) R. A. Periana, G. Bhalla, W. J. Tenn, K. J. H. Young, X. Y. Liu, O. Mironov, CJ Jones, V. R. Ziatdinov, *J. Mol. Cat. A,* **2004**, *220,* 7-25. c) B. L. Conley, W. J. Terin III, K. J. H. Young, S. K. Ganesh, S. K. Meier, V. R. Ziatdinov, O. Mironov, J. Oxgaard, J. Gonzales, W. A. Goddard III and R. A. Periana, *J. Mol. Cat. A,* **2006**, *251,* 8-23. d) J. S. Owen, J. A. Labinger and J. E. Bercaw, *J. Am. Chem Soc.,* **2004,** *126*, 8247-8255.

34. R. H. Crabtree, C. P. Parnell, R. J. Uriarte, *Organometallics,* **1987**, *6,* 696-699.

35. M. Gupta, C. Hagen, W. C. Kaska, R. E. Cramer and C. M. Jensen, *J. Am. Chem. Soc.,* **1997**, *119,* 840-841.

36. W. Xu, G. P. Rosini, M. Gupta, C. M. Jensen, W. C. Kaska, K. Krogh-Jespersena and A. S. Goldman, *Chem. Commun.,* **1997**, *23,* 2273-2274.

37. F. Liu and A. S. Goldman, *Chem. Commun.,* **1999**, *7,* 655-656.

38. C. M. Jensen, *Chem. Commun.,* **1999**, *24,* 2443-2449.

39. I. Gottker-Schnetmann, P. White and M. Brookhart, *J. Am. Chem. Soc.,* **2004**, *126,* 1804-1811.

40. D. Morales-Morales, R. Redon, C. Yung and C. M. Jensen, *Inorg. Chim. Acta,* **2004**, *357,* 2953-2956.

41. I. Gottker-Schnpetmann and M. Brookhart, *J. Am. Chem. Soc.,* **2004**, *126,* 9330-9338.

42. K. Zhu, P D. Achord, X. Zhang, K. Krogh-Jespersen, and A. S. Goldman, *J. Am. Chem. Soc.,* **2004**, *126,* 13044-13053.

43. M. C. Haibach, S. Kundu, M. Brookhart and A. S. Goldman, *Acc. Chem. Res.,* **2012**, *45,* 947-958.

44. T. M. Trnka and R. H. Grubbs, *Acc. Chem. Res.,* **2001**, *34,* 18-29.

45. B. C. Bailey, R. R. Schrock, S. Kundu, A. S. Goldman, Z. Huang and M. Brookhart, *Organometallics,* **2009**, *28,* 355-360.

46. S. Kundu, Y. Choliy, G. Zhuo, R. Ahuja, T. J. Emge, R. Warmuth, M. Brookhart, K. Krogh-Jespersen, and A. S. Goldman, *Organometallics,* **2009**, *28,* 5432-5444.

47. C. Gunanathan and D. Milstein, *Acc. Chem. Res.,* **2011**, *44,* 588-602.

48. E. Balaraman, C. Gunanathan, J. Zhang, L. J. W. Shimon and D. Milstein, *Nat. Chem.,* **2011**, *3,* 609-614.

49. E. Balaraman, E. Khaskin1, G. Leitus and D. Milstein, *Nat. Chem.,* **2013**, *5,* 122-125.

50. E. Balaraman, B. Gnanaprakasam, L. J. W. Shimon, and D. Milstein, *J. Am. Chem. Soc.,* **2010**, *132,* 16756-16758.

51. E. Balaraman, E. Fogler and D. Milstein, *Chem. Commun.,* **2012**, *48,* 1111-1113.

52. E. Balaraman, Y. Ben-David, and D. Milstein, *Angew. Chem. Int. Ed.,* **2011**, *50,* 11702–11705.

53. D. Srimani, M. Feller, Y. Ben-David and D. Milstein, *Chem. Commun.,* **2012**, *48,* 11853-11855.

54. D. Srimani, Y. Ben-David and D. Milstein, *Angew. Chem. Int. Ed.,* **2013**, *52,* 4012-4015.

55. Hudlicky, M. *Oxidations in Organic Chemistry*; Wiley:Washington, D.C., 1990.

56. Ley, S. V.; Madin, A. In *Comprehensive Organic Synthesi*, Trost, B. M.; Fleming, I; Ley,S. V.; Pergamon, Oxford*,* 1991, vol 7, pp. 251-289.

57. C. Gunanathan, Y. Ben-David, D. Milstein, *Science,* **2007**, *317,* 790-792.

58. B. Gnanaprakasam, J. Zhang, and D. Milstein, *Angew. Chem. Int. Ed.,* **2010**, *49,* 1468-1471.

59. A. Nova, D. Balcells, N. D. Schley, G. E. Dobereiner, R. H. Crabtree, and O. Eisenstein, *Organometallics,* **2010**, *29,* 6548-6558.

60. B. Gnanaprakasam, E. Balaraman, Y. Ben-David and David Milstein, *Angew. Chem. Int. Ed.,* **2011**, *50,* 12240-12244.

61. H. Zeng and Z. Guan, *J. Am. Chem. Soc.,* **2011**, *133,* 1159-1161.

62. B. Gnanaprakasam, E. Balaraman, C. Gunanathan, D. Milstein, *J. Polym. Sci. A Polym. Chem.,* **2012**, *50,* 1755-1765.

63. J. Ma, N. Sun, X. Zhang, N. Zhao, F. Xiao and W. Wei, *Catal. Today,* **2009**, *148,* 221.

64. G. A. Olah, A. Goeppert and G. K. S. Prakash, *J. Org. Chem.,* **2009**, *74,* 487-498.

65. a) D. Delledonnea, F. Rivettia and U. Romanob, *Appl. Catal. A,* **2001**, *221,* 241-251. b) D. Delledonnea, F. Rivettia and U. Romanob, *J. Organomet. Chem.,* **1995**, *488,* C15-C19. c) T. Sakakura and K. Kohnoa, *Chem. Commun.,* **2009**, *11,* 1312-1330. d) T. Sakakura, J. Choi and H. Yasuda, *Chem. Rev.,* **2007**, *107,* 2365-2387.

66. a) K. M. K. Yu, C. M. Y. Yeung and S. C. Tsang, *J. Am. Chem. Soc.,* **2007,** *129,* 6360-6361. b) Wa. Leitner, *Agnew. Chem. Int. Ed.,* **1995,** *34,* 2207-2221. c) P. G. Jessopa, Fe. Joob and C. Taic, *Coord. Chem. Rev.,* **2004,** *248,* 2425-2442. d) C. Federsel, R. Jackstell and M. Beller, *Angew. Chem. Int. Ed.,* **2010,** *49,* 6254-6257.

67. a) M. Abla, J. Choi and T. Sakakura, *Chem. Commun.,* **2001**, *21,* 2238-2239. b) M. Abla, J. Choi and T. Sakakura, *Green Chem.,* **2004**, *6,* 524-525.

68. Turculet, L. PSiP Transition-Metal Pincer Complexes: Synthesis, Bond Activation, and Catalysis. In *Pincer and Pincer-Type Complexes: Applications in Organic Synthesis and Catalysis*; K. J. Szabó and O. F. Wendt); Wiley-VCH Verlag GmbH & Co. KGaA, Weinheim, Germany.

69. H. Kameo, S. Ishii and H. Nakazaura, *Dalton Trans.,* **2012**, *41*, 11386-11392.

70. C. Zhu, J. Takaya and N. Iwasawa, *Chem. Lett.,* **2012**, *41,* 967-969.

71. M. Mazzeo, M. Lamberti, I. D'Auria, S. Milione, J. C. Peters and C. Pellechia, *J. Polym. Sci., Part A: Polym. Chem.,* **2010**, *48,* 1374-1382.

72. E. J. Derrah, S. Lateira, G. Bouhadir, K. Miqueu and D. Bourissou, *Chem. Commun.,* **2011**, *47,* 8611-8613.

73. G. S. Day, B. Pan, D. L. Kellenberger, B. M. Foxman and C. M. Thomas, *Chem. Commun.,* **2011**, *47,* 3634-3636.

74. B. Pan, M. W. Bezpako, B. Foxman, and C. M. Thomas, *Organometallics,* **2011**, *30,* 5560-5563.

75. Y. Gloaguen, W. Jacobs, B. de Bruin, M. Lutz and J. I. van der Vlugt, *Inorg. Chem.,* **2013**, *52,* 1682-1684.

76. E. J. Derrah, C. Martin, S. Mallet-Ladeira, K. Miqueu, G. Bouhadir and D. Bourissou, *Organometallics,* **2013**, *32,* 1121-1128.

77. M. Mazzeo, M. Strianese, O. Kuhl and J. C. Peters, *Dalton Trans.,* **2011**, *40,* 9026-9033.

78. N. P. Mankad, E. Rivard, S. B. Harkins and J. C. Peters, *J. Am. Chem. Soc.,* **2005**, *127,* 16032-16033.

79. M. Mazzeo, M. Lamberti, A. Massa, A. Scettri, C. Pellechia and J. C. Peters, *Organometallics,* **2008**, *27,* 5741-5743.

80. R. C. Bauer, Y. Gloaguen, M. Lutz, J. N. H. Reek, B. de Bruin and J. I. van der Vlugt, *Dalton Trans.,* **2011**, *40,* 8822-8829.

81. H. Ogawa and M. Yamashita, *Dalton Trans.,* **2013**, *42,* 625-629.

82. M. E. El-Zaria, H. Arii and H. Nakamura, *Inorg. Chem.,* **2011**, *50,* 4149-4161.

83. A. F. Hill, S. B. Lee, J. Park, R. Shang and A. C Willis, *Organometallics,* **2010**, *29,* 5661-5669.

84. A. M. Spokoyny, M. G. Reuter, C. L. Stern, M. Ratner, T. Seideman and C. A. Mirkin, *J. Am. Chem. Soc.,* **2009**, *131,* 9482-9483.

85. M. Hasegawa, Y. Segawa, M. Yamashita and K. Nozaki, *Agnew. Chem. Int. Ed.,* **2012**, *51,* 6956-6960.

86. Y. Segawa, M. Yamashita and K. Nozaki, *J. Am. Chem Soc.,* **2009**, *131,* 9201-9203.

87. Y. Segawa, M. Yamashita and K. Nozaki, *Organometallics,* **2009**, *28,* 6234-6242.

88. S. J. Mitton, R. McDonald and L. Turculet, *Angew. Chem. Int. Ed.,* **2009**, *48,* 8568-8571.

89. M. C. MacInnis, R. McDonald, M. J. Ferguson, S. Tobisch and L. Turculet, *J. Am. Chem. Soc.,* **2011**, *133,* 13622-13633.

90. M. Aizenberg and D. Milstein, *J. Am. Chem. Soc.,* **1995**, *117,* 6456-6464.

91. M. Stradiotto, K. L. Fujdala and T. D. Tilley, *Chem. Commun.,* **2001**, *13,* 1200-1201.

92. P. Sangtrirutnugul and T. D. Tilley, *Organometallics,* **2008**, *27,* 2223-2230.

93. P. Sangtrirutnugul, M. Stradiotto and T. D. Tilley, *Organometallics,* **2006**, *25,* 1607-1617.

94. J. Y. Corey and J. Braddock-Wilking, *Chem. Rev.,* **1999**, *99,* 175-292.

95. J. Y. Corey, *Chem. Rev.,* **2011**, *111,* 863-1071.

96. D. Huang, W. E. Streib, J. C. Bollinger, K. G. Caulton, R. F. Winter and T. Scheiring, *J. Am. Chem. Soc.,* **1999**, *121,* 8087-8097.

97. D. Huang, J. C. Bollinger, W. E. Streib, K. Folting, V. Young Jr., O. Eisenstein and K. G. Caulton, *Organometallics,* **2000**, *19,* 2281-2290.

98. W. Baratta, E. Herdtweck and P. Rigo, *Angew. Chem. Int. Ed.,* **1999**, *38,* 1629-1631.

99. D. Huang, J. C. Huffman, J. C. Bollinger, O. Eisenstein and K. G. Caulton, *J. Am. Chem. Soc.,* **1997**, *119,* 7398-7399.

100. L. A. Watson, O. V. Ozerov, M. Pink, and K. G. Caulton, *J. Am. Chem. Soc.,* **2003**, *125,* 8426-8427.

101. B. Askevold, M. M. Khusniyarov, E. Herdtweck, K. Meyer, and S. Schneider, *Angew. Chem. Int. Ed.,* **2010**, *49,* 7566-7569.

102. A. C. Sykes, P. White and M. Brookhart, *Organometallics,* **2006**, *25,* 1664-1675.

103. M. Kanzelberger, X. Zhang, T. J. Emge, A. S. Goldman, J. Zhao, C. Incarvito and J. F. Hartwig, *J. Am. Chem. Soc.,* **2003**, *125,* 13644-13645.

104. J. Zhao, A. S. Goldman, J. F. Hartwig, *Science,* **2005**, *307,* 1080-1082.

105. Z. Huang, J. Zhou, and J. F. Hartwig, *J. Am. Chem. Soc.,* **2010**, *132,* 11458-11460.

106. D. F. MacLean, R. McDonald, M. J. Ferguson, A. J. Caddella and L. Turculet, *Chem. Commun.,* **2008**, *41,* 5146–5148.

107. S. J. Blanksby and G. B. Ellison, Acc. Chem. Res., **2003**, *36*, 255-263.

108. University of Reading. http://www.gelest.com/goods/pdf/Library/10BondDiss.pdf 2016 (accessed December 27, 2015).

109. T. Matsuo and H. Kawaguchi, *J. Am. Chem. Soc.,* **2006**, *128,* 12362-12363.

110. S. Park, D. Bézier and M. Brookhart, *J. Am. Chem. Soc.,* **2012**, *134,* 11404-11407.

111. A. J. Ruddy, S. J. Mitton, R. McDonald and L. Turculet, *Chem. Commun.,* **2012**, *48,* 1159-1161.

112. The Chemistry of Pincer Compounds. D. Morales-Morales, C. Jensen; Elsevier, Oxford, 2007.

113. Organometallic Pincer Chemistry. G. van Koten, D. Milstein; Springer, New York, 2013.

114. W. Leis, H. A. Mayer, W. C. Kaska, *Coord. Chem. Rev.,* **2008**, *252*, 1787-1797.

115. D. Pugh, A. A. Danopoulos, *Coord. Chem. Rev.,* **2007**, *251*, 610-64.

116. L. C. Liang, P. S. Chien and P-Y. Lee, *Organometallics,* **2008**, *27,* 3082-3093.

117. P. Y. Lee and L. C Liang, *Inorg. Chem.,* **2009**, *48,* 5480-5487.

118. R. B. Lansing, Jr., K. I. Goldberg and R. Kemp, *Dalton. Trans.,* **2011**, *40,* 8950-8958.

119. J. J. Davidson, J. C. DeMott, C. Douvris, C. M. Fafard, N. Bhuvanesh, C-H. Chen, D. E. Herbert, C-I. Lee, B. J. McCulloch, B. M. Foxman and O. V. Ozerov, *Inorg. Chem.,* **2015**, *54*, 2916-2935.

120. P. O. Lagaditis, P. E. Sues, J. F. Sonnenberg, K. Y. Wan, A. J. Lough and R. H. Morris, *J. Am. Chen. Soc.,* **2014**, *126*, 1367-1380.

121. J. Takaya and N. Iwasawa, *Chem. Eur. J.,* **2014**, *20*, 11812-11819.

122. J. Takaya and N. Iwasawa, *Organometallics,* **2009**, *28*, 6636-6638.

123. Mitton, S. J. Synthesis and Reactivity of Group 10 Silyl Pincer Complexes. PhD Dissertation. Dalhousie University, Halifax, NS, 2013.

124. S. J. Mitton, R. Macdonald and L. Turculet, *Organometallics,* **2009**, *28*, 5122-5136.

125. J. R. Fulton, A. W. Holland, D. J. Fox and R. G. Bergman, *Acc. Chem. Res.*, **2002**, *35*, 44-56.

126. T. B. Gunnoe, *Eur. J. Inorg. Chem.*, **2007**, 1185-1203.

127. J. H. Vincent, B. L. Scott and G. J. Kubas*Inorg, Chem.*, **1999**, *21*, 115-124.

128. R. G. Bergman, *Polyhedron*, **1995**, *14*, 3227-3237.

129. D. Conner, K. M. Jayaprakash, T. R. Cundari and T. B. Gunnoe, *Organometallics* **2004,** *23,* 2724-2733.

130. T. R. Cunari, T. V. Grimes and T. B. Gunnoe, *J. Am. Chem. Soc.* **2007**, 129, 13172-13182.

131. Y. Fang, M. Lail, N. A. Foley, T. B. Gunnoe, K. A. Barskat, T. R. Cundari and J. L. Petersen, *J. Am. Chem. Soc.* **2006**, 128, 7982-7994.

132. J. F. Hartwig, *Nature*, **2008**, *455*, 314-3122.

133. J. F. Hartwig, *Inorg. Chem.*, **2007**, *46*, 1936-1947.

134. D. S. Glueck, *Dalton Trans.*, **2008**, 5276-5286.

135. M. Murata and S. L. Buchwald, *Tetrahderon,* **2004**, *60,* 7397-7403.

136. M. T, Whited, E. Rivard and J. C. Peters, *Chem. Commun.*, **2006**, 1613-1615.

137. L. Turculet, J. D. Feldman and T. D. Tilley, *Organometallics,* **2003**, *22,* 4627-4629.

138. M. C. MacInnis, R. McDonald, M. J. Ferguson, S. Tobisch and L. Turculet, *J. Am. Chem. Soc.,* **2011**, *133,* 13622-13633.

139. Morgan, E. Rhodium and Iridium Pincer Complexes Supported by Bis(phosphino)silyl Ligation: Applications in Bond Cleavage Chemistry. PhD Dissertation, Dalhousie University, Halifax, NS, 2013.

140. Ruddy, A. Synthesis, Characterization, and Reactivity of Transition Complexes Supported by Heteropolydentate Ligation. PhD Dissertation. Dalhousie University, Halifax, NS, 2014.

Appemdix A: Crystallographic Experimental Details

Table A-1. Crystallographic experimental details for (Cy-PSiP'-Ph)PdCl (**2-7**)

A. Crystal Data	
formula	$C_{37}H_{43}ClP_2PdSi$
formula weight	719.59
crystal dimensions (mm)	0.31 x 0.26 x 0.11
crystal system	orthorhombic
space group	$P2_12_12_1$ (No. 19)
unit cell parameters[a]	
a (Å)	9.9605 (6)
b (Å)	14.0365 (8)
c (Å)	24.9317 (14)
V (Å^3)	3485.7 (3)
Z	4
ρ_{calcd} (g cm^{-3})	1.371
μ (mm^{-1})	0.760
B. Data Collection and Refinement Conditions	
diffractometer	Bruker D8/APEX II CCD[b]
radiation (λ [Å])	graphite-monochromated Mo Kα (0.71073)
temperature (°C)	–100
scan type	ω scans (0.3°) (15 s exposures)
data collection 2Θ limit (deg)	55.00
total data collected	30923 ($-12 \le h \le 12$, $-18 \le k \le 18$, $-32 \le l \le 32$)
independent reflections	8000 (R_{int} = 0.0460)
number of observed reflections (*NO*)	7111 [$F_o^2 \ge 2\sigma(F_o^2)$]
structure solution method	Patterson/structure expansion (*DIRDIF–2008*[c])
refinement method	full-matrix least-squares on F^2 (*SHELXL–97*[d])
absorption correction method	Gaussian integration (face-indexed)
range of transmission factors	0.9211–0.7991
data/restraints/parameters	8000 / 0 / 381
Flack absolute structure parameter[e]	0.40(2)
goodness-of-fit (*S*)[f] [all data]	1.055
final *R* indices[g]	
R_1 [$F_o^2 \ge 2\sigma(F_o^2)$]	0.0314
wR_2 [all data]	0.0763
largest difference peak and hole	0.768 and –0.332 e Å^{-3}

[a]Obtained from least-squares refinement of 3686 reflections with $4.36° < 2\Theta < 36.18°$.

[b]Programs for diffractometer operation, data collection, data reduction and absorption correction were those supplied by Bruker.

[c]Beurskens, P. T.; Beurskens, G.; de Gelder, R.; Smits, J. M. M.; Garcia-Granda, S.; Gould, R. O. (2008). The *DIRDIF-2008* program system. Crystallography Laboratory, Radboud University Nijmegen, The Netherlands.

[d]Sheldrick, G. M. *Acta Crystallogr.* **2008**, *A64*, 112–122.

[e]Flack, H. D. *Acta Crystallogr.* **1983**, *A39*, 876–881; Flack, H. D.; Bernardinelli, G. *Acta Crystallogr.* **1999**, *A55*, 908–915; Flack, H. D.; Bernardinelli, G. *J. Appl. Cryst.* **2000**, *33*, 1143–1148. The Flack parameter will refine to a value near zero if the structure is in the correct configuration and will refine to a value near one for the inverted configuration. The value observed herein is indicative of racemic twinning, and was accomodated during the refinement (using the *SHELXL-97* TWIN instruction [see reference *c*]).

[f]$S = [\Sigma w(F_o^2 - F_c^2)^2/(n-p)]^{1/2}$ (n = number of data; p = number of parameters varied; $w = [\sigma^2(F_o^2) + (0.0404P)^2 + 0.0821P]^{-1}$ where $P = [\text{Max}(F_o^2, 0) + 2F_c^2]/3$).

[g]$R_1 = \Sigma||F_o| - |F_c||/\Sigma|F_o|$; $wR_2 = [\Sigma w(F_o^2 - F_c^2)^2/\Sigma w(F_o^4)]^{1/2}$.

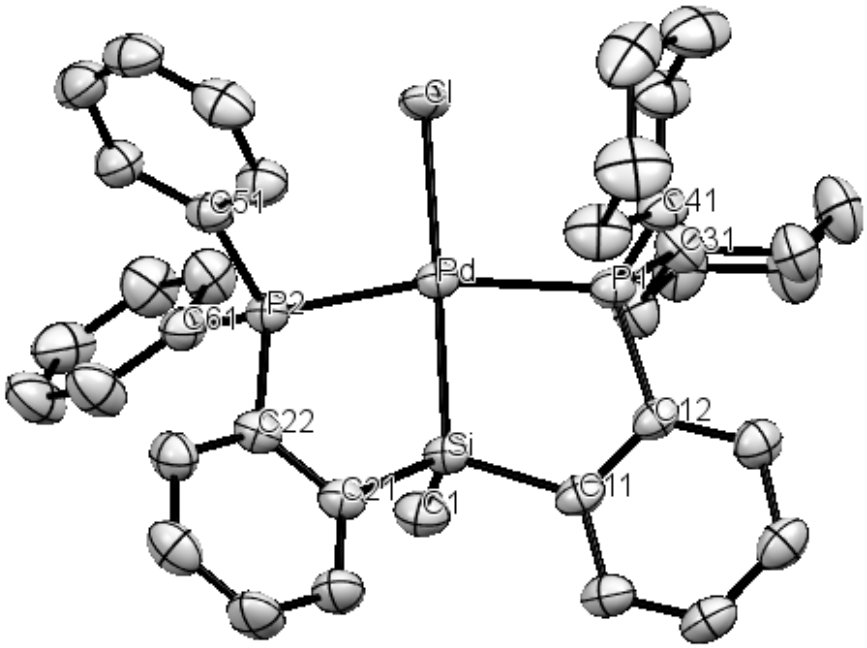

Figure A-1. ORTEP drawing of (Cy-PSiP'-Ph)PdCl] (**2-7**).

Table A-2. Crystallographic experimental details for (Cy-PSiP'-Ph)NiCl (**2-8**)

A. Crystal Data	
formula	$C_{37}H_{43}ClNiP_2Si$
formula weight	671.90
crystal dimensions (mm)	0.30 x 0.27 x 0.12
crystal system	orthorhombic
space group	$P2_12_12_1$ (No. 19)
unit cell parameters[a]	
a (Å)	9.8265 (3)
b (Å)	14.0961 (4)
c (Å)	24.8588 (7)
V (Å^3)	3443.32 (17)
Z	4
ρ_{calcd} (g cm^{-3})	1.296
μ (mm^{-1})	0.793
B. Data Collection and Refinement Conditions	
diffractometer	Bruker PLATFORM/APEX II CCD[b]
radiation (λ [Å])	graphite-monochromated Mo Kα (0.71073)
temperature (°C)	–100
scan type	ω scans (0.3°) (15 s exposures)
data collection 2Θ limit (deg)	55.04
total data collected	30991 ($-12 \le h \le 12$, $-18 \le k \le 18$, $-32 \le l \le 32$)
independent reflections	7928 (R_{int} = 0.0346)
number of observed reflections (*NO*)	7303 [$F_o^2 \ge 2\sigma(F_o^2)$]
structure solution method	Patterson/structure expansion (*DIRDIF–2008*[c])
refinement method	full-matrix least-squares on F^2 (*SHELXL–97*[d])
absorption correction method	Gaussian integration (face-indexed)
range of transmission factors	0.9108–0.7956
data/restraints/parameters	7928 / 0 / 381
Flack absolute structure parameter[e]	0.455(8)
goodness-of-fit (*S*)[f] [all data]	1.031
final *R* indices[g]	
R_1 [$F_o^2 \ge 2\sigma(F_o^2)$]	0.0266
wR_2 [all data]	0.0695
largest difference peak and hole	0.497 and –0.219 e Å^{-3}

[a]Obtained from least-squares refinement of 9997 reflections with $4.46° < 2\Theta < 49.02°$.

[b]Programs for diffractometer operation, data collection, data reduction and absorption correction were those supplied by Bruker.

[c]Beurskens, P. T.; Beurskens, G.; de Gelder, R.; Smits, J. M. M.; Garcia-Granda, S.; Gould, R. O. (2008). The *DIRDIF-2008* program system. Crystallography Laboratory, Radboud University Nijmegen, The Netherlands.

[d]Sheldrick, G. M. *Acta Crystallogr.* **2008**, *A64*, 112–122.

[e]Flack, H. D. *Acta Crystallogr.* **1983**, *A39*, 876–881; Flack, H. D.; Bernardinelli, G. *Acta Crystallogr.* **1999**, *A55*, 908–915; Flack, H. D.; Bernardinelli, G. *J. Appl. Cryst.* **2000**, *33*, 1143–1148. The Flack parameter will refine to a value near zero if the structure is in the correct configuration and will refine to a value near one for the inverted configuration. The value observed herein is indicative of racemic twinning, and was accomodated during the refinement (using the *SHELXL-97* TWIN instruction [see reference *c*]).

[f]$S = [\Sigma w(F_o^2 - F_c^2)^2/(n-p)]^{1/2}$ (n = number of data; p = number of parameters varied; $w = [\sigma^2(F_o^2) + (0.0404P)^2 + 0.3900P]^{-1}$ where $P = [\text{Max}(F_o^2, 0) + 2F_c^2]/3$).

[g]$R1 = \Sigma||F_o| - |F_c||/\Sigma|F_o|$; $wR2 = [\Sigma w(F_o^2 - F_c^2)^2/\Sigma w(F_o^4)]^{1/2}$.

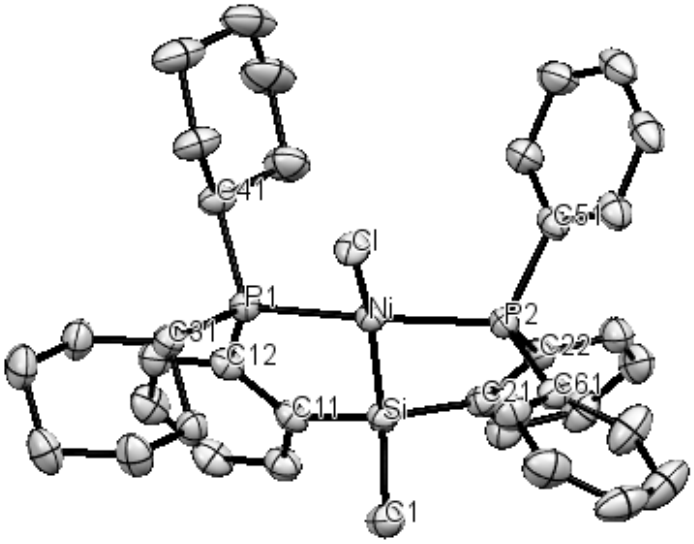

Figure A-2. ORTEP drawing of (Cy-PSiP'-Ph)NiCl] (**2-8**).

Table A-3. Crystallographic experimental details for [(Cy-PSiP*-^{i}Pr)PdCl]$_2$ (**2-24b**)·OEt_2

A. Crystal Data	
formula	$C_{60}H_{110}Cl_2O_2P_4Pd_2Si_2$
formula weight	1327.23
crystal dimensions (mm)	0.21 x 0.20 x 0.11
crystal system	monoclinic
space group	$P2_1/c$ (No. 14)
unit cell parameters[a]	
a (Å)	14.0874 (6)
b (Å)	20.5176 (8)
c (Å)	23.0364 (9)
β (deg)	94.6356 (6)
V (Å^3)	6636.7 (5)
Z	4
ρ_{calcd} (g cm^{-3})	1.328
μ (mm^{-1})	0.793
B. Data Collection and Refinement Conditions	
diffractometer	Bruker PLATFORM/APEX II CCD[b]
radiation (λ [Å])	graphite-monochromated Mo Kα (0.71073)
temperature (°C)	–100
scan type	ω scans (0.3°) (15 s exposures)
data collection 2Θ limit (deg)	55.17
total data collected	59528 (-18 ≤ h ≤ 18, -26 ≤ k ≤ 26, -29 ≤ l ≤ 29)
independent reflections	15349 (R_{int} = 0.0534)
number of observed reflections (*NO*)	11836 [$F_o^2 \geq 2\sigma(F_o^2)$]
structure solution method	Patterson/structure expansion (*DIRDIF–2008*[c])
refinement method	full-matrix least-squares on F^2 (*SHELXL–2014*[d])
absorption correction method	Gaussian integration (face-indexed)
range of transmission factors	0.9604–0.8536
data/restraints/parameters	15349 / 28[e] / 644
goodness-of-fit (*S*)[f] [all data]	1.036
final R indices[g]	
R_1 [$F_o^2 \geq 2\sigma(F_o^2)$]	0.0417
wR_2 [all data]	0.1165
largest difference peak and hole	1.199 and –0.618 e Å^{-3}

[a]Obtained from least-squares refinement of 9670 reflections with $4.34° < 2\Theta < 45.08°$.

[b]Programs for diffractometer operation, data collection, data reduction and absorption correction were those supplied by Bruker.

[c]Beurskens, P. T.; Beurskens, G.; de Gelder, R.; Smits, J. M. M.; Garcia-Granda, S.; Gould, R. O. (2008). The *DIRDIF-2008* program system. Crystallography Laboratory, Radboud University Nijmegen, The Netherlands.

[d]Sheldrick, G. M. *Acta Crystallogr.* **2015**, *C71*, 3–8

[e]Distances within the disordered solvent diethyl ether molecules were given idealized target values during refinement: d(O1SA–C1SA) = d(O1SA–C3SA) = d(O1SB–C1SB) = d(O1SB–C3SB) = d(O2SA–C5SA) = d(O2SA–C7SA) = d(O2SB–C5SB) = d(O2SB–C7SB) = 1.46(1) Å; d(C1SA–C2SA) = d(C3SA–C4SA) = d(C1SB–C2SB) = d(C3SB–C4SB) = d(C5SA–C6SA) = d(C7SA–C8SA) = d(C5SB–C6SB) = d(C7SB–C8SB) = 1.54(1) Å; d(O1SA···C2SA) = d(O1SA···C4SA) = d(O1SB···C2SB) = d(O1SB···C4SB) = d(O2SA···C6SA) = d(O2SA···C8SA) = d(O2SB···C6SB) = d(O2SB···C8SB) = 2.43(1) Å; d(C1SA···C3SA) = d(C1SB···C3SB) = d(C5SA···C7SA) = d(C5SB···C7SB) = 2.38(1) Å.

[f]$S = [\Sigma w(F_o^2 - F_c^2)^2/(n-p)]^{1/2}$ (n = number of data; p = number of parameters varied; $w = [\sigma^2(F_o^2) + (0.0581P)^2 + 4.1050P]^{-1}$ where $P = [\mathrm{Max}(F_o^2, 0) + 2F_c^2]/3$).

[g]$R1 = \Sigma||F_o| - |F_c||/\Sigma|F_o|$; $wR2 = [\Sigma w(F_o^2 - F_c^2)^2/\Sigma w(F_o^4)]^{1/2}$.

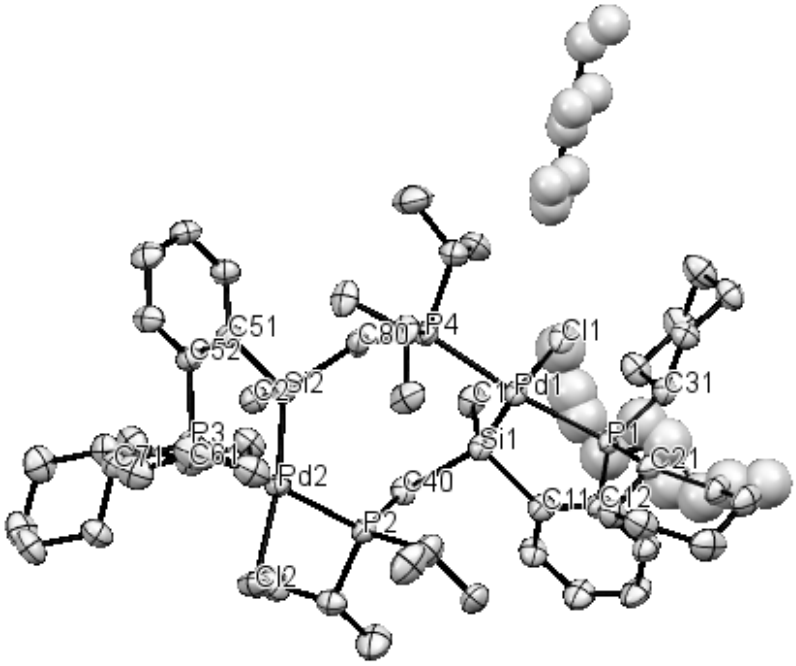

Figure A-3. ORTEP drawing of $[(\text{Cy-PSiP*-}^{i}\text{Pr})\text{PdCl}]_2 \bullet \text{Et}_2\text{O}$ (**2-24b**).